

WRDC-TR-90-4130

ADA232740



**Kinetic and Rheological Studies of a Model In-Situ  
Molecular Composite System (PAA/DNI-3A)**

Yih-Fang Chen  
AdTech System Research, Inc.  
1342 N. Fairfield Road  
Dayton, OH 45432

and

Charles Y-C. Lee  
Polymer Branch  
Nonmetallic Materials Division  
WPAFB, OH 45433

January 1991

**Best Available Copy**

Final Report for Period April 1989 to June 1990

Approved for Public Release; Distribution Unlimited

MATERIALS LABORATORY  
WRIGHT RESEARCH AND DEVELOPMENT CENTER  
AIR FORCE SYSTEM COMMAND  
WRIGHT-PATTERSON AIR FORCE BASE, OHIO 45433-6533

**BEST AVAILABLE COPY**

20040219269

## NOTICE

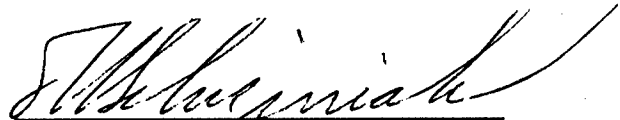
WHEN GOVERNMENT DRAWINGS, SPECIFICATIONS, OR OTHER DATA ARE USED FOR ANY PURPOSE OTHER THAN IN CONNECTION WITH A DEFINITELY GOVERNMENT-RELATED PROCUREMENT, THE UNITED STATES GOVERNMENT INCURS NO RESPONSIBILITY OR ANY OBLIGATION WHATSOEVER. THE FACT THAT THE GOVERNMENT MAY HAVE FORMULATED OR IN ANY WAY SUPPLIED THE SAID DRAWINGS, SPECIFICATIONS, OR OTHER DATA, IS NOT TO BE REGARDED BY IMPLICATION, OR OTHERWISE IN ANY MANNER CONSTRUED, AS LICENSING THE HOLDER, OR ANY OTHER PERSON OR CORPORATION; OR AS CONVEYING ANY RIGHTS OR PERMISSION TO MANUFACTURE, USE, OR SELL ANY PATENTED INVENTION THAT MAY IN ANY WAY BE RELATED THERETO.

THIS REPORT HAS BEEN REVIEWED BY THE OFFICE OF PUBLIC AFFAIRS (ASD/PA) AND IS RELEASABLE TO THE NATIONAL TECHNICAL INFORMATION SERVICE (NTIS). AT NTIS IT WILL BE AVAILABLE TO THE GENERAL PUBLIC INCLUDING FOREIGN NATIONS.

THIS TECHNICAL REPORT HAS BEEN REVIEWED AND IS APPROVED FOR PUBLICATION.

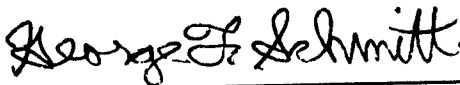


R. C. Evers  
Polymer Branch  
Nonmetallic Materials Division



T. E. Helminiak, Chief  
Polymer Branch  
Nonmetallic Materials Division

FOR THE COMMANDER



for Merrill L. Minges, Director  
Nonmetallic Materials Division

IF YOUR ADDRESS HAS CHANGED, IF YOU WISH TO BE REMOVED FROM OUR MAILING LIST, OR IF THE ADDRESSEE IS NO LONGER EMPLOYED BY YOUR ORGANIZATION PLEASE NOTIFY WRDC/MLBP, WRIGHT-PATTERSON AFB, OH 45433-6533 TO HELP MAINTAIN A CURRENT MAILING LIST.

COPIES OF THIS REPORT SHOULD NOT BE RETURNED UNLESS RETURN IS REQUIRED BY SECURITY CONSIDERATIONS, CONTRACTUAL OBLIGATIONS, OR NOTICE ON A SPECIFIC DOCUMENT.

Unclassified

SECURITY CLASSIFICATION OF THIS PAGE

REPORT DOCUMENTATION PAGE				Form Approved OMB No. 0704-0188	
1a. REPORT SECURITY CLASSIFICATION <b>Unclassified</b>			1b. RESTRICTIVE MARKINGS		
2a. SECURITY CLASSIFICATION AUTHORITY			3. DISTRIBUTION/AVAILABILITY OF REPORT Approved for public release; distribution is unlimited.		
2b. DECLASSIFICATION/DOWNGRADING SCHEDULE					
4. PERFORMING ORGANIZATION REPORT NUMBER(S) WRDC-TR-90-4130			5. MONITORING ORGANIZATION REPORT NUMBER(S)		
6a. NAME OF PERFORMING ORGANIZATION Materials Lab, WRDC, AFSC		6b. OFFICE SYMBOL (If applicable) WRDC/MLBP	7a. NAME OF MONITORING ORGANIZATION		
6c. ADDRESS (City, State, and ZIP Code) Wright-Patterson AFB OH 45433-6533			7b. ADDRESS (City, State, and ZIP Code)		
8a. NAME OF FUNDING/SPONSORING ORGANIZATION		8b. OFFICE SYMBOL (If applicable)	9. PROCUREMENT INSTRUMENT IDENTIFICATION NUMBER		
8c. ADDRESS (City, State, and ZIP Code)			10. SOURCE OF FUNDING NUMBERS		
			PROGRAM ELEMENT NO. 61102F	PROJECT NO. 2303	TASK NO. Q3
11. TITLE (Include Security Classification) Kinetic and Rheological Studies of a Model In-Situ Molecular Composite System (PAA/DNI-3A)					
12. PERSONAL AUTHOR(S) Yih-Fang Chen and Charles Y-C Lee					
13a. TYPE OF REPORT Interim		13b. TIME COVERED FROM Apr 89 TO Jun 90	14. DATE OF REPORT (Year, Month, Day) January 1991		15. PAGE COUNT 138
16. SUPPLEMENTARY NOTATION					
17. COSATI CODES			18. SUBJECT TERMS (Continue on reverse if necessary and identify by block number)		
FIELD	GROUP	SUB-GROUP			
07	04				
11	04				
19. ABSTRACT (Continue on reverse if necessary and identify by block number) A model compound of In-Situ Molecular Composite system, poly(amic dialkylamide) was prepared and characterized in an attempt to better understand the rod conversion for designing a processing scheme for these materials. The conversion kinetics and the chemorheology of the system were studied by using FTIR and TICA. The activation energy was found to be higher than the values reported for poly(amic esters). The rod conversion kinetics was controlled by rheology. Two different kinetic rates were observed before and after the vitrification point. A Fixed-Time-Interval method for using FTIR data to analyze kinetic rate was developed. The effect of pressurization on the thermal behavior of the model system was analyzed. This study clearly indicated that the rod conversion chemistry is rheologically controlled.					
20. DISTRIBUTION/AVAILABILITY OF ABSTRACT <input checked="" type="checkbox"/> UNCLASSIFIED/UNLIMITED <input type="checkbox"/> SAME AS RPT. <input type="checkbox"/> DTIC USERS			21. ABSTRACT SECURITY CLASSIFICATION Unclassified		
22a. NAME OF RESPONSIBLE INDIVIDUAL Charles Y-C Lee			22b. TELEPHONE (Include Area Code) 513-255-9155		22c. OFFICE SYMBOL WRDC/MLBP

## FOREWORD

This report was prepared by the Polymer Branch, Nonmetallic Materials Division. The work was initiated under Project No. 2303, "Nonmetallic and Composite Materials," Task No. 2303Q3, work unit Directive 2303Q307, "Structure Resin." It was administrated under direction of Materials Laboratory, Wright Research and Development Center, Air Force Systems Command, Wright-Patterson Air Force Base, Ohio, with Dr. R.C. Evers as the Materials Laboratory Project Scientist. Coauthors were Dr. Yih-Fang Chen (Adtech System Research, Inc.) and Dr. Charles Y-C. Lee, Materials Laboratory (WRDC/MLBP). This report covers research conducted from April 1989 to June 1990.

## TABLE OF CONTENTS

	Page
SECTION 1. INTRODUCTION .....	1
SECTION 2. EXPERIMENTAL .....	5
SECTION 3. BACKGROUND .....	8
3.1 Possible Chemistry Description .....	8
3.2 Temperature Range of the Reactions and FTIR Measurement..	8
3.3 First Order Reaction Kinetics Based on Normalized Concentration.....	13
3.4 First Order Reaction Kinetics Based on Fixed-Time-Interval Data.....	16
SECTION 4. RESULTS AND DISCUSSION.....	18
4.1 Chemistry Correlated with DSC and TGA/MS Results .....	18
4.2 FTIR Absorption Spectra and Subtraction Results .....	23
4.3 FTIR Absorption Bands for PAA/DNI-3A and Polyimide.....	31
4.4 $([C]_t - [C]_r) / ([C]_0 - [C]_r)$ Concentration Ratio Analysis and Kinetic Parameters.....	36
4.5 $\Delta A$ Absorbance Difference Analysis and Kinetic Parameters....	44
4.6 The TICA Results and Correlation with the Two Kinetic Rates.	55
SECTION 5. SUMMARY.....	61
REFERENCES .....	62
APPENDIX A Illustrated Examples for Kinetic Data Calculation from Sections 3.3 and 3.4 .....	A-1
APPENDIX B Report of TGA/MS Results of PAA/DNI and DNI Systems from SRL .....	B-1
APPENDIX C Absorption Spectra from FTIR for PAA/DNI-3A .....	C-1
APPENDIX D Subtraction Spectra from FTIR for PAA/DNI-3A .....	D-1

THIS DOCUMENT CONTAINED  
BLANK PAGES THAT HAVE  
BEEN DELETED

## LIST OF FIGURES

Figure	Page
1. Chemistry of PAA/DNI-3A for in-situ rod reinforced molecular composite ..	2
2. Synthesis route for PAA/DNI-3A and polyimide.....	6
3. Possible reaction routes for nadic group.....	11
4. TGA/MS spectra for (a) PAA/DNI-3A, and (b) DNI-3A.....	19
5. DSC thermogram for PAA/DNI-3A under (a) ambient, and (b) 750psi pressure, and for DNI-3A under (c) ambient, and (d) 750psi pressure.....	21
6. FTIR absorbance for PAA/DNI-3A at (a) 240°C, t =20 min, (b) 260°C, t=10 min, and (c) 280°C, t=10 min, respectively, and the subtraction results for (d) [A(t=5min)-A(0)], and (e) [A(t=180min)-A(0)] at 280°C.....	26
7. Normalized absorption at increasing peak 1725 cm <sup>-1</sup> and decreasing peak 1690 cm <sup>-1</sup> for PAA/DNI-3A during imidization at (a) 280°C, (b) 260°C, and (c) 240°C.....	33
8. $\ln ([C]_t/[C]_\tau) / ([C]_0/[C]_\tau)$ versus time for PAA/DNI-3A at 1725 cm <sup>-1</sup> at (a) 240°C, (b) 260°C, and (c) 280°C, and at 1690 cm <sup>-1</sup> at (d) 240°C, (e) 260°C, and (f) 280°C.....	37
9. $\ln \Delta A$ versus time for PAA/DNI-3A at 1725 cm <sup>-1</sup> at (a) 240°C, (b) 260°C, and (c) 280°C, and at 1690 cm <sup>-1</sup> at (d) 240°C, (e) 260°C, and (f) 280°C.....	46
10. Arrhenius plot for imidization of PAA/DNI-3A at (a) 1725 and (b) 1690 cm <sup>-1</sup>	53
11. Comparison of Arrhenius plot for imidization of PAA/DNI-3A and PMR-15.	54
12. TICA spectra of PAA/DNI-3A for (a) temperature scan, and (b) isothermal scan at 240°C, and (c) isothermal scan at 280°C.....	56
13. Relationship between softening and reaction rate for PAA/DNI-3A.....	60

## LIST OF TABLES

		Page
TABLE 1.	The kinetic parameters of imidization in the literature .....	10
TABLE 2.	The assigned imide peaks in the literature.....	32
TABLE 3.	The kinetic parameters of imidization from $([C]_t - [C]_\tau) / ([C]_0 - [C]_\tau)$ data at 1725 and 1690 $\text{cm}^{-1}$ .....	43
TABLE 4.	The kinetic parameters of imidization from $\Delta A$ data at 1725 and 1690 $\text{cm}^{-1}$ .....	52

## SECTION 1

### INTRODUCTION

The concept of In-Situ Molecular Composites (ISMC) was introduced previously [1,2]. These ISMC systems will undergo an intramolecular thermal elimination (ring closure) to form the rigid-rod polyimide, and the evolved pendants can crosslink to form an in-situ network. The feasibility of the conversion (ring-closure only) has been proven spectroscopically [3]. However, to yield useful properties, the ISMC materials will have to consolidate, to attain complete conversion to generate high aspect ratio rods, and to remain molecularly dispersed. These factors are very much controlled by the rheology of the systems during processing. Sufficiently low viscosity is required for consolidation and rod conversion, but too low a viscosity will cause the aggregation of the rod molecules. The successful conversion of the aforementioned poly(amic dialkylamides) into molecular composites will necessitate a careful definition of the processing window.

In an attempt to understand better the process of rod conversion so as to design a processing scheme for these materials, the kinetics of rod conversion and its relationship with the rheology of a prototype system, poly(amic amide/DNI-3A) (PAA/DNI-3A) where DNI-3A is an alkyl dinadiimide derived from 3,3'-iminobispropylamine and nadic anhydride, was studied. The structure and imidization of PAA/DNI-3A is shown in Fig.1. FTIR was used to follow the degree of imide conversion. Analysis of the kinetic algorithm showed that systematic errors could be introduced if the final concentration of reactant was not accurately known. A modified fixed-time-interval approach was developed and was used to analyze the kinetic data. Chemorheology of the system was studied by using TICA



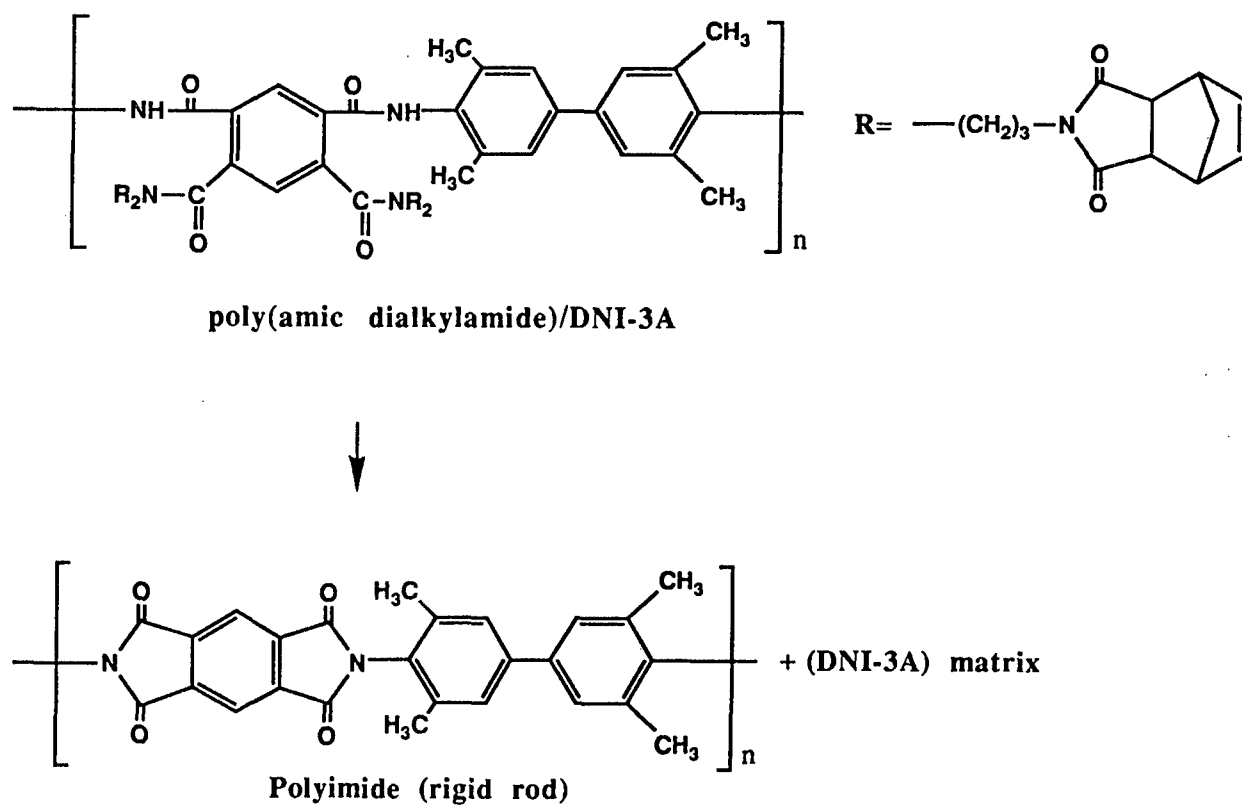


Fig.1. Chemistry of PAA/DNI-3A for in-situ rod reinforced molecular composite

DNI-3A matrix network

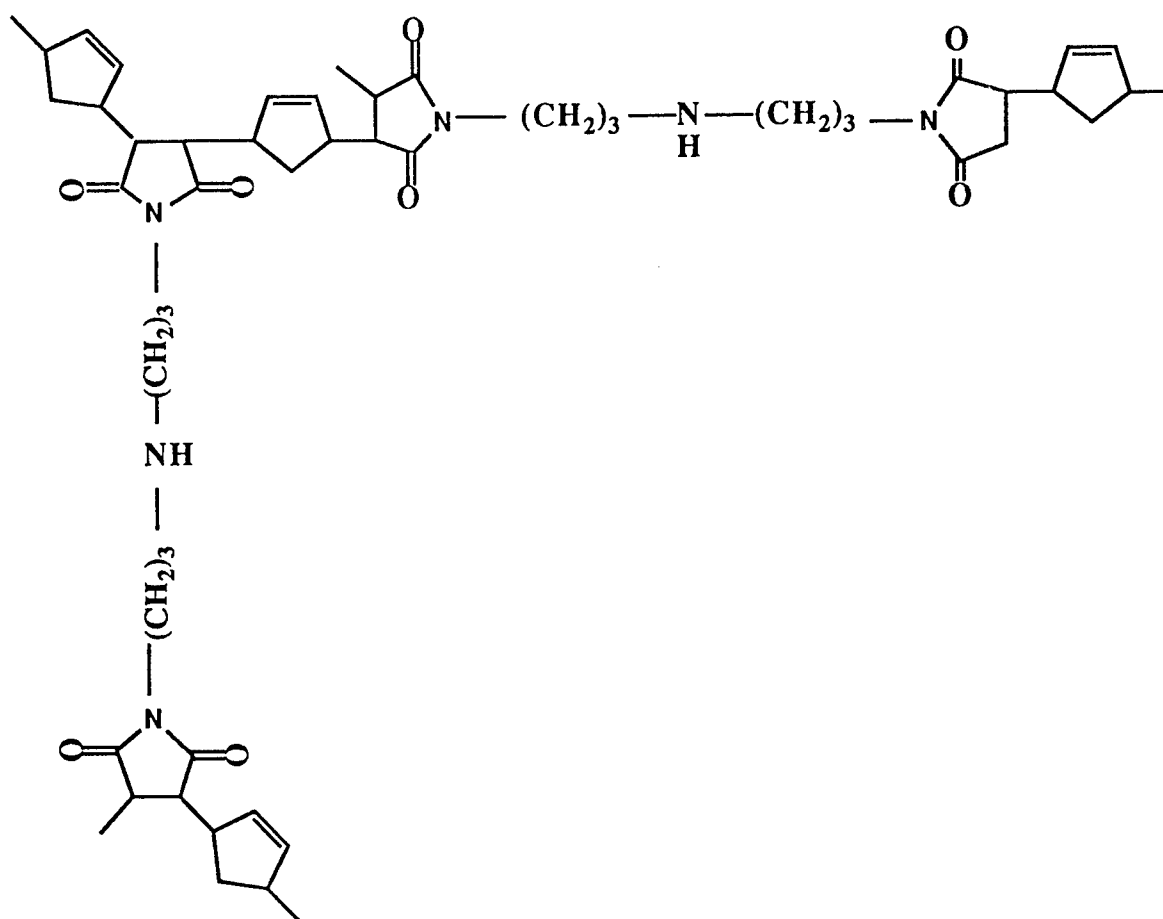


Fig.1. (continued)

in isothermal and temperature scan modes. The DSC of the model system polymer and the model leaving group under ambient and pressurized condition was analyzed.

## SECTION 2

### EXPERIMENTAL

The poly(amic amide) samples (PAA/DNI-3A) (sample #A90501) used in this study was prepared by Tan [1,2]. The synthesis of this compound is based on a previously published synthesis route for poly(amic dialkyl amide) [4]. The details of the synthesis of this compound will be published separately [1,2]. The syntheses reaction is summarized in Fig. 2. PMDA (pyromellitic dianhydride) and TMB (tetramethyl benzidine) as the starting monomers were reacted to yield a poly(amic amide), which was sequentially converted to polyisoimide, and finally to poly(amic dialkyl amide). The leaving group of this compound is an alkyl group terminated with norbornene.

Film samples of PAA/DNI-3A were solvent casted from 0.4% concentration DMAc solutions. About 10 ml of this solution was placed on a 3.5" petri dish. Vacuum was applied for 24 hours to remove the solvent. The film was then immersed in acetone overnight to remove residual DMAc. The film was subsequently rinsed with acetone several times and dried in air. Small pieces of the films were sandwiched between KCl plates for FTIR studies. The plates were mounted inside a temperature controlled fixture for kinetic studies.

After placing the fixture inside the IR chamber, the film was heated at the rate of about 40°C/min to the desired temperature. When the system reached a predetermined temperature, the timer was started and an initial IR scan was recorded. Subsequent spectra were recorded at appropriate time intervals. The spectra were stored in an on-line computer for later use. After the last spectrum was recorded the heater was turned off and the film was allowed to cool. The final IR scan for the cooled sample was also recorded.

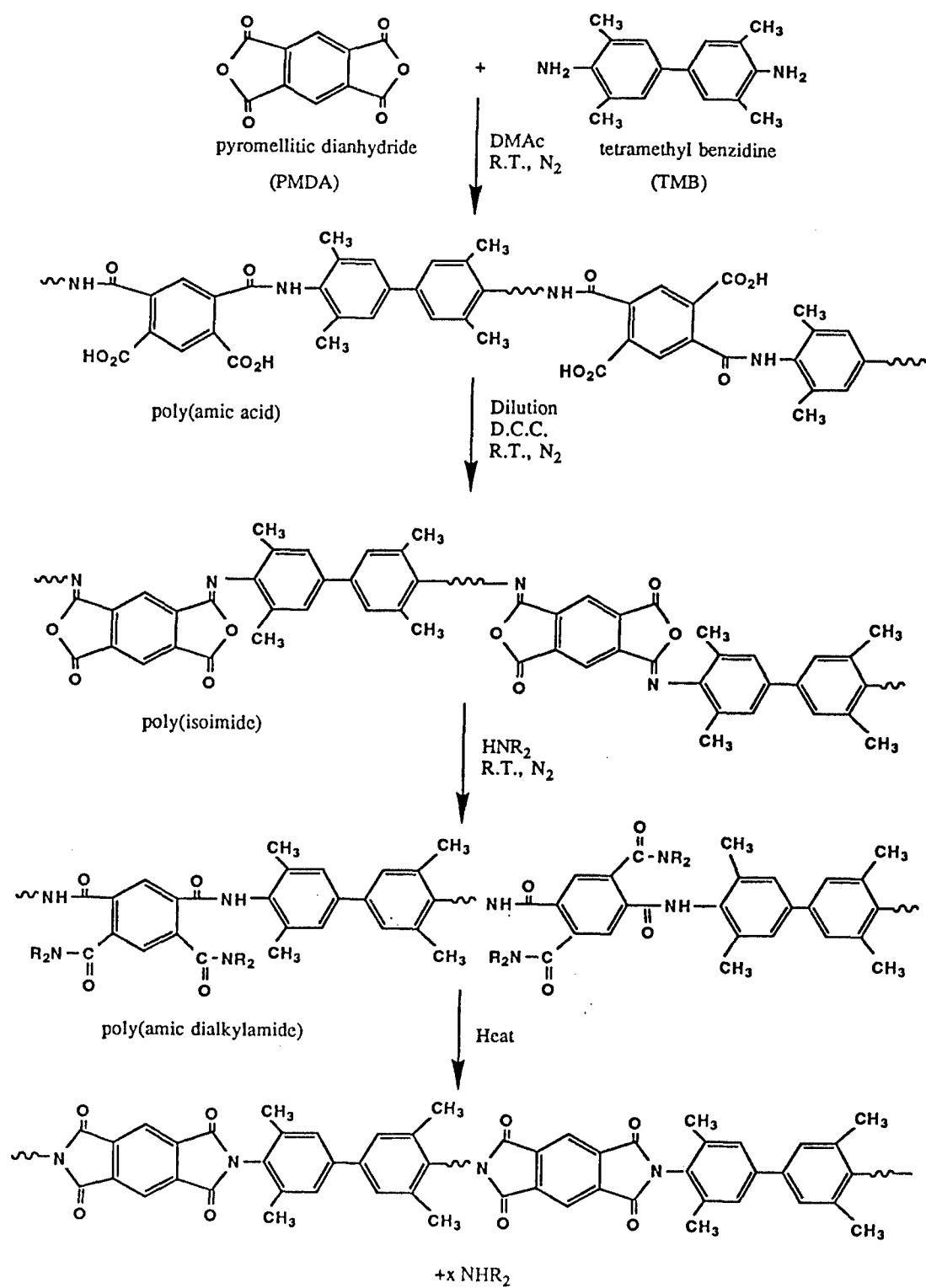


Fig.2. Synthesis route for PAA/DNI-3A and polyimide

The details of TICA specimens preparation and experimentation were described elsewhere [5]. A piece of glass cloth of 3"x4" was prepared by pulling two strands of fibers every half inch in the width direction. The cloth was immersed in a 4% DMAc solution of the polymer and placed in a desiccator for vacuuming and drying. Then the cloth was immersed in acetone overnight to remove residual DMAc. Before being dried in air the cloth was rinsed with acetone several times. The dried cloth was then cut in halves and folded into strips of 1.2 cm wide, 6.4 cm long and 0.2 cm thick, with the cut edges folded inside the strips. The specimen was made by stacking two strips with the ends sandwiched by two metal plates held together by a screw at the center. The TICA specimen was mounted on the RDS instrument with the end metal plates as fixtures. The instrument was set at "torsion" mode and the control mode was set at "cure".

## SECTION 3

### BACKGROUND

#### 3.1 Possible Chemistry Description

The PAA/DNI-3A chemistry is similar to PMR-15 [6]. The monomers used in PMR-15 include a dialkyl ester of aromatic tetracarboxylic acid such as BTDE, an aromatic diamine like MDA, and a monoalkyl ester of norbornene 2,3-dicarboxylic acid (NE). They are dissolved in a low boiling alkyl alcohol. After heating to 150-220°C temperature range, the the solvent was removed and the monomers undergo in-situ condensation and cyclodehydration to yield norbornenyl end-capped low molecular weight imide prepolymer. Under pressurized condition, the end-capped prepolymer undergoes addition polymerization (crosslinking) at 260-315°C without evolution of volatiles.

The same types of reactions occur in the current PAA/DNI-3A system. The high molecular weight poly(amic amide) will undergo ring closure imidization probably at a higher reaction temperature. A leaving group with a reactive end-cap will be released from the reaction. This leaving amine group,  $\text{NH}(\text{nadic-3A})_2$ , may undergo crosslinking reaction and degrade due to the instability of the aliphatic bonds in its structure.

#### 3.2 Temperature Range of the Reactions and the FTIR Measurement

The polyimide formation reactions from different prepolymers such as poly(amic acid), poly(amic ester) or poly(amic amide) are similar. Most of the data in literature were from poly(amic acid) system and in solution state. The activation energy and mechanism for the imide formation in the solution state can be different from that in the solid state. It has been shown that the solvent-polymer interaction caused difficulty in the removal of solvent in the

final stage [7,8] and affected the imidization rate [9]. The condensation reaction product, water, also induced hydrolysis of the polymer and cause rapid degradation [10].

The kinetics of the formation of imide showed that it was a first order reaction and is linearly proportional to the concentration of amic acid. Recently, a second order reaction mechanism of maleimide formation was reported [11]. It was argued that the imidization rate is proportional to the product of the amic acid concentration and the catalyst acetic anhydride concentration. Nevertheless, most reports agreed that the imide formation reaction being a first order reaction. Most of the research on imide formation kinetics were based on FTIR technique. The temperature range for the imide formation and the associated kinetic data including pre-exponent constant and the activation energy constant are listed in Table 1.

For PMR type polyimide, the crosslinking reaction of the nadic group, occurs at a higher temperature. The reaction mechanism still remains controversial. Some possible reaction routes found in the literature are shown in Fig.3 [20,21]. The crosslinking reaction of the nadic group involves a retro-Diels Alder reaction in which the nadic group cracks down to form maleimide and cyclopentadiene. The cyclopentadiene has boiling temperature about 41°C which is much lower than the crosslinking temperature. In order to incorporate the cyclopentadiene compound in the crosslinking reaction, a high pressure environment has to be maintained to suppress the evolution of pentadiene.

Experiments also showed this crosslinking reaction for the PMR system to be a first order reaction. The kinetic data of this reaction was determined by DSC thermoanalysis. Only one set of kinetic data was found in the literature [15], and the values are:

$$A=2.5 \times 10^{15} \text{ (min}^{-1}\text{)}, E=44\pm 2 \text{ Kcal/mole, } T=275\text{-}325^{\circ}\text{C with pressure.}$$



Table 1. The kinetic parameters of imdization in the literature

$k_0(\text{min}^{-1})$	E (Kcal/mole)	Reaction Temp ( $^{\circ}\text{C}$ )	Reference
	28.2	150-200	[9]*a
	23 $\pm$ 7 (slow) 26 $\pm$ 3 (fast)	161-188	[12]*b
4.6 E 10	26 $\pm$ 4		[13]*c
	19.5		[14]*d
8.4 E 8	24 $\pm$ 6	120-204	[15]*e
	10 $\pm$ 1	100-170	[16]*f
	14-65	150-250	[17]*g
6.8 E 10	26	140-170	[18]*h
	8.6 $\pm$ 2.3	140-200	[19]*i
	12 (2nd order rxn)	27-80	[11]*j
*a. BTDA + DABP in diglyme solvent, by FTIR, 720 and 1780 $\text{cm}^{-1}$			
*b 4,4'-diaminodiphenyl ether + PMDA in DMAc solvent, by FTIR, 725 $\text{cm}^{-1}$			
*c, *d, dianhydride + diamine (not specified), 720 & 1380 $\text{cm}^{-1}$ ( recommended)			
*e NE + MDA + BTDE in methanol (PMR system), by FTIR, 1370 $\text{cm}^{-1}$			
*f PMR-15 by RDS method			
*g PMDA/ODA, E=28, BTDA/ODA, E=22, BPDA/ODA, E=16, BPDA/ODA, E=14, Toray photoneece, E=26, PMDA/ODA ethyl ester, E=65, all by FTIR, 1780 $\text{cm}^{-1}$			
*h BTDA + DDS + siloxane oligomer in NMP/CHP cosolvent for solution imidization, by FTIR, 725 $\text{cm}^{-1}$			
*i PMDA + ODA in NMP solvent, by Fluorescence Spectroscopy			
*j Maleamic acid --> maleimide, 2nd order reaction, by $^1\text{H}$ -NMR			

(Scola, 1985 [21])

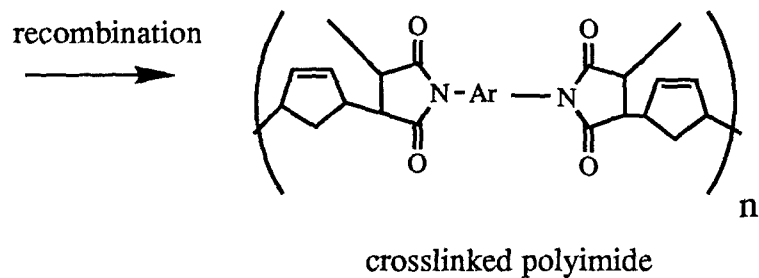
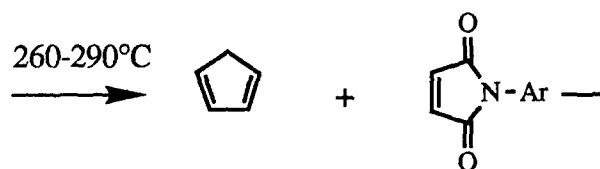
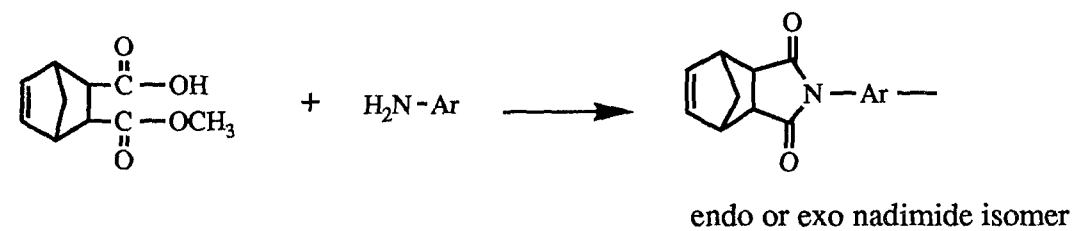


Fig.3. Possible reaction routes for nadic group

(Gaylord, 1981 [20])

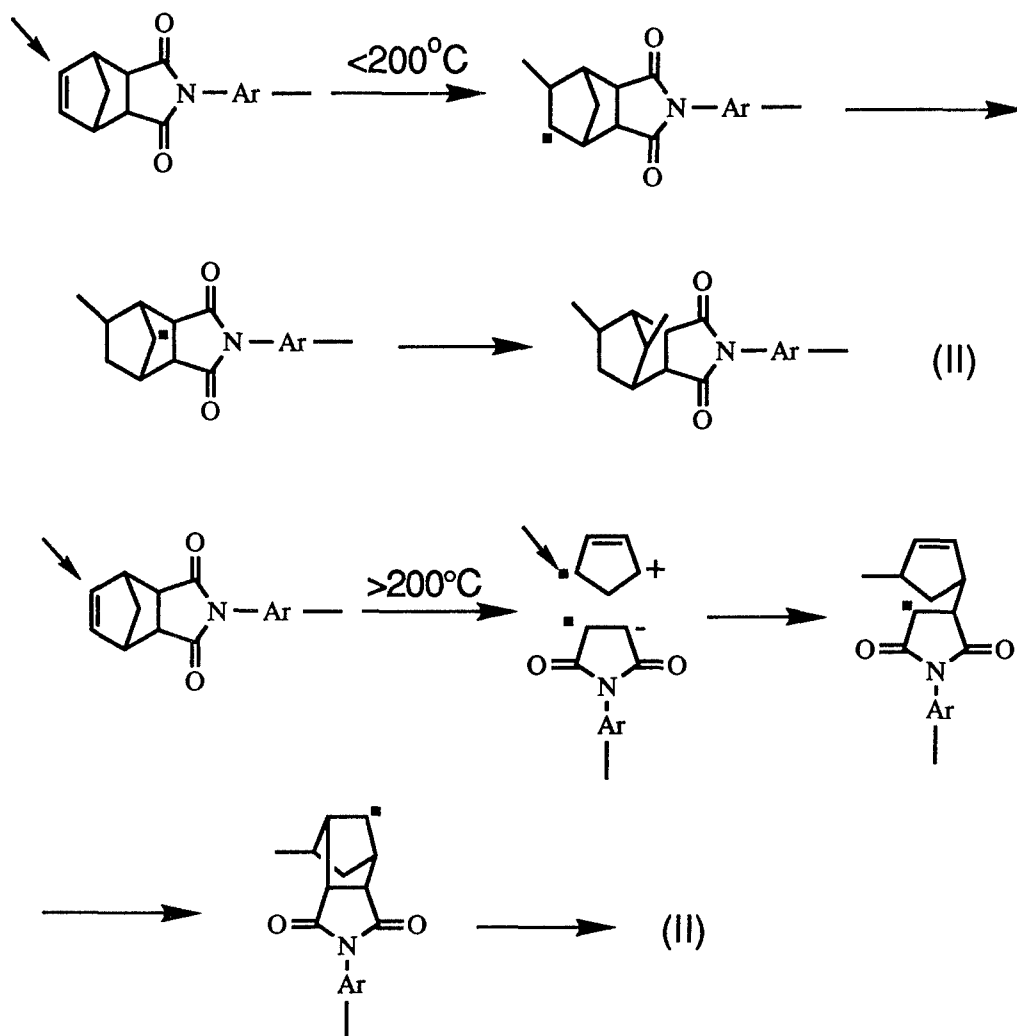


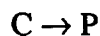
Fig.3. (continued)

Myers [16] used PMR-15 prepreg by RDS instrument to obtain the activation energy of the crosslinking reaction to be  $14 \pm 2$  Kcal/mole, a value much smaller than Lauver's data.

### 3.3 First Order Reaction Kinetics Based on Normalized Concentration

From FTIR data, the first order reaction kinetic parameters can be obtained by two methods. One is based on the reactant or product normalized concentration, and the other is based on fixed-time-interval data. These two techniques will be analyzed in detail in this and the next sections. But first let's examine the first order reaction kinetics.

The first order chemical reaction



is represented by the following differential equation:

$$\frac{d[p]_t}{dt} = -\frac{d[c]_t}{dt} = k[c]_t \quad (1a)$$

The initial conditions are defined as:

$$\text{i.c. @ } t=0, [c] = [c]_0, [p] = [p]_0 \quad (1b)$$

The following equation holds for the first order reaction:

$$[p]_0 + [c]_0 = [p]_t + [c]_t = [p]_\infty + [c]_\infty = \text{constant.} \quad (1c)$$

Please note that in this report the notation  $[c]_\infty$  represents the reactant concentration at infinite reaction time and is therefore zero. With the conditions (1b) and (1c), the

differential equation (1a) can be solved by direct integration method to obtain the solution of  $[c]_t$  and  $[p]_t$ ,

$$\begin{aligned} [c]_t &= [c]_0 e^{-kt} \\ [p]_t - [p]_0 &= [c]_0 (1 - e^{-kt}) \end{aligned} \quad (2)$$

For accurate determination of the first order kinetics parameters, either the initial product concentration  $[p]_0$  or the final reactant concentration has to be accurately determined. In infrared spectroscopy the concentration can be extracted from the absorbance according to Beer's Law, which is,

$$\text{Beer's Law:} \quad A = ab[c] = -\log_{10} T \quad (3)$$

where  $A$  is the absorbance,

$a$  is the absorptivity,  $[\text{cm}^2/\text{mole}]$ ,

$b$  is the path length,  $[\text{cm}]$ ,

$[c]$  is the concentration of the absorbing species,  $[\text{mole}/\text{cm}^3]$

$T$  is the transmittance,

If the systems contains some inert species (an absorption peak that does not change in intensity in the course of the reaction being studied) which absorb at the same frequency, then

$$A(\nu_c, t) = A_c(t) + A_i = a_c b [c]_t + a_i b [I] \quad (4)$$

$$A(\nu_p, t) = A_p(t) + A_{i'} = a_p b [p]_t + a_{i'} b [I']$$

where  $A(\nu_c, t)$  and  $A(\nu_p, t)$  are the apparent absorbance at peak frequency for C and P moieties respectively,  $A_c(t)$  and  $A_p(t)$  are the true absorbance of C and P at time  $t$ ,  $A_i$  and  $A_{i'}$  are the absorbance of inert species I and I' respectively.

In equation (4),  $A_c(t)$  and  $A_{pr}(t)$  are the desired quantities for the kinetic study, but  $A(v_c, t)$  and  $A(v_p, t)$  are the experimentally measured data. The background absorbance can be removed by subtracting different spectra:

$$A(v_c, t_1) - A(v_c, t_2) = A_c(t_1) - A_c(t_2) = a_c b ([c]_{t_1} - [c]_{t_2}) \quad (5)$$

$$A(v_p, t_1) - A(v_p, t_2) = A_p(t_1) - A_p(t_2) = a_p b ([p]_{t_1} - [p]_{t_2})$$

This subtraction result is the change in absorbance as a result of the reaction. Normalizing the subtraction data with the total change between  $t=0$  at the beginning of the experiment and  $t=\tau$  at the end of the experiment, will yield

$$\frac{A(v_c, 0) - A(v_c, t)}{A(v_c, 0) - A(v_c, \tau)} = \frac{[c]_0 - [c]_t}{[c]_0 - [c]_\tau} \quad (6a)$$

$$\frac{A(v_p, t) - A(v_p, 0)}{A(v_p, \tau) - A(v_p, 0)} = \frac{[p]_t - [p]_0}{[p]_\tau - [p]_0} \quad (6b)$$

with

$$\frac{[c]_0 - [c]_t}{[c]_0 - [c]_\tau} = \frac{[p]_t - [p]_0}{[p]_\tau - [p]_0} \quad (6c)$$

The ratio terms shown in equation (6c) represent the normalized degree of reaction conversion. If  $[c]_\tau$  is sufficiently close to zero ( $[c]_\tau \sim [c]_\infty = 0$ ) then the data obtained according to equation (6a) and (6b) can be analyzed by replacing  $\tau$  by  $\infty$  and using the kinetic equation (2). Thus the logarithm of  $[c]/[c]_0$  (or  $[A(t)-A(\infty)]/[A(0)-A(\infty)]$ ) versus time  $t$  plot will yield a straight line with the slope being the desired reaction constant  $k$ . But if  $[c]_\tau$  is not zero, equation (6) will not be equivalent to equation (2), but instead be

$$1 - \frac{A(t)-A(0)}{A(\tau)-A(0)} = \frac{A(t)-A(\tau)}{A(0)-A(\tau)} = \frac{[p]_t - [p]_\tau}{[p]_0 - [p]_\tau} = \frac{[c]_t - [c]_\tau}{[c]_0 - [c]_\tau} \neq e^{-kt} \quad (7)$$

The logarithm of  $([c]_t - [c]_\tau)/([c]_0 - [c]_\tau)$  versus time  $t$  plot in this case will not give the correct quantity  $k$ . The analysis in the following section then has to be taken.

### 3.4 First Order Reaction Kinetics Based on Fixed-Time-Interval Data

From equation (2) one can immediately obtain the following equation,

$$\begin{aligned} [c]_{t_1} - [c]_{t_2} &= [c]_0(e^{-kt_1} - e^{-kt_2}) \\ [p]_{t_1} - [p]_{t_2} &= -[c]_0(e^{-kt_1} - e^{-kt_2}) \end{aligned} \quad (8)$$

Equation (5) can be rewritten in the following general form,

$$\Delta A(t_1, t_2) = k' (e^{-kt_1} - e^{-kt_2}) \quad (9)$$

where  $\Delta A(t_1, t_2)$  represents either  $A(c, t_1) - A(c, t_2)$  or  $A(p, t_1) - A(p, t_2)$  and  $k' = a_c b[c]_0$  or  $-a_p b[c]_0$ . Taking the logarithm of equation (9) yields

$$\begin{aligned} \ln \Delta A(t_1, t_2) &= \ln \{ k' (e^{-kt_1} - e^{-kt_2}) \} \\ &= \ln k' - kt_1 + \ln \{ 1 - e^{-k(t_1 - t_2)} \} \end{aligned} \quad (10)$$

Now if  $(t_1 - t_2)$  is set to be constant (equally spaced time data), equation (10) can be rewritten as

$$\begin{aligned} \ln \Delta A(t_1, t_2) &= \ln k' - kt_1 + \ln \{ 1 - e^{-k(t_1 - t_2)} \} \\ &= k'' - kt_1 \end{aligned} \quad (11)$$

with  $k''$  being a constant as well.

From equation (11) with equally spaced data, the plot of  $[\ln \Delta A(t_1, t_2)]$  verse  $t_1$  will generate the slope  $(-k)$ , which is the desired reaction rate constant at that particular temperature. The example for using these two different approaches to calculate the kinetic data are shown in Appendix A for comparison.



## SECTION 4

### RESULTS AND DISCUSSION

#### 4.1 Chemistry Correlated with DSC and TGA/MS Results

To further characterize the chemistry of PAA/DNI-3A system (sample #A90501) at elevated temperature, the system was analyzed by TGA/MS spectra. The report from SRL is shown in Appendix B. The result, shown in Fig.4a, illustrated that cyclopentadiene ( $C_5H_6$ ) started to evolve  $\sim 150^\circ C$  as the product of the reverse Diels Alder reaction. No other product were released in this temperature range. The next volatile product started above  $300^\circ C$  with  $m/e$  being 138 and was assigned as  $C_3H_6NC_3H_5NCO$ . This is part of the secondary amine from DNI group. Fig.4b showed the TGA/MS result of the model compound, DNI-3A (also see Appendix B for the SRL report). It suggested that the sample be consumed by degradation. The expected product cyclopentadiene was observed at  $220^\circ C$ , which was  $10^\circ C$  below the corresponding data from poly(amic amide)/DNI-3A.

The DSC experiments were run for DNI-3A and PAA/DNI-3A under both ambient and high pressure (750 psi) environments. The DSC result for PAA/DNI-3A systems under ambient pressure condition is shown in Fig.5a. The region between  $200^\circ C$  to  $350^\circ C$  can be interpreted as a composite of an endotherm superposed on an exotherm. The endotherm started at about  $200^\circ C$ . The exotherm started at a higher temperature and showed a peak at about  $280^\circ C$ . At even higher temperature, the exothermic reaction overshadowed the endothermic reaction. The peak at  $343^\circ C$  was the tail section of the exotherm. This interpretation can be substantiated by studying the pressured DSC result shown in Fig.5b. The exotherm is due to the ring closure imidization reaction and the crosslinking reaction of the nadic end groups. The endotherm is from the evolution of cyclopentadiene. Under the pressurized condition, the evolution of cyclopentadiene was suppressed and the DSC

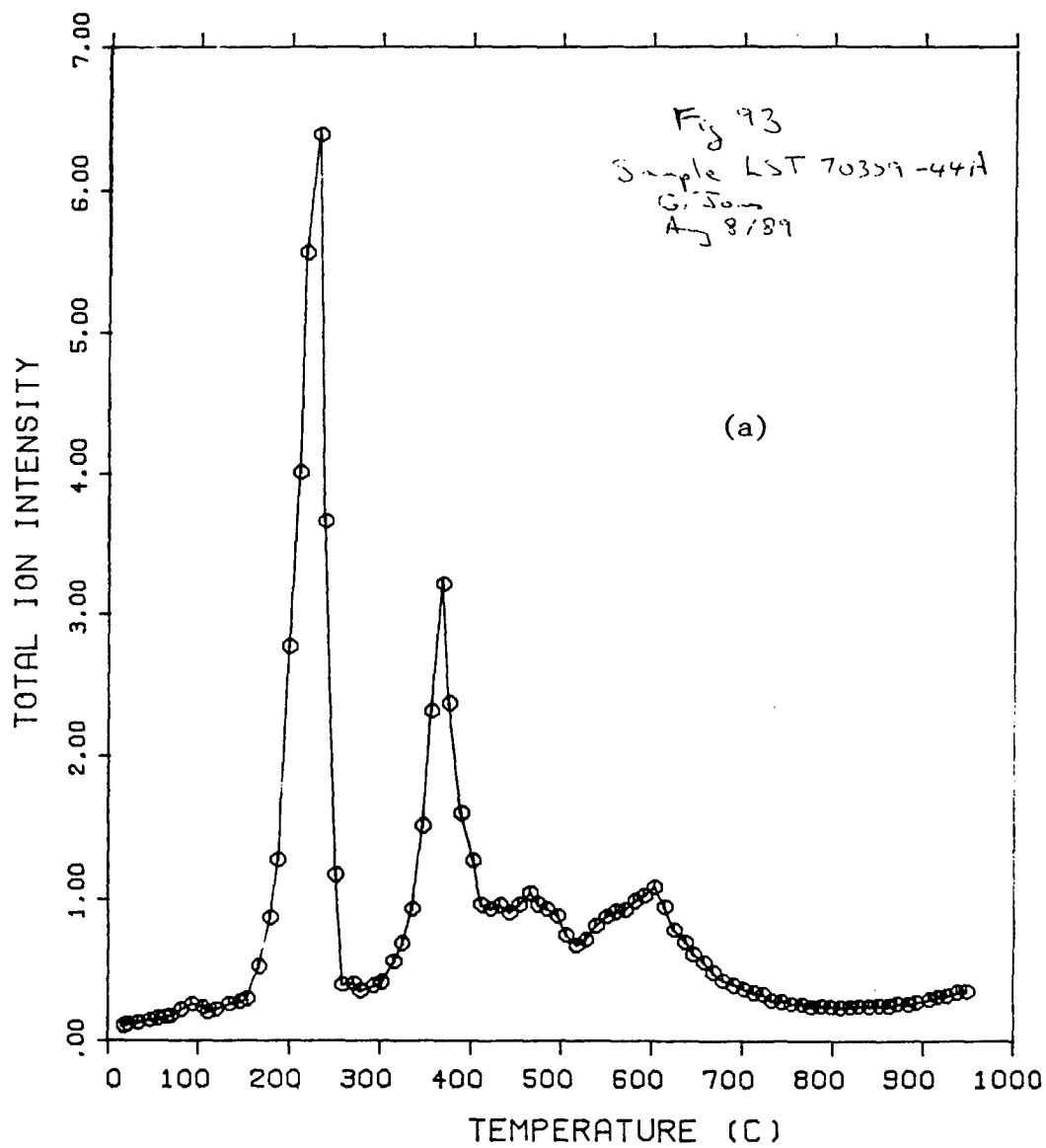


Fig.4. TGA/MS spectra for (a) PAA/DNI-3A, and (b) DNI-3A

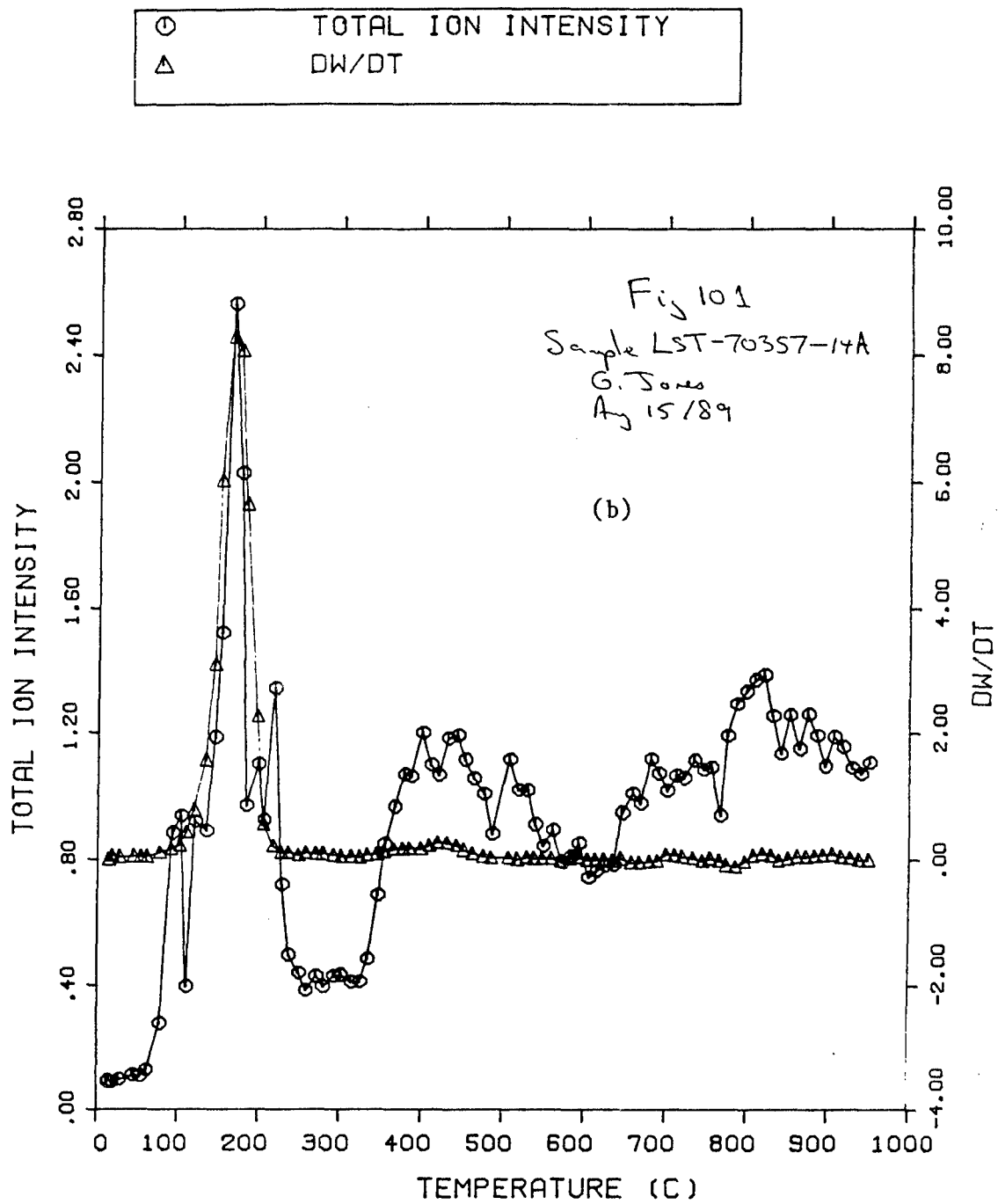


Fig.4. (continued)

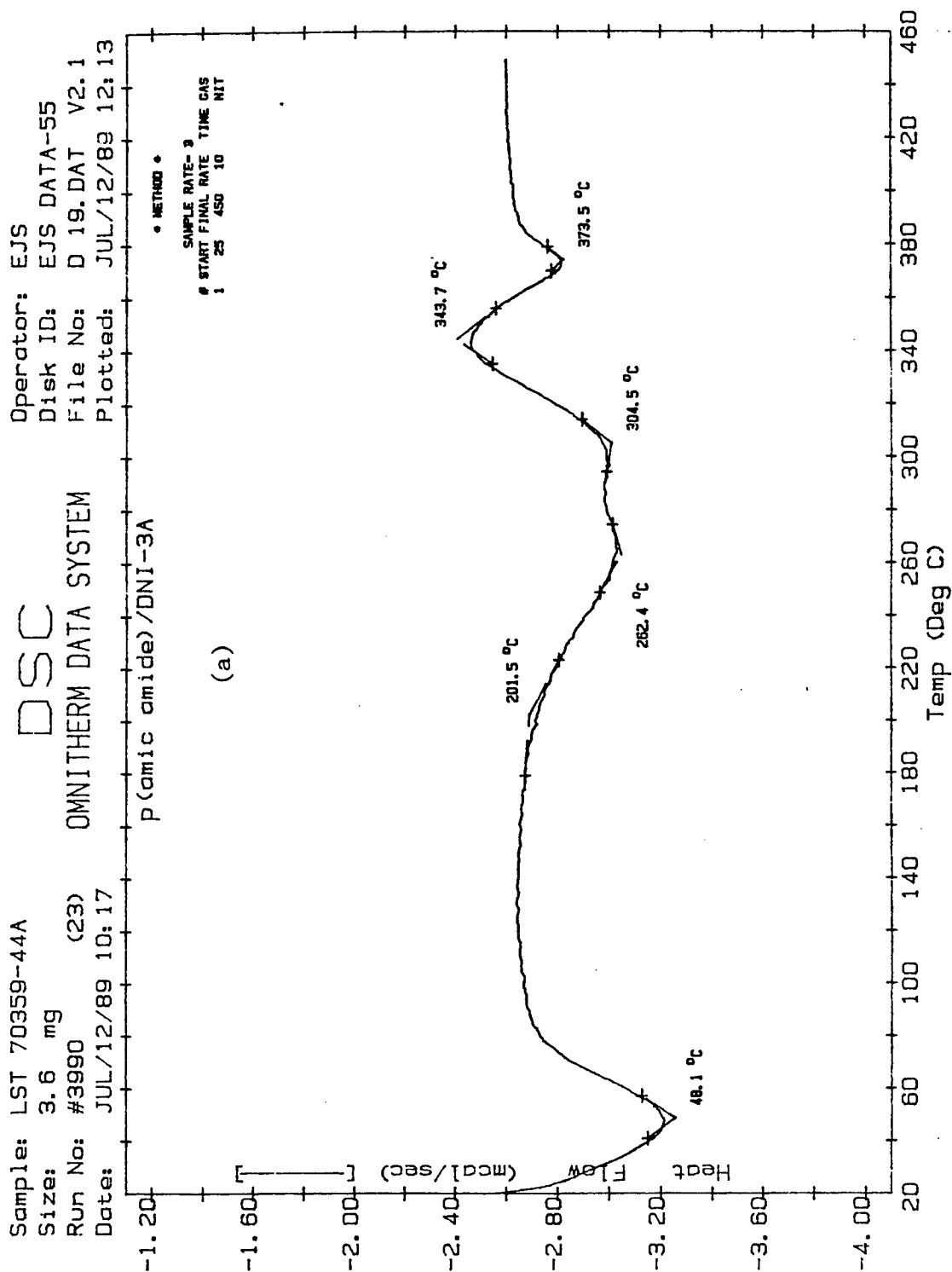


Fig.5. DSC thermogram for PAA/DNI-3A under (a) ambient, and (b) 750psi pressure, and for DNI-3A under (c) ambient, and (d) 750psi pressure

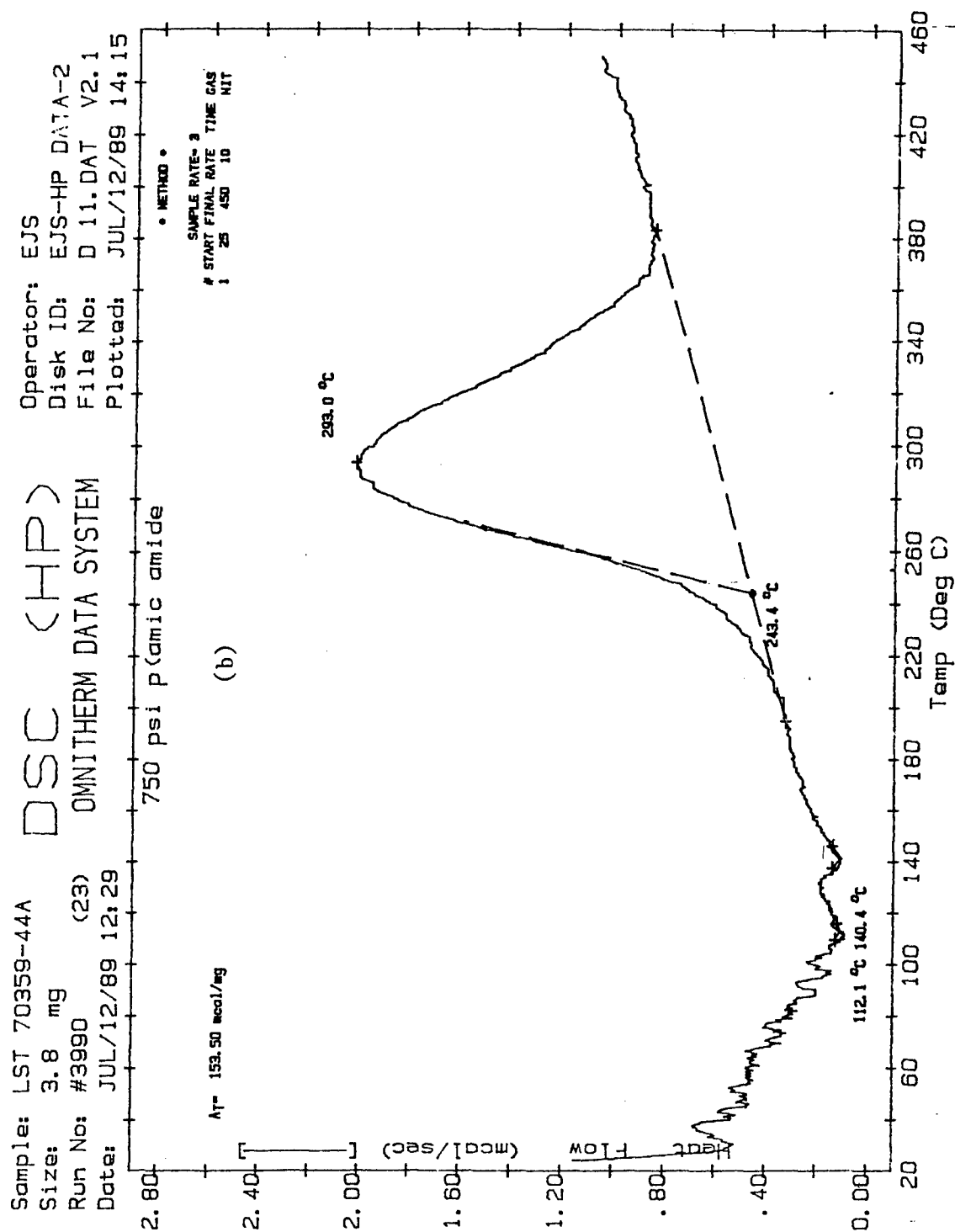


Fig.5. (continued)

showed only the exothermic component. The exotherm showed a well-behaved profile and peaked at  $\sim 290^{\circ}\text{C}$ . The high temperature tail section of the exotherm corresponded nicely with the high temperature peak ( $343^{\circ}\text{C}$ ) shown in Fig.5a.

The DSC result of the model leaving group, DNI-3A, is shown in Figs.5c and 5d. The unpressurized DSC result in Fig.5c shows a melting endotherm at about  $92^{\circ}\text{C}$ . Another endotherm starts at about  $200^{\circ}\text{C}$ . This endotherm is due to the evaporation of the cyclopentadiene which is released from the decomposition of the nadic end group. The decomposed end groups can not crosslink at higher temperature. Thus no appreciable exotherm is shown in Fig.5c. The pressurized DSC in Fig.5d shows a similar melting endotherm at about  $90^{\circ}\text{C}$ . Evolution of cyclopentadiene is suppressed by the pressure. Two exotherms can be detected peaking at  $272^{\circ}\text{C}$  and  $322^{\circ}\text{C}$  respectively. Crosslinking reactions will occur at higher temperature if the cyclopentadiene evolution can be suppressed by external pressure.

## **4.2 FTIR Spectra and Subtraction Results**

FTIR was used to study the imidization kinetics. In this study three different temperatures were chosen for the PAA/DNI-3A film reaction, namely, 240, 260 and  $280^{\circ}\text{C}$ . The typical FTIR results were shown in Figs.6a to 6c. The detail spectra for the polymers during the imidization were shown in Appendix C. The spectra changes were enhanced by subtracting the spectrum at  $t=0$  from the spectrum collected at different times. The base line was offset by an arbitrary unit to display the negative side of the subtraction. The typical subtraction results were shown in Figs.6d and 6e. The details of the resultant charts from subtraction are shown in Appendix D.

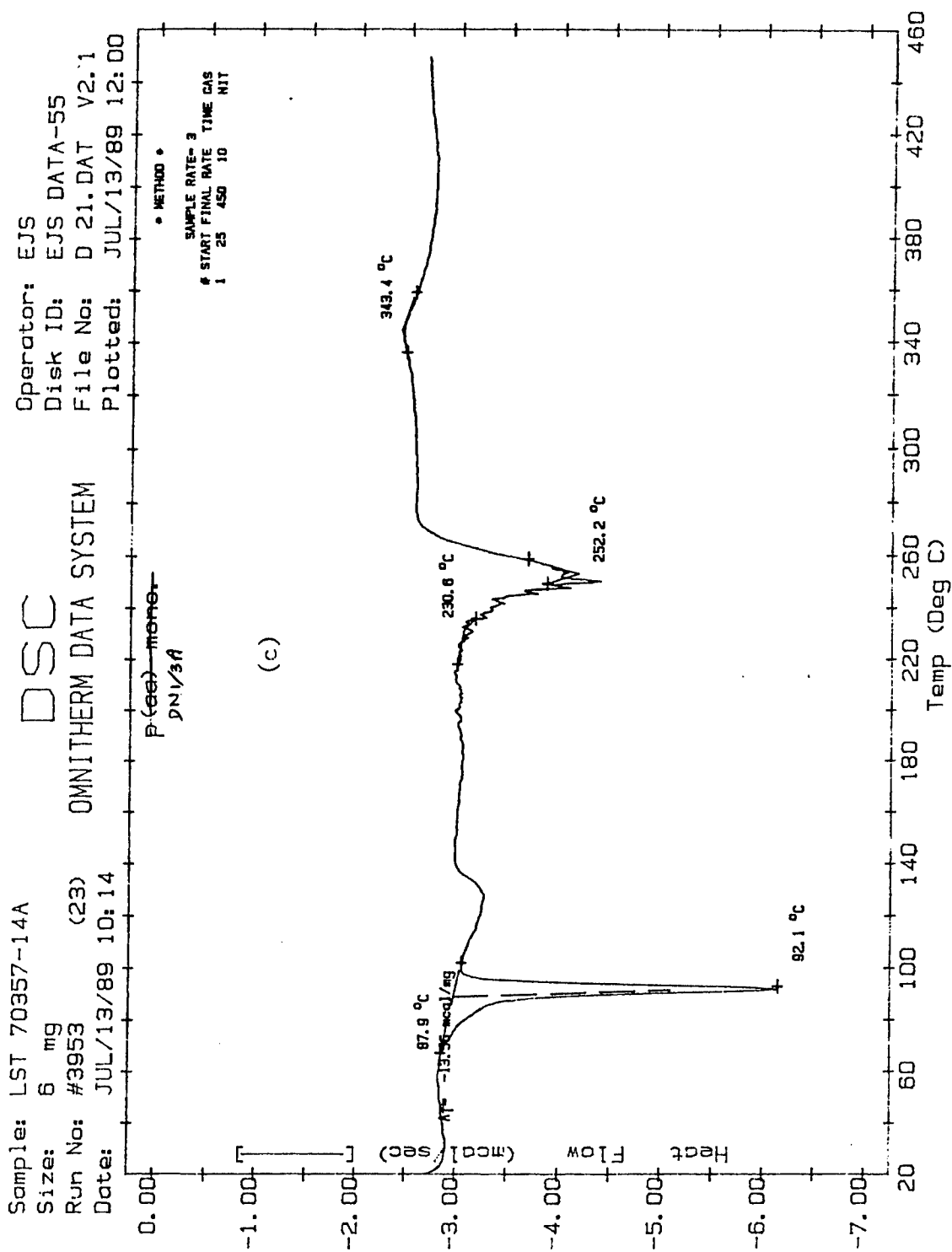


Fig.5. (continued)

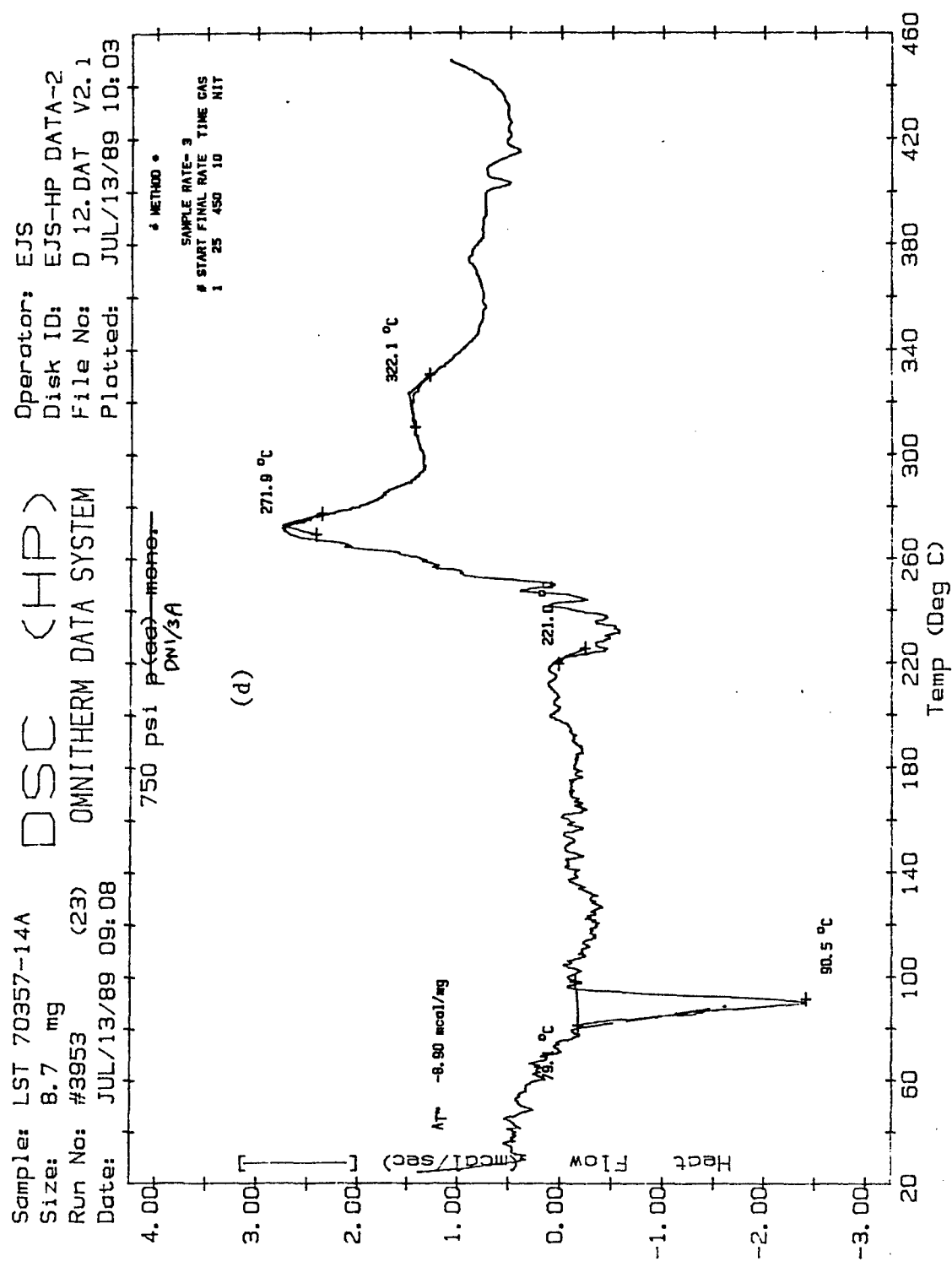


Fig.5. (continued)



# BECKMAN

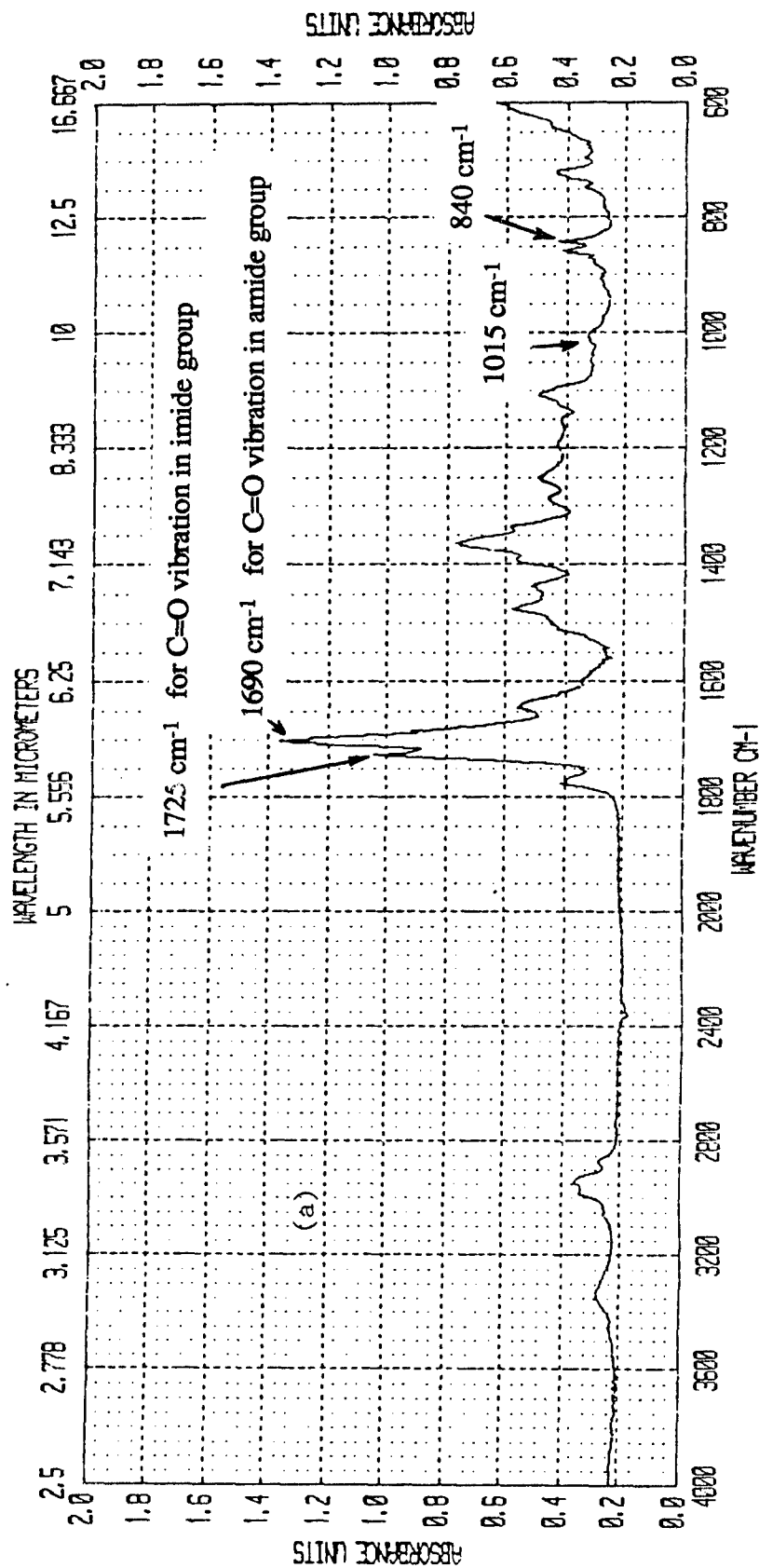


Fig. 6. FTIR absorbance for PAA/DNI-3A at (a) 240°C, t=20 min, (b) 260°C, t=10 min, and (c) 280°C, t=10 min, respectively, and the subtraction results for (d)  $[A(t=5\text{min})-A(0)]$ , and (e)  $[A(t=180\text{min})-A(0)]$  at 280°C

BECKMAN

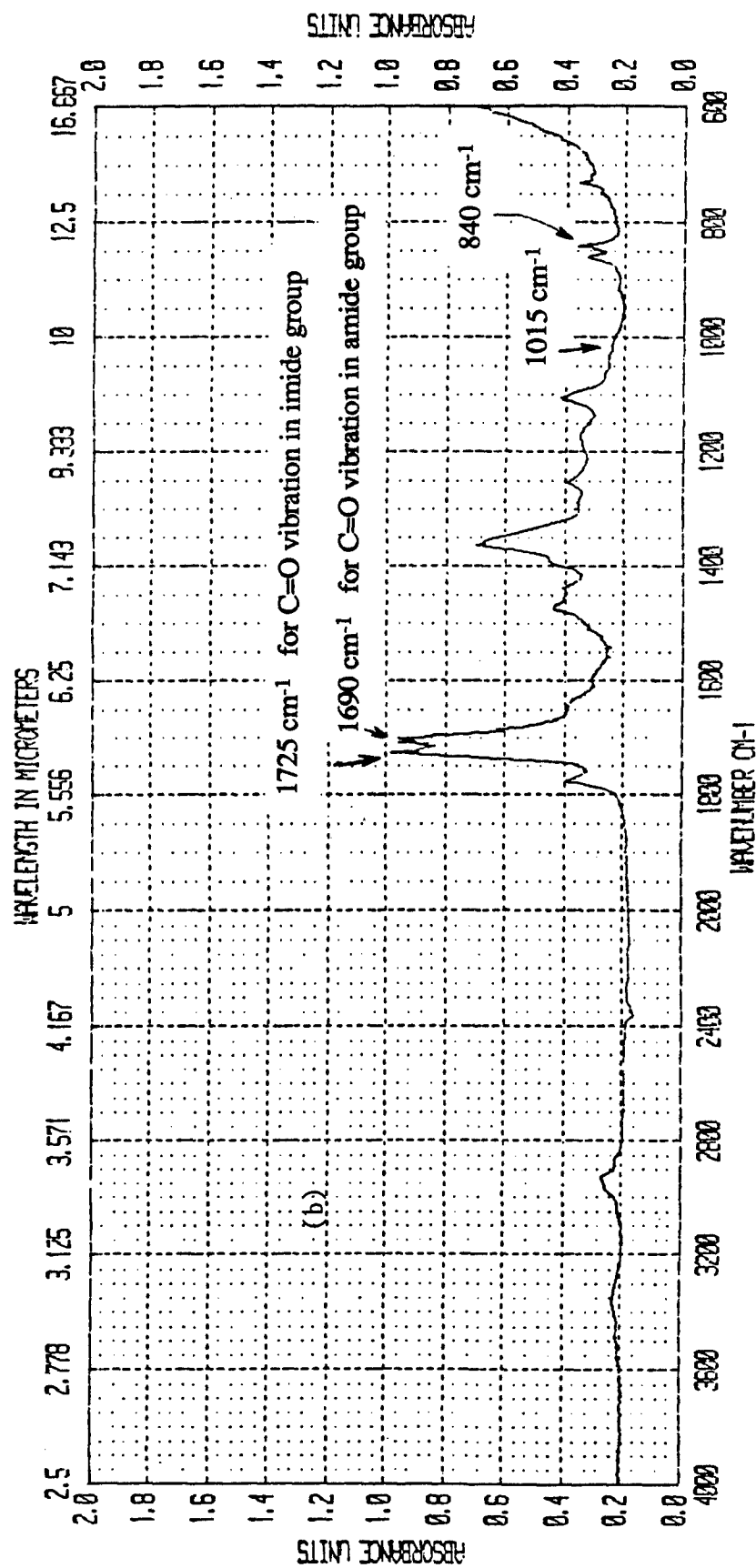


Fig. 6. (continued)

# BECKMAN

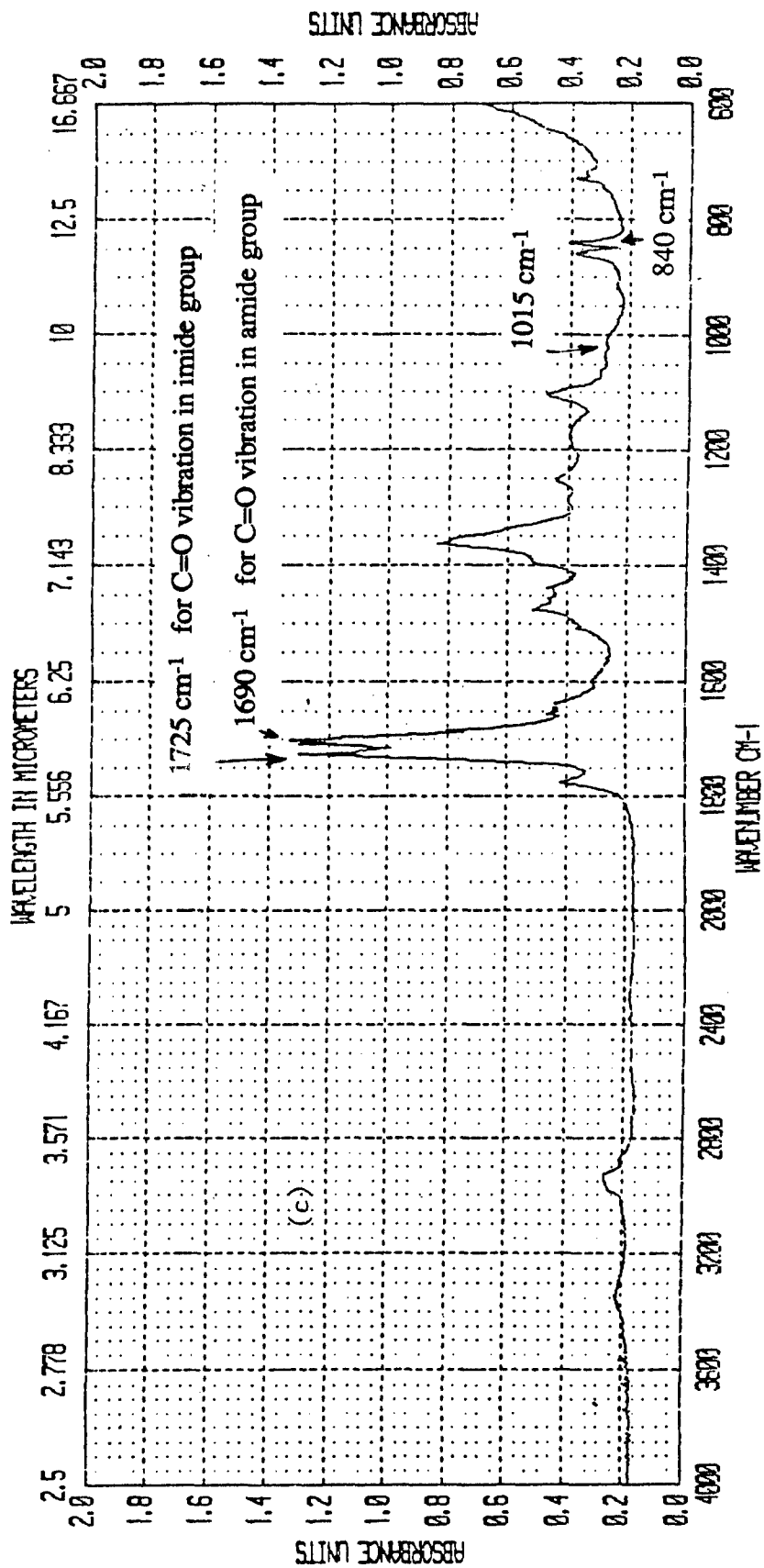


Fig.6. (continued)

# BECKMAN

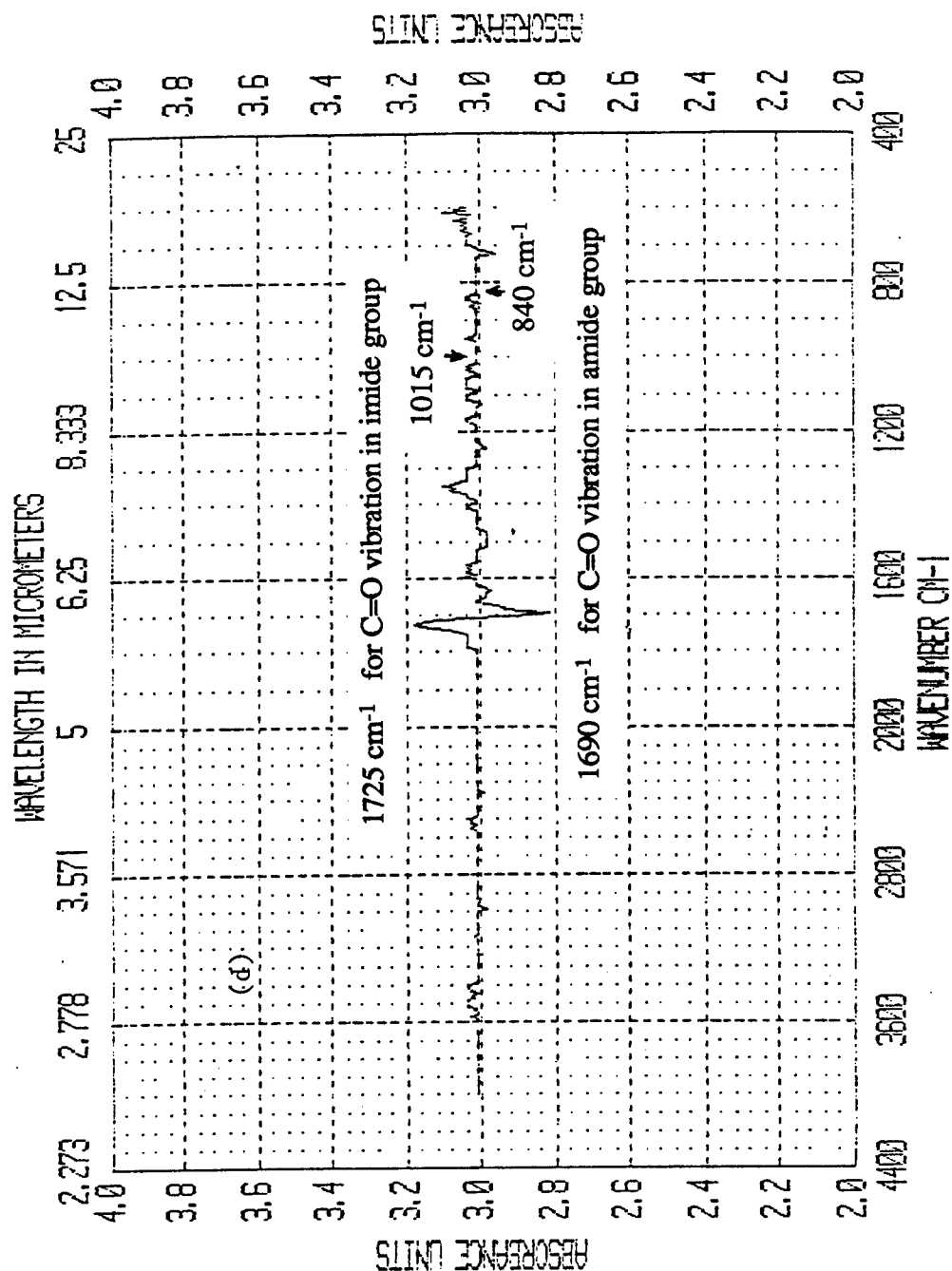


Fig.6. (continued)

# BECKMAN

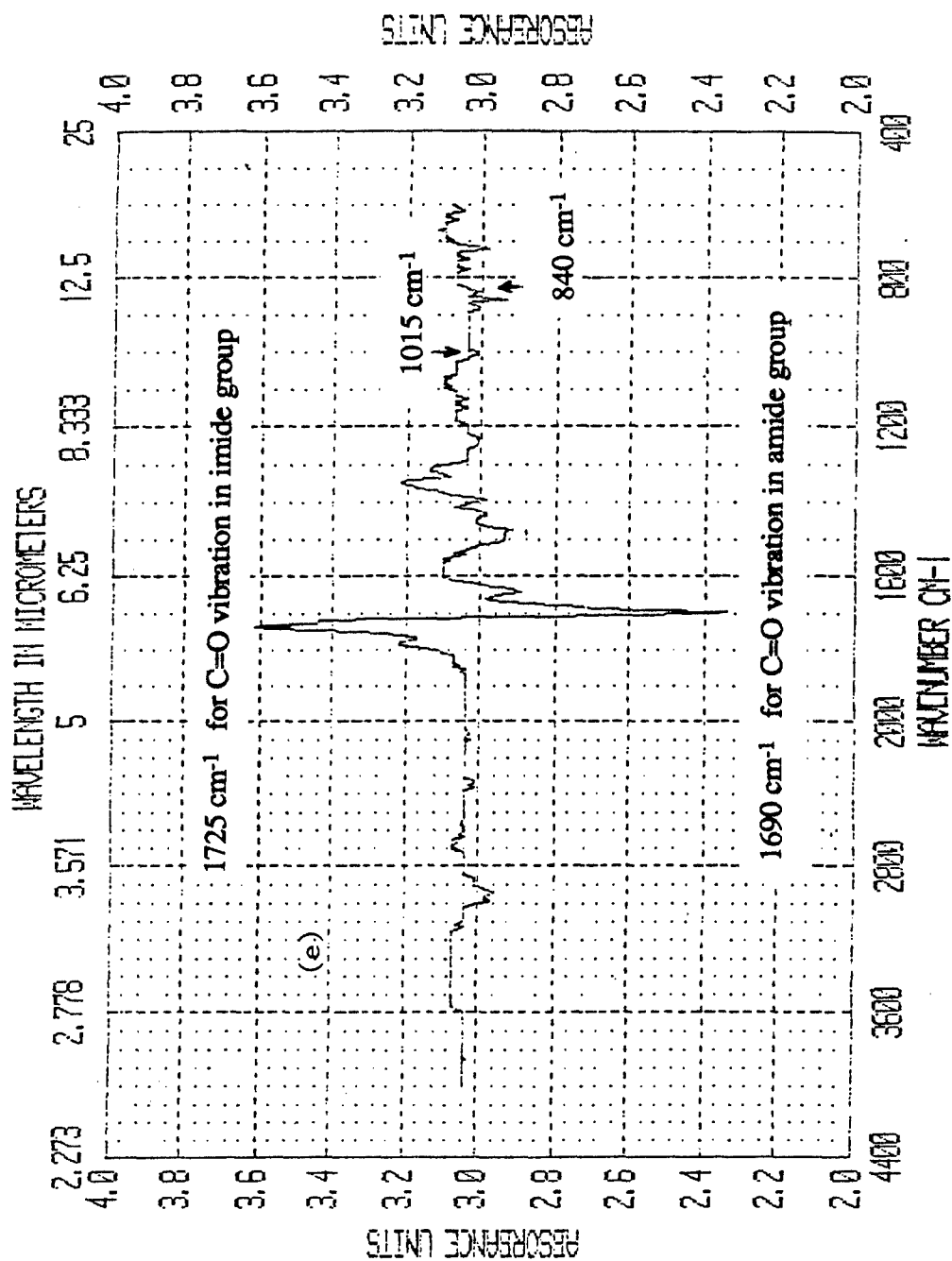


Fig.6. (continued)

In comparing the FTIR spectra from different samples, one should notice the thickness effect since different thickness cause different amount of peak intensity. From the literature the internal reference is chosen at  $840\text{ cm}^{-1}$  (C-H out-of-plane bending from p-substituted benzene) [22] or  $1015\text{ cm}^{-1}$  (C-H in-plane bending from p-substituted benzene) peak [23,24]. In this report the  $1015\text{ cm}^{-1}$  was chosen. (Indeed, both bands do not change much). With this reference peak the relative thickness was calibrated and the correct peak intensity was obtained.

#### 4.3 FTIR Absorption Bands for PAA/DNI-3A and Polyimide

The characteristic bands of amide or imide is from its carbonyl vibration. The band at  $1690\text{ cm}^{-1}$  was assigned as the stretching vibration of the secondary amide. The  $1640\text{ cm}^{-1}$  peak is assigned to the tertiary amide. For imide, the peaks assigned are  $1775$  ( $1780$ ),  $1725$ ,  $1350$  ( $1370$ ), and  $735$  ( $720$ )  $\text{cm}^{-1}$  [9,12,13,17,18,22-29] (see Table 2.) The increasing or decreasing of the aforementioned peaks during imidization was observed. But not every peaks can be quantitatively characterized due to the noise in the data. The most significant changes of the peaks are those of  $1690$  and  $1725\text{ cm}^{-1}$ . The former one is an amide peak along the unreacted backbone while the latter one is associated with the resultant imide [30]

The comparison of the normalized data from increasing intensity of  $1725\text{ cm}^{-1}$  peak with that from the decreasing intensity of  $1690\text{ cm}^{-1}$  peak at  $280^{\circ}\text{C}$  is shown in Fig.7a. The good agreement between the increase of  $1725\text{ cm}^{-1}$  peak and the decrease of  $1690\text{ cm}^{-1}$  peak at  $280^{\circ}\text{C}$  suggested that there is no intermediate formed during the amide-imide conversion. Similar plots for  $260^{\circ}\text{C}$  and  $240^{\circ}\text{C}$  experiments are shown in Figs. 7b and 7c. The agreement between these two peaks were not that good at  $240^{\circ}\text{C}$  due to the noise effect on the relative small value of the denominator  $\Delta A(0,\tau)$ . But they are still in the same range

Table 2. The assigned imide peaks in the literature

Ref.No.	Absorption Peaks (cm <sup>-1</sup> )
9.	720*,1725, 1780 (* used for kinetics, ref. 995 for Aromatic ring vibration)
12.	725
13.	1380*, 1780 (recommended)
17.	1780
18.	725 (ref 1480 for aromatic structure)
22.	720, 1370, 1720, 1780 (ref. 820 for C-H)
23.	1720,1780 (ref.1012)
24.	725, 1380 (ref 1015 for aromatic ring vibr.)
25.	1380, 1780
26.	1380,1720,1780
27.	730, 1370*, 1780 (* recommended)
28.	700, 1776
29.	725, 1778 (ref 1480 for aromatic structure)

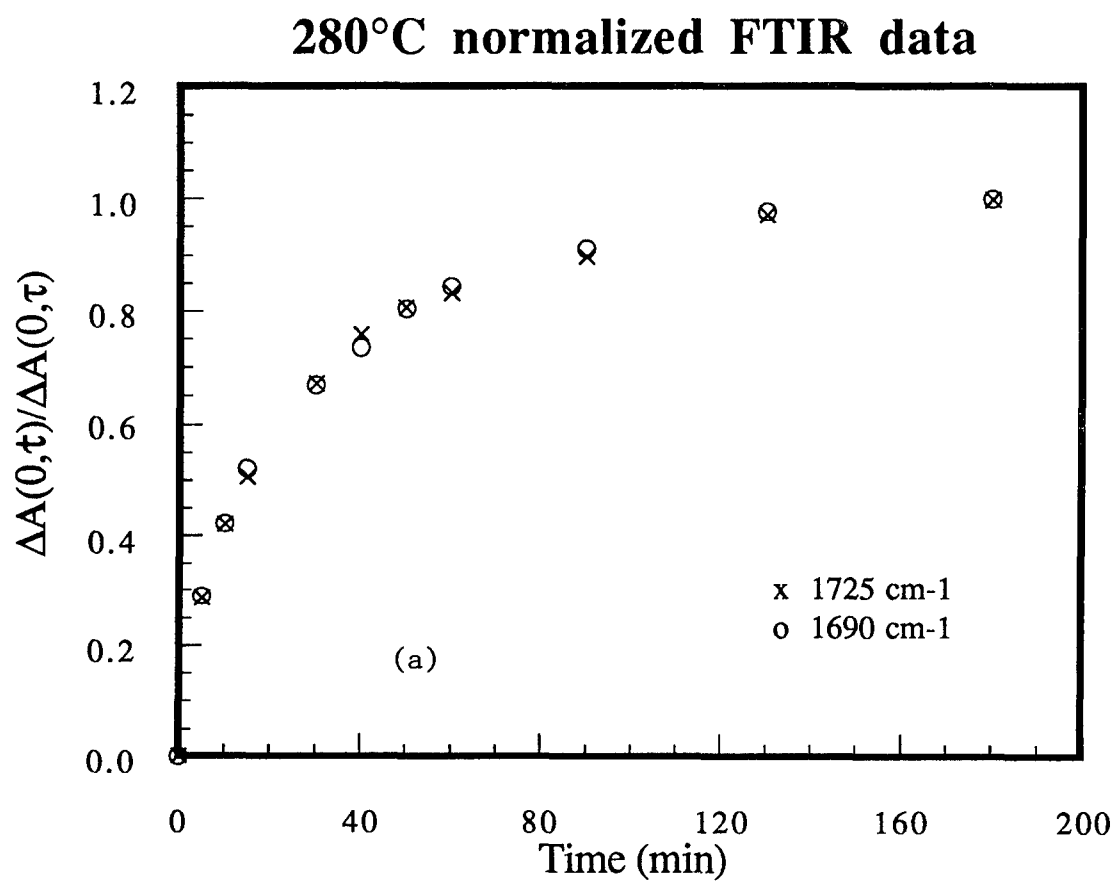


Fig.7. Normalized absorption at increasing peak 1725 cm<sup>-1</sup> and decreasing peak 1690 cm<sup>-1</sup> for PAA/DNI-3A during imidization at (a) 280°C, (b) 260°C, and (c) 240°C



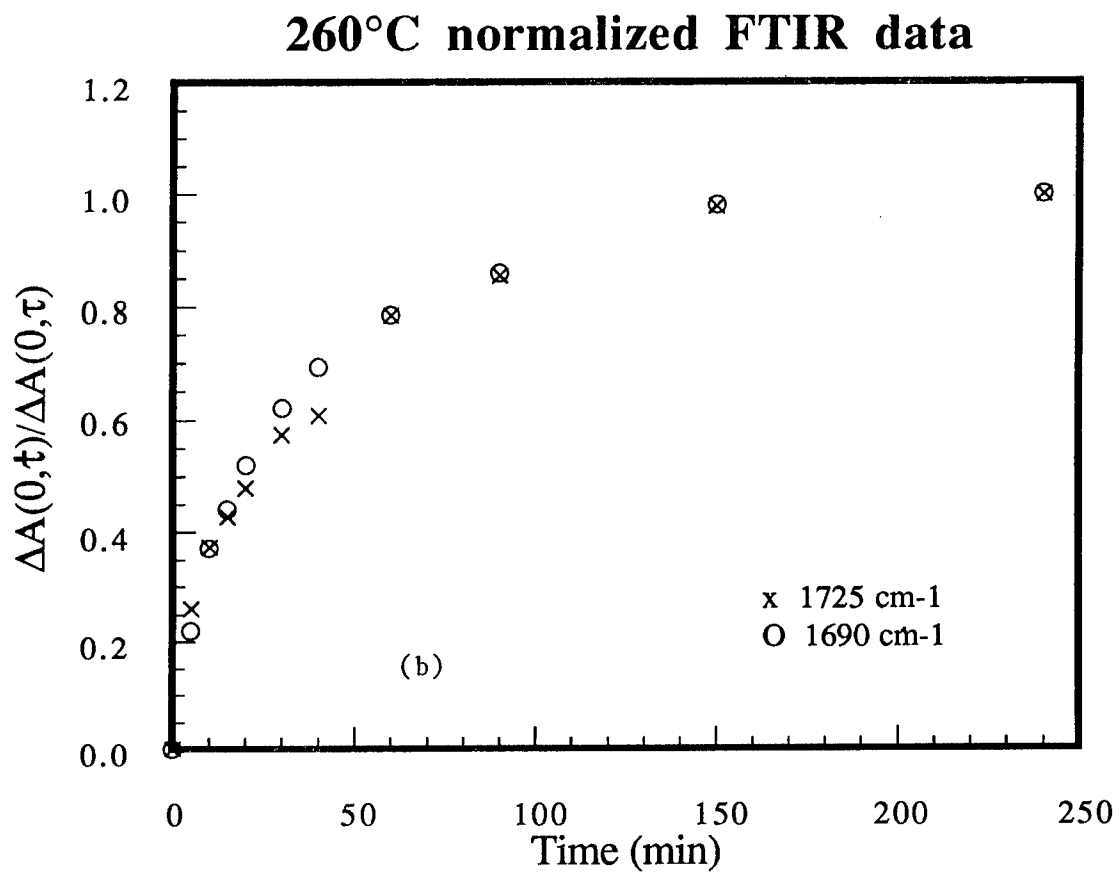


Fig.7. (continued)

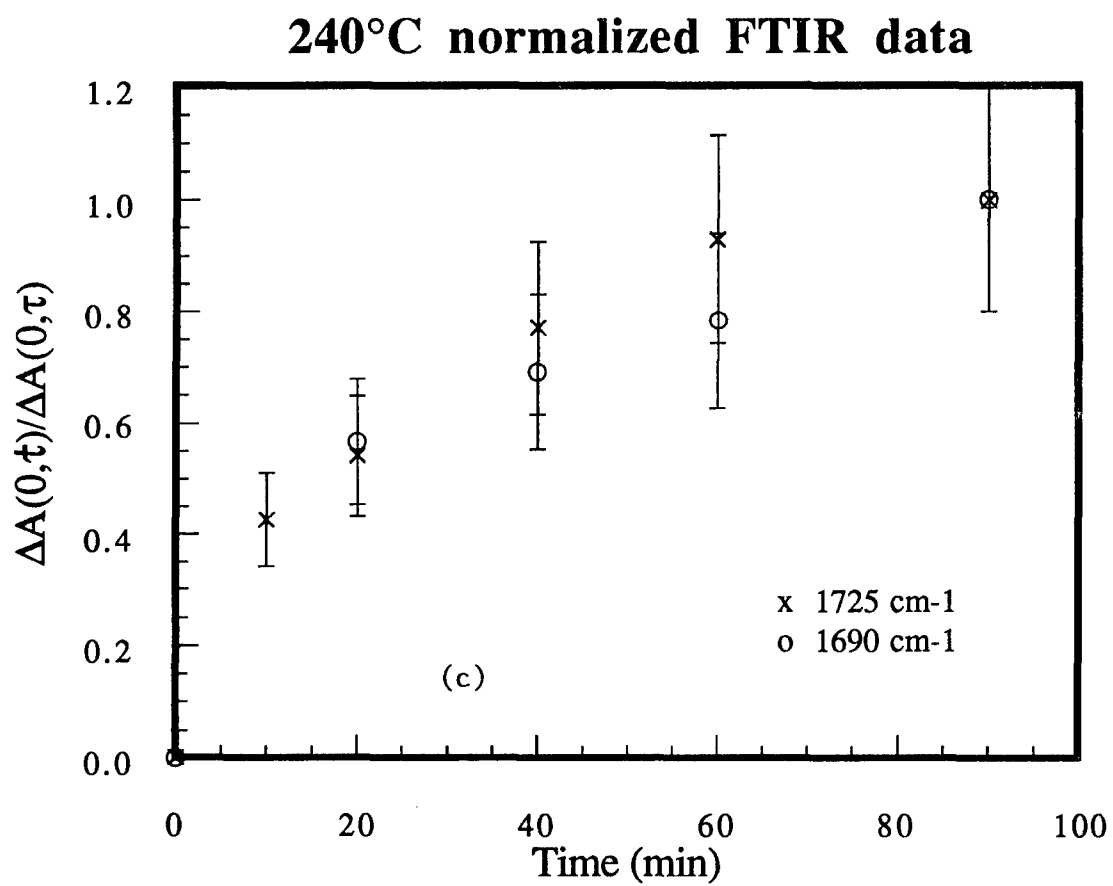


Fig.7. (continued)

after the error from noise ( $\pm 20\%$ ) is taken into account. It is worth noting that the imidization at these two temperatures for 4 hours is not complete.

#### 4.4. $([C]_t - [C]_\tau) / ([C]_0 - [C]_\tau)$ Concentration Ratio Analysis and Kinetic Parameters

As explained in Section 3.3, the kinetic data can be characterized by equations (6) or (7). At  $280^\circ\text{C}$  let  $\tau = 180$  minutes. It was noticed that the imidization is very close to completion at  $280^\circ\text{C}$  for 180 minutes (this point will be verified in Section 4.5), i.e.,  $A(180 \text{ min}) \sim A(\infty)$  at  $280^\circ\text{C}$ . From Beer's Law, the path-independent characteristic absorbance of any moieties for different specimen at any temperature  $T$  can be represented by the following equation:

$$\begin{aligned} \Delta A(0, \infty)_{280^\circ\text{C}} / b_{280^\circ\text{C}} &= \Delta A(0, \infty)_T / b_T \\ \text{or} \quad \Delta A(0, \infty)_T &= \Delta A(0, \infty)_{280^\circ\text{C}} * b_T / b_{280^\circ\text{C}} \end{aligned} \quad (12)$$

where  $\Delta A(0, \infty)_{280^\circ\text{C}}$  is  $A(0) - A(\infty)$  at  $280^\circ\text{C}$ . The path (or thickness) ratio,  $b_T / b_{280^\circ\text{C}}$ , can be calibrated by the absorbance of the internal reference peak at  $1015 \text{ cm}^{-1}$ . [Note: This peak was not very obvious in the absorption spectrum, but can be readily detected in the computer "pick-peak" option.] In equation (12) the notation  $\infty$  can be interchanged with time  $\tau$  without losing any generality. This equation provides an easy way to calculate the corresponding value of  $\Delta A(0, \infty)_T$  for different specimen at temperature  $T$ . The function  $\ln\{([C]_t - [C]_\tau) / ([C]_0 - [C]_\tau)\}$  (or  $\ln\{[A(t) - A(\tau)] / \Delta A(0, \infty)_T\}$  with the understanding that  $\Delta A(0, \infty)_T$  comes from equation (12)) were plotted verse time. The results were shown in Figs.8a-8c for  $1725 \text{ cm}^{-1}$  and Figs.8d-8f for  $1690 \text{ cm}^{-1}$  at different temperatures. From the plots it is observed that there are two first order stages during the whole reaction process. The slopes of the curves, which were the  $(-k)$  values at that temperature, were calculated by the least square method. These  $k$  values are listed in Table 3.

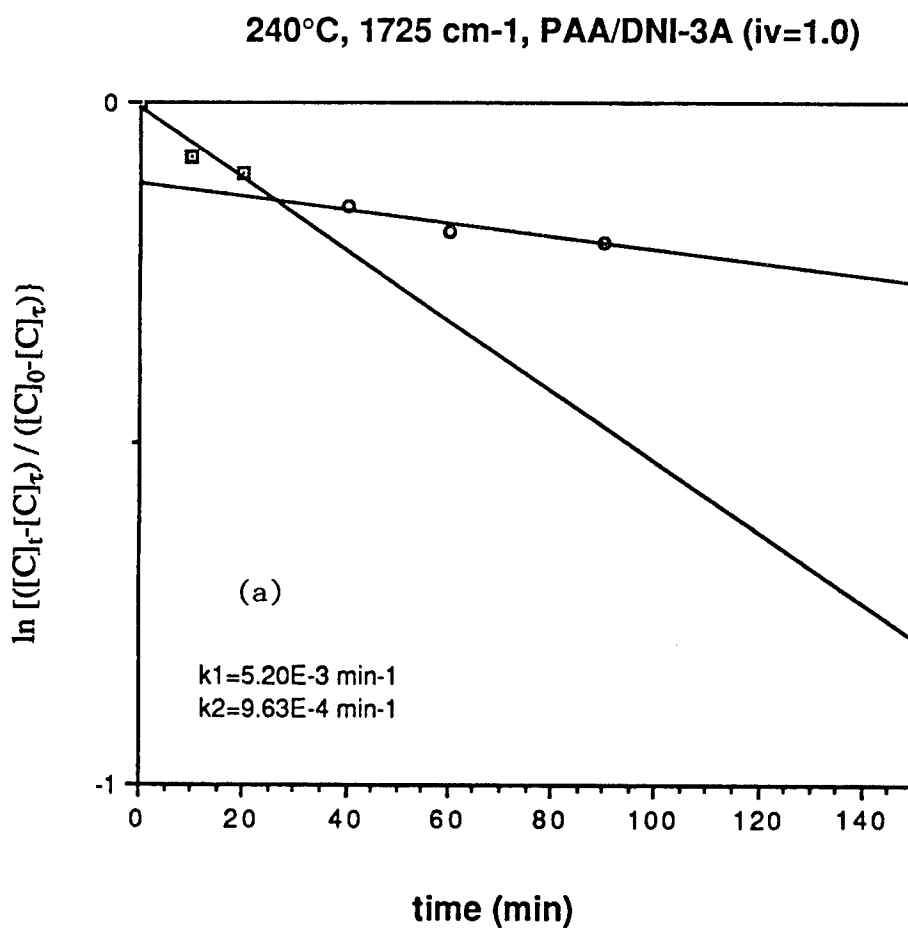


Fig. 8.  $\ln [(C)_t - (C)_e] / [(C)_0 - (C)_e]$  versus time for PAA/DNI-3A at 1725 cm<sup>-1</sup> at (a) 240°C, (b) 260°C, and (c) 280°C, and at 1690 cm<sup>-1</sup> at (d) 240°C, (e) 260°C, and (f) 280°C

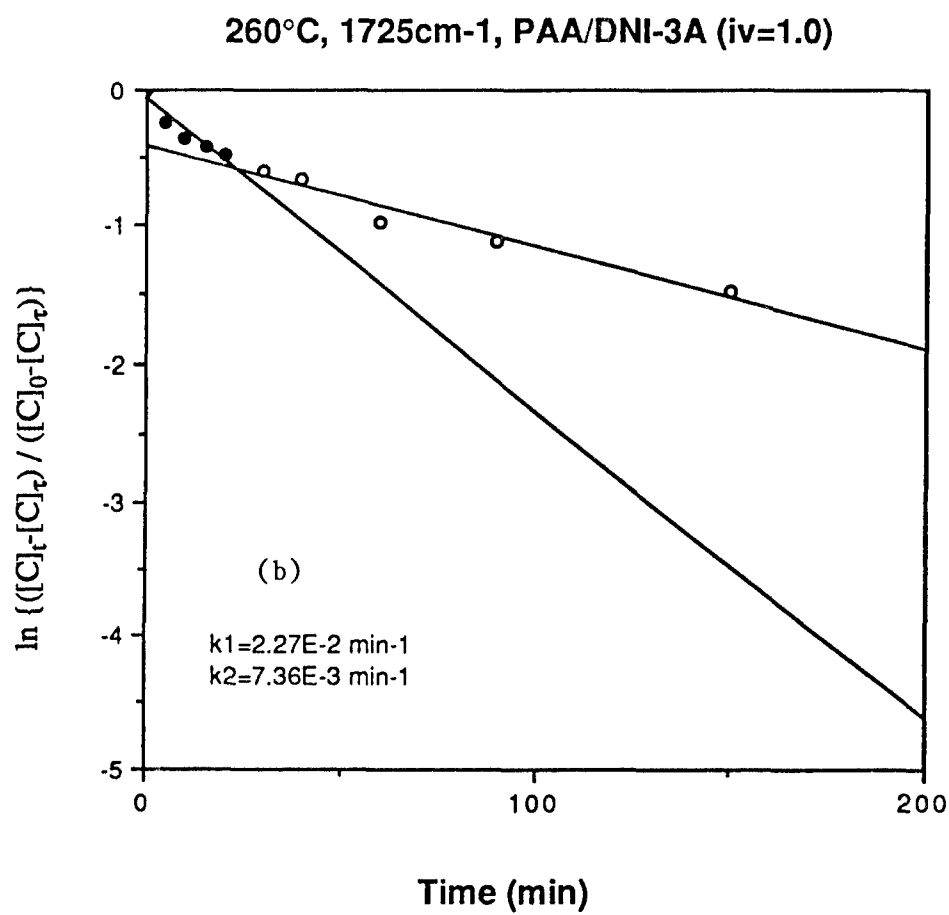


Fig.8. (continued)

280°C, 1725 cm<sup>-1</sup>, PAA/DNI-3A (iv=1.0)

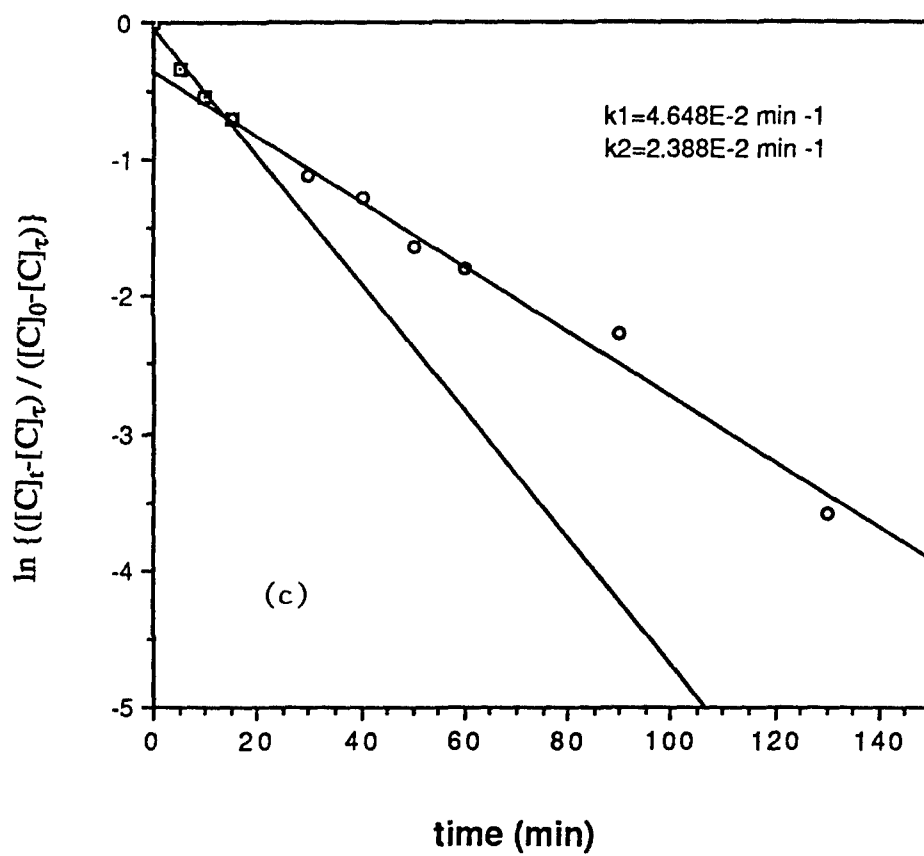


Fig.8. (continued)

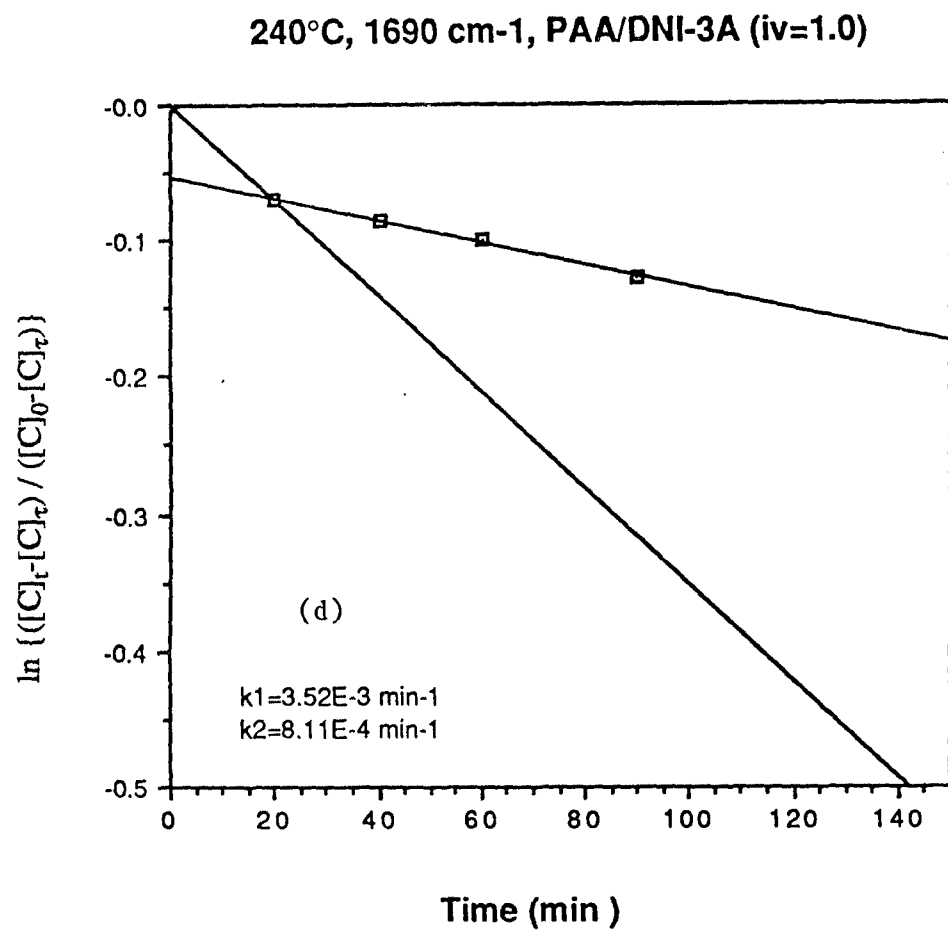


Fig.8. (continued)

260°C, 1690 cm<sup>-1</sup>, PAA/DNI-3A (iv=1.0)

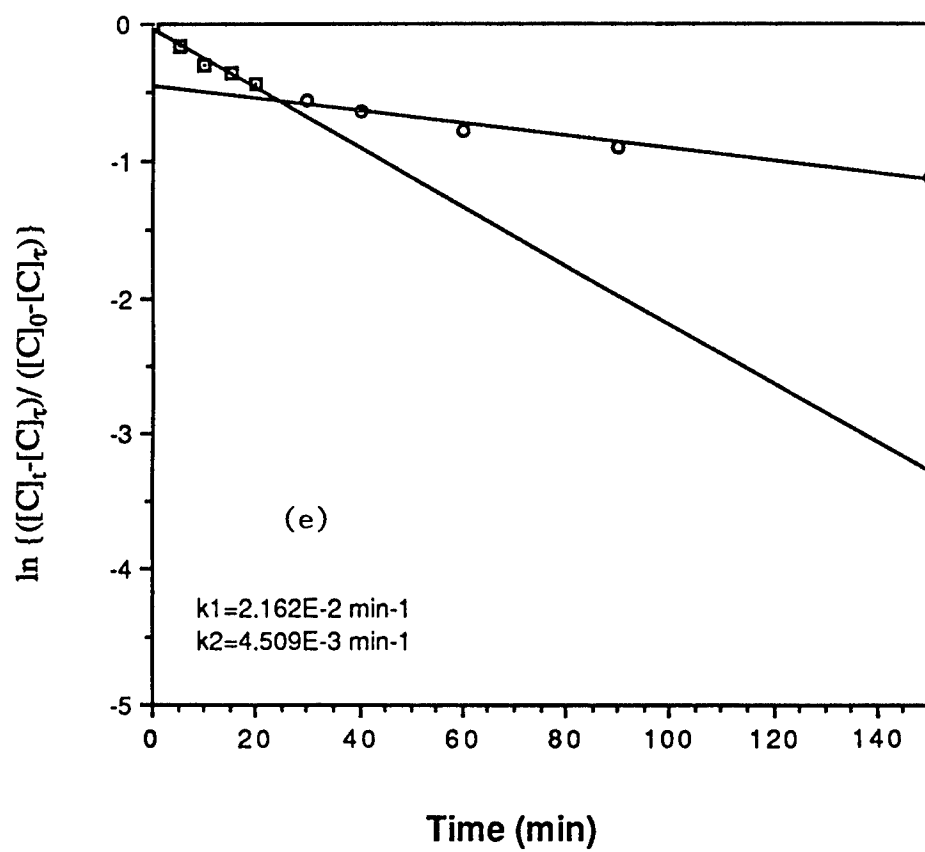


Fig.8. (continued)



280°C, 1690 cm<sup>-1</sup>, PAA/DNI-3A (iv=1.0)

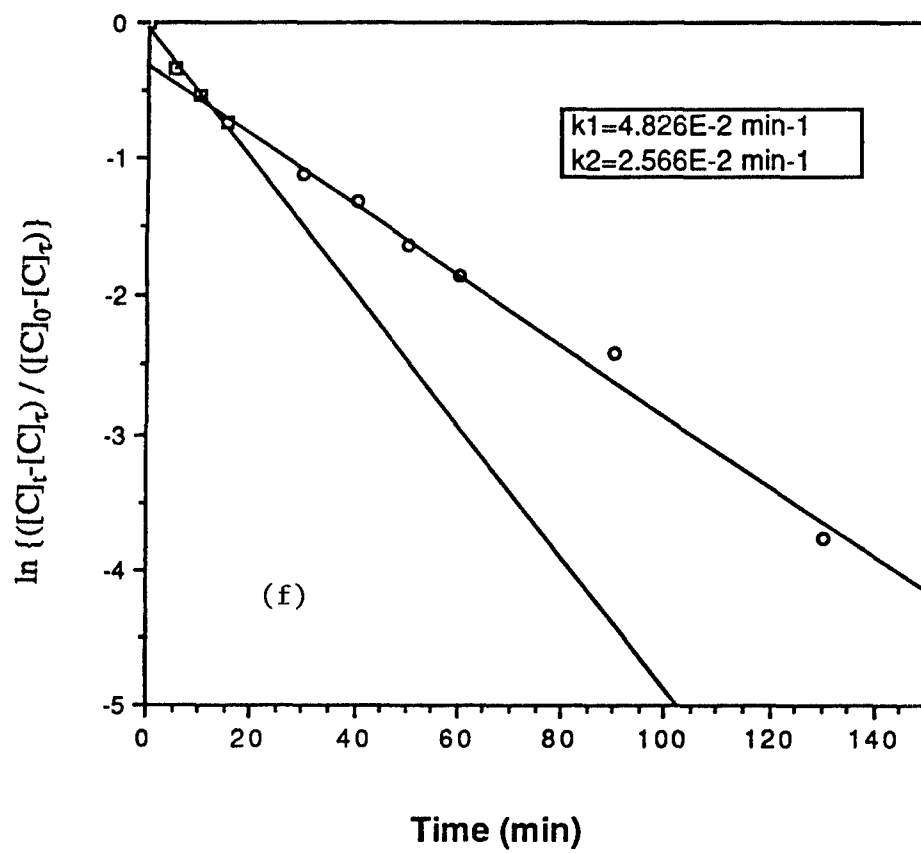


Fig.8. (continued)

Table 3. The kinetic parameters of imidization from

$([C]_t - [C]_\tau) / ([C]_0 - [C]_\tau)$  data

(a) at 1725  $\text{cm}^{-1}$

$k_1$ ( $\text{min}^{-1}$ )			$k_2$ ( $\text{min}^{-1}$ )		
280°C	260°C	240°C	280°C	260°C	240°C
4.684E-2	2.27E-2	5.20E-3	2.388E-2	7.36E-3	9.63E-4

(b) at 1690  $\text{cm}^{-1}$

$k_1$ ( $\text{min}^{-1}$ )			$k_2$ ( $\text{min}^{-1}$ )		
280°C	260°C	240°C	280°C	260°C	240°C
4.826E-2	2.162E-2	3.52E-3	2.566E-2	4.51E-3	8.11E-4

#### 4.5 $\Delta A$ Absorbance Difference Analysis and Kinetic Parameters

The above analysis based on concentration ratio data,  $([C]_t - [C]_\tau)/([C]_0 - [C]_\tau)$ , is subject to error in calculating the kinetic data  $k$  values because of the possible non-zero value of  $[C]_\tau$  as mentioned in Section 3.3. The data were following the absorbance difference,  $\Delta A$ , analysis mentioned in Section 3.4. Since the initial data set was not in equally spaced time basis, the interpolation of the data is required. There are two ways to interpolate the data, direct and indirect. The direct interpolation simply was done from the original data set while the indirect way would be done after some massage of the original data. It is noted that the raw data shown in Figs.8a-f are not smoothly distributed. When the equally spaced time data were directly interpolated from these scattered data, the logarithm of the difference,  $\ln[\Delta A(t_1, t_2)]$ , for each pair of data will become very scattering. Significant error will be generated by this way of data treatment. It is this sensitivity that the indirect way, the least-square-fitted curves in Figs.8a-f, were used to interpolate the equally spaced time data for the  $\Delta A/[A(\tau) - A(0)]$  readings. The  $\Delta A$  data were then obtained by multiplying  $[A(\tau) - A(0)]$  with the interpolation values. After this conversion the  $\Delta A$  values really represent the true difference between any two different times no matter how the  $([C]_t - [C]_\tau)/([C]_0 - [C]_\tau)$  data were distorted from the true first-order one by the non-zero  $[C]_\tau$  value since the  $([C]_0 - [C]_\tau)$  values do not play any role in the  $\Delta A$  terms. In principle, this is just the interpolation of  $[C]_t$  or  $A(c, t)$  value, nothing to do with  $[C]_\tau$  value. Recall that, from Section 3.4,

$$\begin{aligned} \ln \Delta A(t_1, t_2) &= \ln k' - kt_1 + \ln \{1 - e^{-k(t_1 - t_2)}\} \\ &= k'' - kt_1 \end{aligned} \quad (11)$$

The  $\Delta t = t_1 - t_2 = 5$  minute in the fast reaction period and  $\Delta t = t_1 - t_2 = 10$  minutes in the slow reaction period were then taken for  $\Delta A$  readings. The results of  $[\ln \Delta A]$  verse  $t_1$ , based on

equation (11), were plotted and shown in Figs.9a-9c for  $1725\text{ cm}^{-1}$  and Figs.9d-9f for  $1690\text{ cm}^{-1}$  band. From each curves the slopes, i.e., the  $(-k)$  values, was computed by the least square method. The resultant  $k$  values are listed in Table 4.

From this Table it is clear that the corresponding  $k$  values derived from the concentration ratio,  $([C]_t - [C]_\tau) / ([C]_0 - [C]_\tau)$ , method and from fixed-time-interval data,  $\Delta A$ , method are very close (within 2%). This implies that the  $\tau (=180\text{ min}) \sim \infty$  assumption is reasonable and that  $[C]_\tau$  is indeed close to zero. Besides, by using the  $k$  values obtained from  $280^\circ\text{C}$  to back calculate the degree of conversion,  $[C]_{\tau=180\text{ min}}$  is only 1% of  $[C]_0$ . (Please note that this value is calculated from the  $1725\text{ cm}^{-1}$  data. If the calculation is based on the  $1690\text{ cm}^{-1}$  data,  $[C]_{\tau=180\text{ min}}$  is about 0.8% of  $[C]_0$ . In doing such calculation, the transition from  $k_1$  to  $k_2$  is set at time equal to 12 minutes as shown in Figs. 8 and 13.) Using the  $1725\text{ cm}^{-1}$  data and the same calculation techniques, the corresponding time for the residue concentration,  $[C]_t$ , to reach 1% of  $[C]_0$  is about 20 hours at  $260^\circ\text{C}$  and 80 hours at  $240^\circ\text{C}$ , respectively.

From the  $k$  values at different temperatures the Arrhenius plot can be employed to compute the activation energy and pre-exponent constant. Figs.10a and 10b and Table 4 show the results. It is noticed from the results that the activation energy is about  $34 \pm 3$  Kcal/mole for the fast reaction and  $48 \pm 2$  Kcal/mole for the slow reaction. Compared to the data from literature, the two values of activation energy are much higher, and the overall reaction constant,  $k$ , at the same temperature are quite different. However, the literature data are mostly the ring closure of amic ester while the reaction being studied in this report was amic amide.

A comparison of the  $k$  values for slow reactions between the current PAA/DNI-3A system and the PMR-15 system is given in Fig.11. Although the fast reaction constants were not

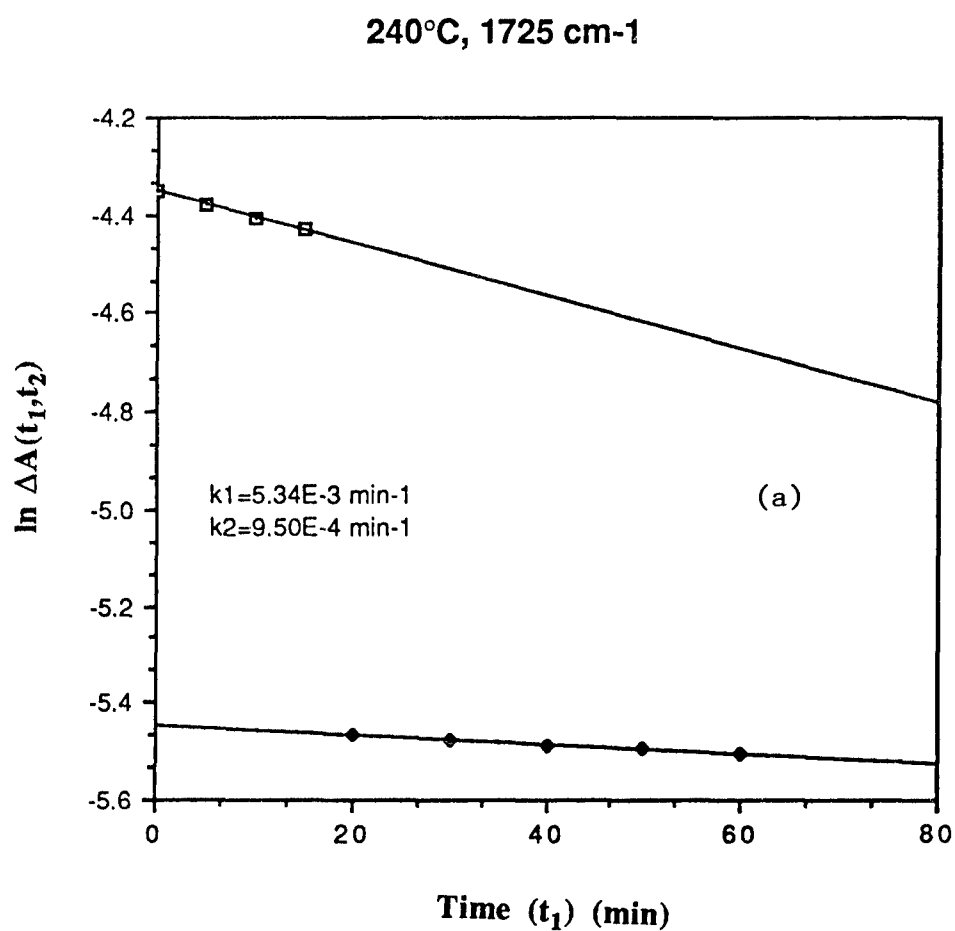


Fig.9. ln  $\Delta A$  versus time for PAA/DNI-3A at 1725 cm<sup>-1</sup> at (a) 240°C, (b) 260°C, and (c) 280°C, and at 1690 cm<sup>-1</sup> at (d) 240°C, (e) 260°C, and (f) 280°C

260°C, 1725cm<sup>-1</sup>

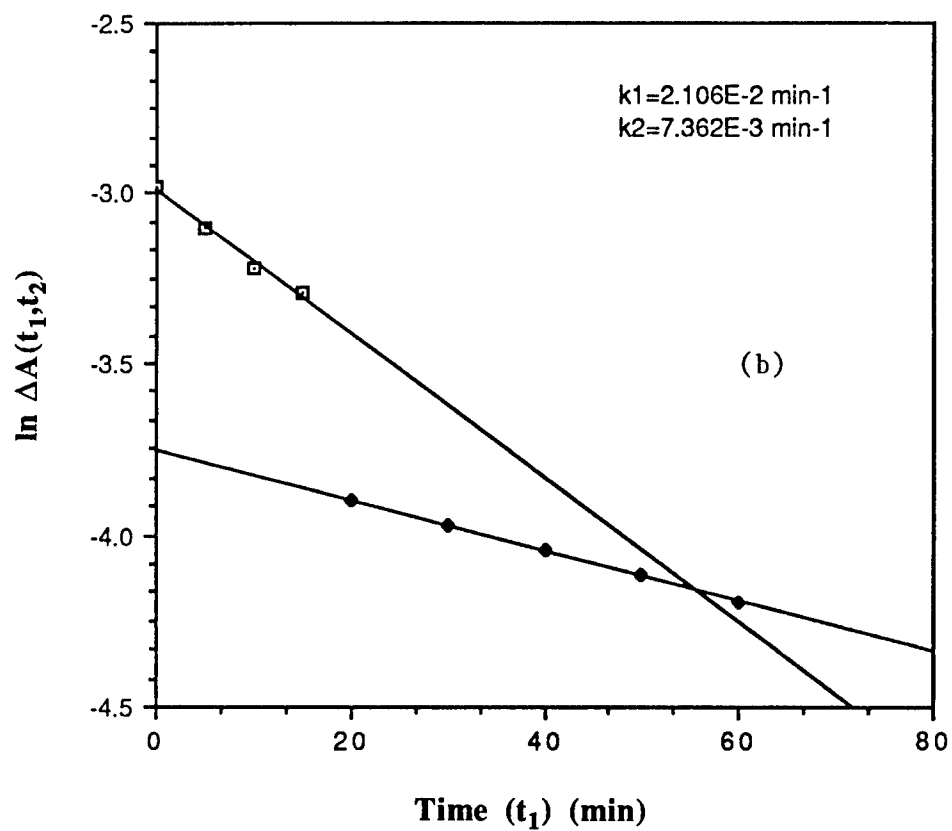


Fig.9. (continued)

280, 1725cm-1

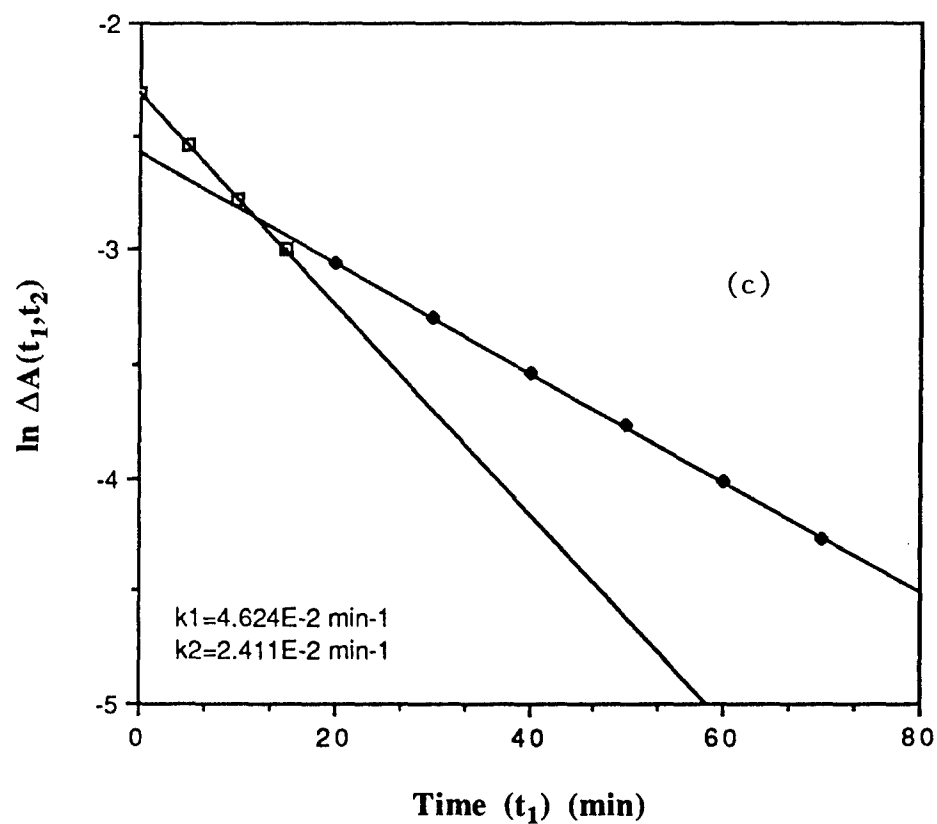


Fig.9. (continued)

240°C, 1690 cm<sup>-1</sup>

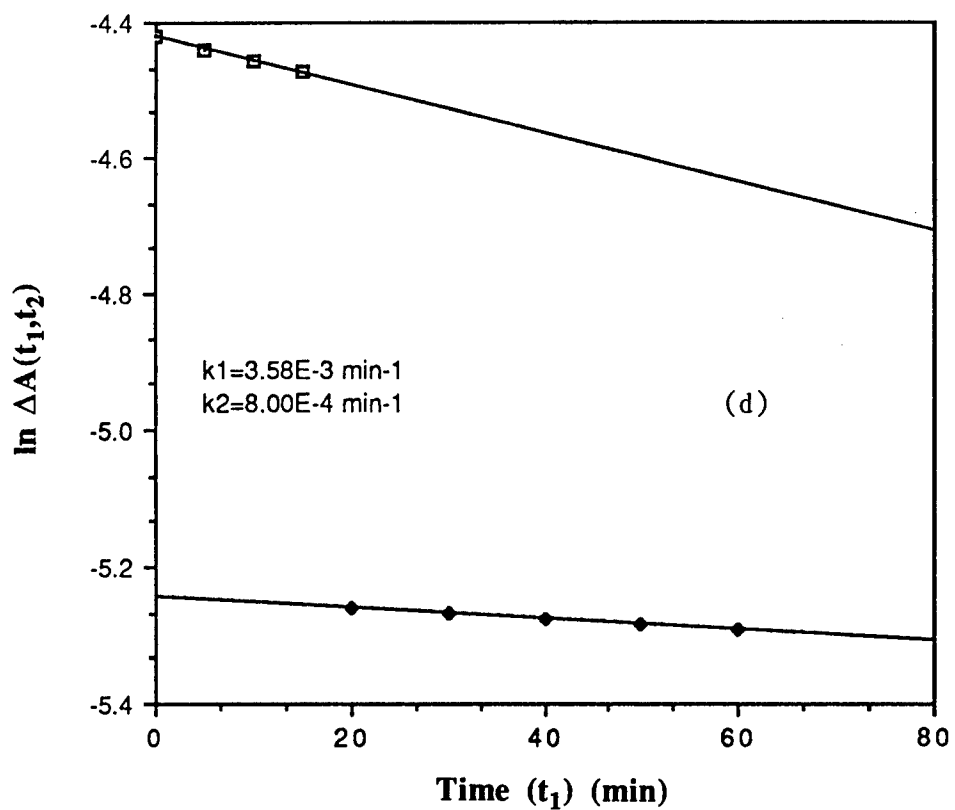


Fig.9. (continued)



260°C, 1690 cm<sup>-1</sup>

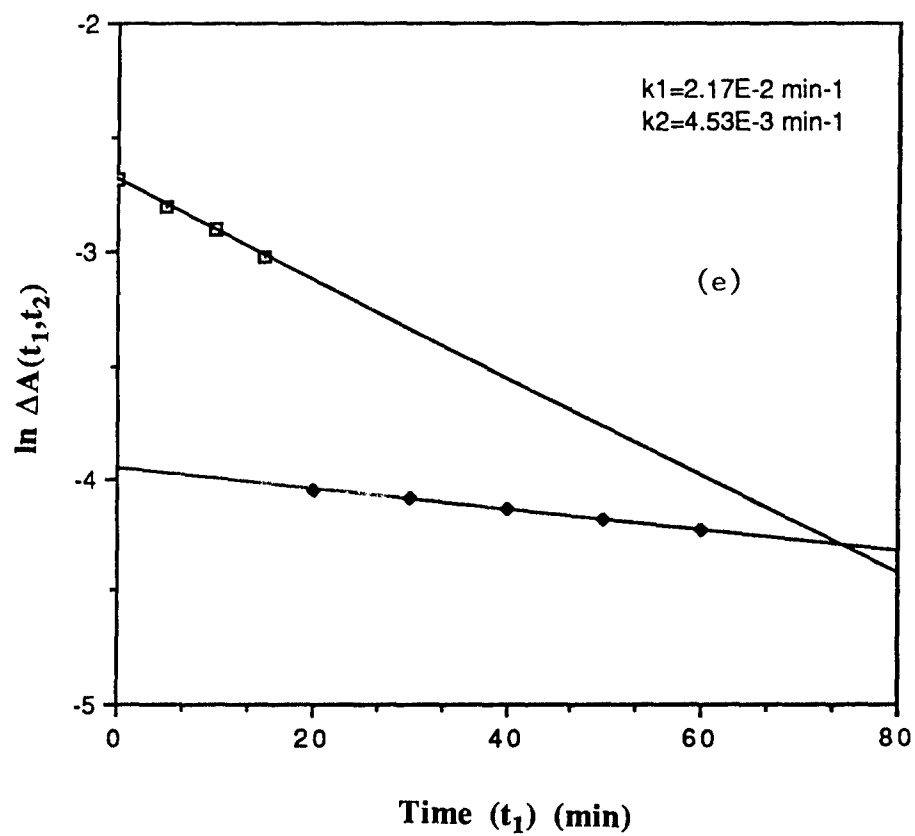


Fig.9. (continued)

280,1690cm<sup>-1</sup>

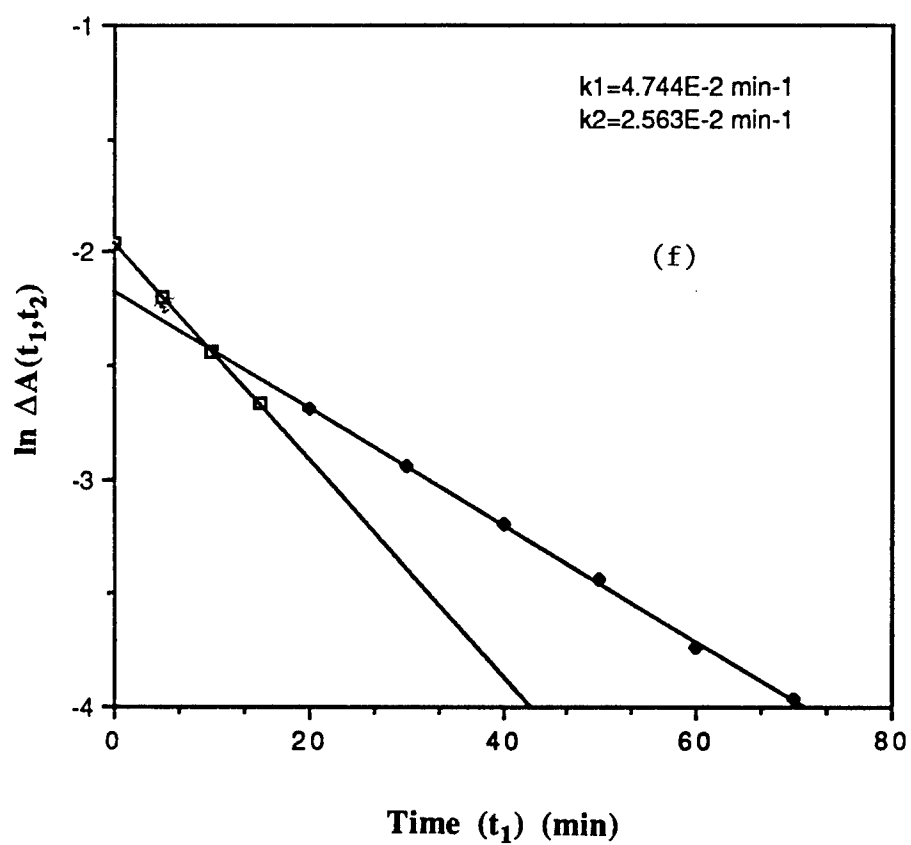


Fig.9. (continued)

Table 4. The kinetic parameters of imidization from  $\Delta A$  data

(a) at  $1725\text{ cm}^{-1}$

$k_1\text{ (min}^{-1}\text{)}$			$k_2\text{ (min}^{-1}\text{)}$		
280°C	260°C	240°C	280°C	260°C	240°C
4.624E-2	2.106E-2	5.34E-3	2.411E-2	7.362E-3	9.50E-4
$K_0 = 5.75\text{ E10, } E_1 = 31\text{ Kcal/mole}$			$K_0 = 3.19\text{ E16, } E_2 = 46\text{Kcal/mole}$		

(b) at  $1690\text{ cm}^{-1}$

$k_1\text{ (min}^{-1}\text{)}$			$k_2\text{ (min}^{-1}\text{)}$		
280°C	260°C	240°C	280°C	260°C	240°C
4.744E-2	2.17E-2	3.58E-3	2.563E-2	4.53E-3	8.00E-4
$K_0 = 1.57\text{ E13, } E_1 = 37\text{ Kcal/mole}$			$K_0 = 4.72\text{ E10, } E_2 = 49\text{ Kcal/mole}$		

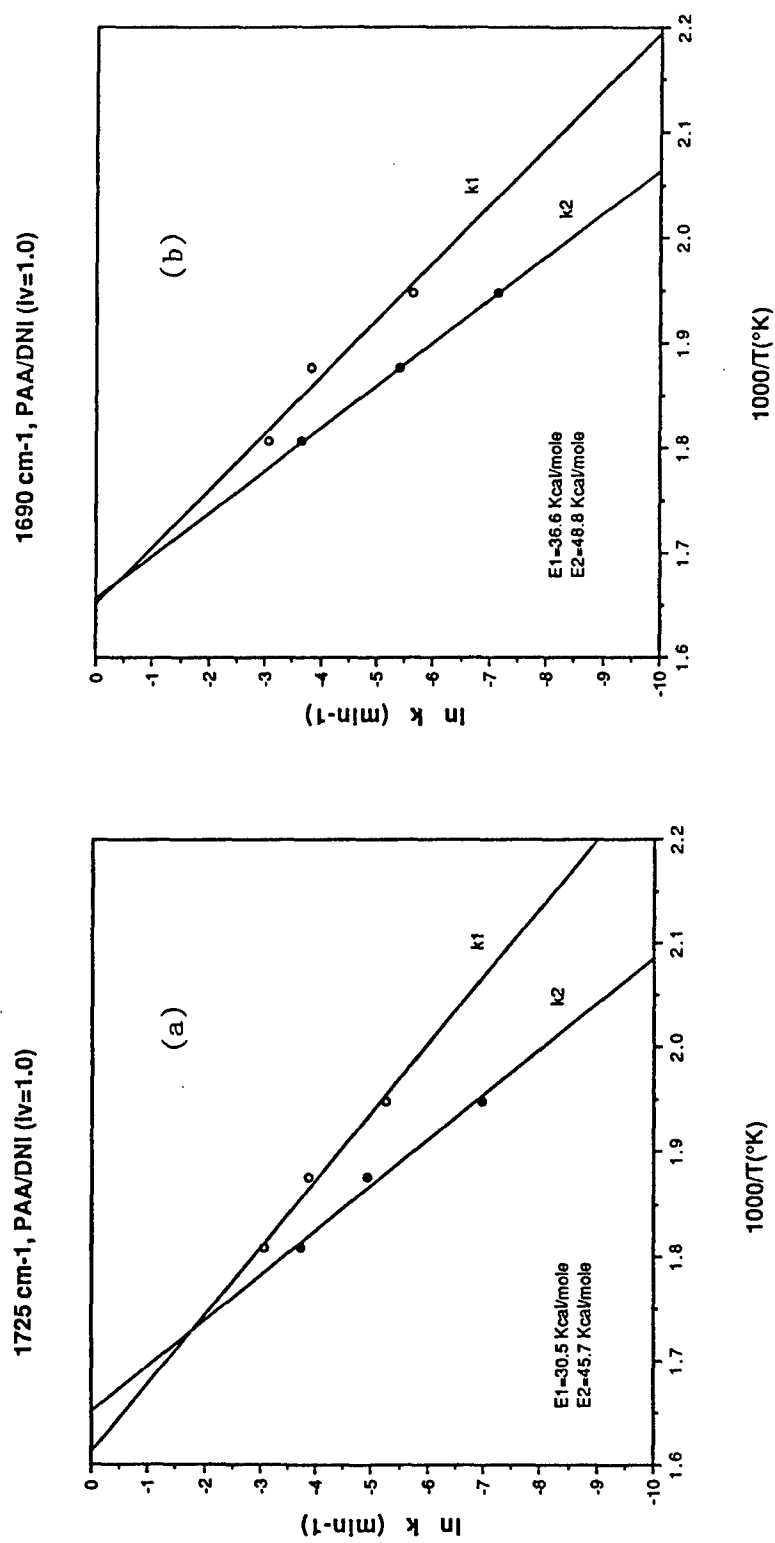


Fig.10. Arrhenius plot for imidization of PAA/DNI-3A at (a) 1725, and (b) 1690 cm<sup>-1</sup>

### Comparison of PAA/DNI-3A and PMR-15

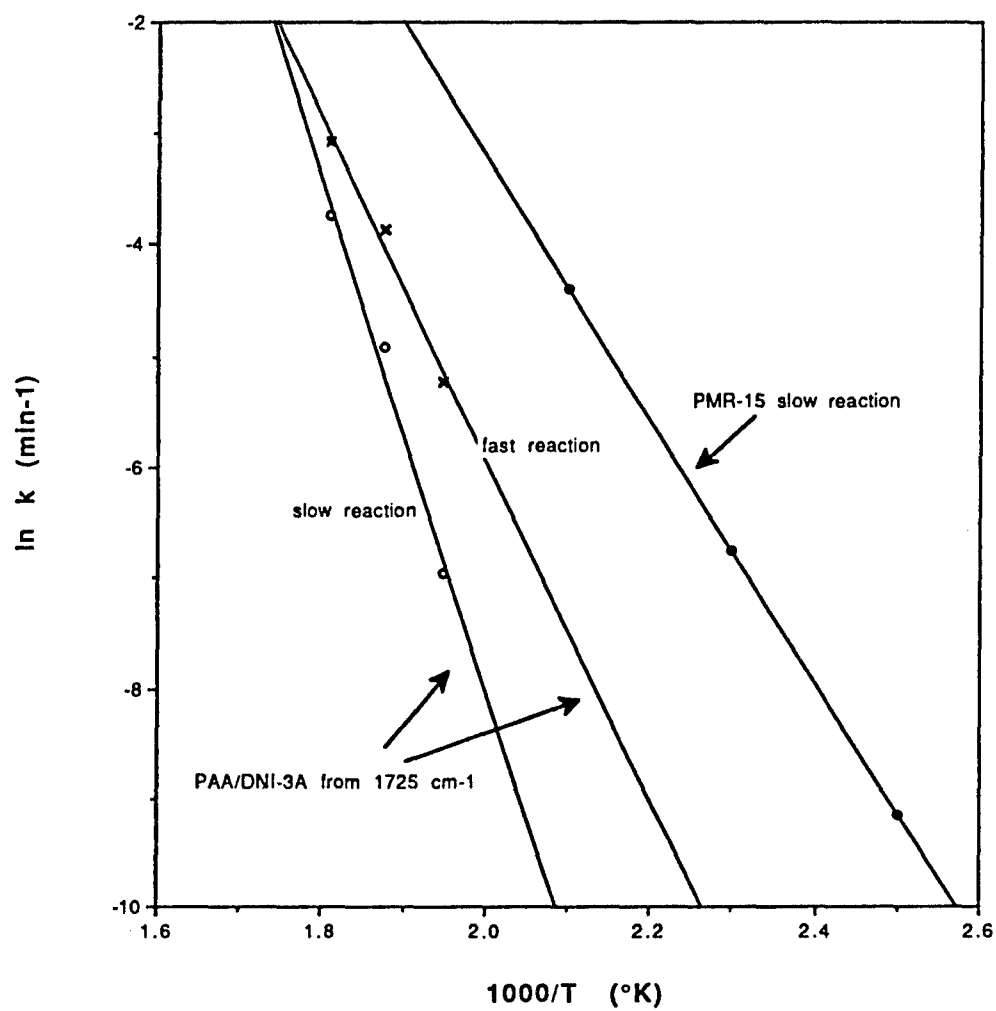


Fig.11. Comparison of Arrhenius plot for imidization of PAA/DNI-3A and PMR-15

shown in the same report, the author [15] did point out that the fast reaction constants should be one to three orders of magnitude larger than the rate constants of the slower reaction. This large difference of rate constants did not happen in the PAA/DNI-3A systems since the reaction kinetics was controlled by the system viscosity and the viscosity change during the solid state processing for PAA/DNI-3A is not very significant compared to the PMR systems. Furthermore, from Fig.11, it shows that for the PAA/DNI-3A system the  $k$  curves have steeper slopes and are located in the higher temperature range for similar  $k$  values than for the PMR systems. This means that the PAA/DNI-3A systems have much smaller processing window and also only in a shorter higher temperature range can the reaction occur in a reasonable rate.

#### **4.6 The TICA Results and Correlation with the Two Kinetic Rates**

The TICA experiments were conducted with RDS in both cure mode and isothermal scans. The results are shown in Figs.12a-12c. The cure scan illustrated that the material began to soften at about 200°C and the softening rate is very slow. At 250°C the viscosity reached the minimum and increased again due to additional reaction. The softening window was very narrow.

The isothermal scans were conducted at 280 and 240°C respectively. The moduli curves from both temperature scans showed the typical softening at the beginning, followed by the vitrification process. The FTIR kinetic results showed that there were two reaction rates associated with the ring closure reaction, a fast reaction ( $k_1$ ) at the beginning followed by a slower rate ( $k_2$ ). Clearly, this change in rate was related to the rheology of the material. When the material was in the softening stage, the reaction proceeded according to rate  $k_1$ . After the system vitrified, the glassy state rheology slowed down the conversion rate, and the remaining conversion proceeded according to rate  $k_2$ .

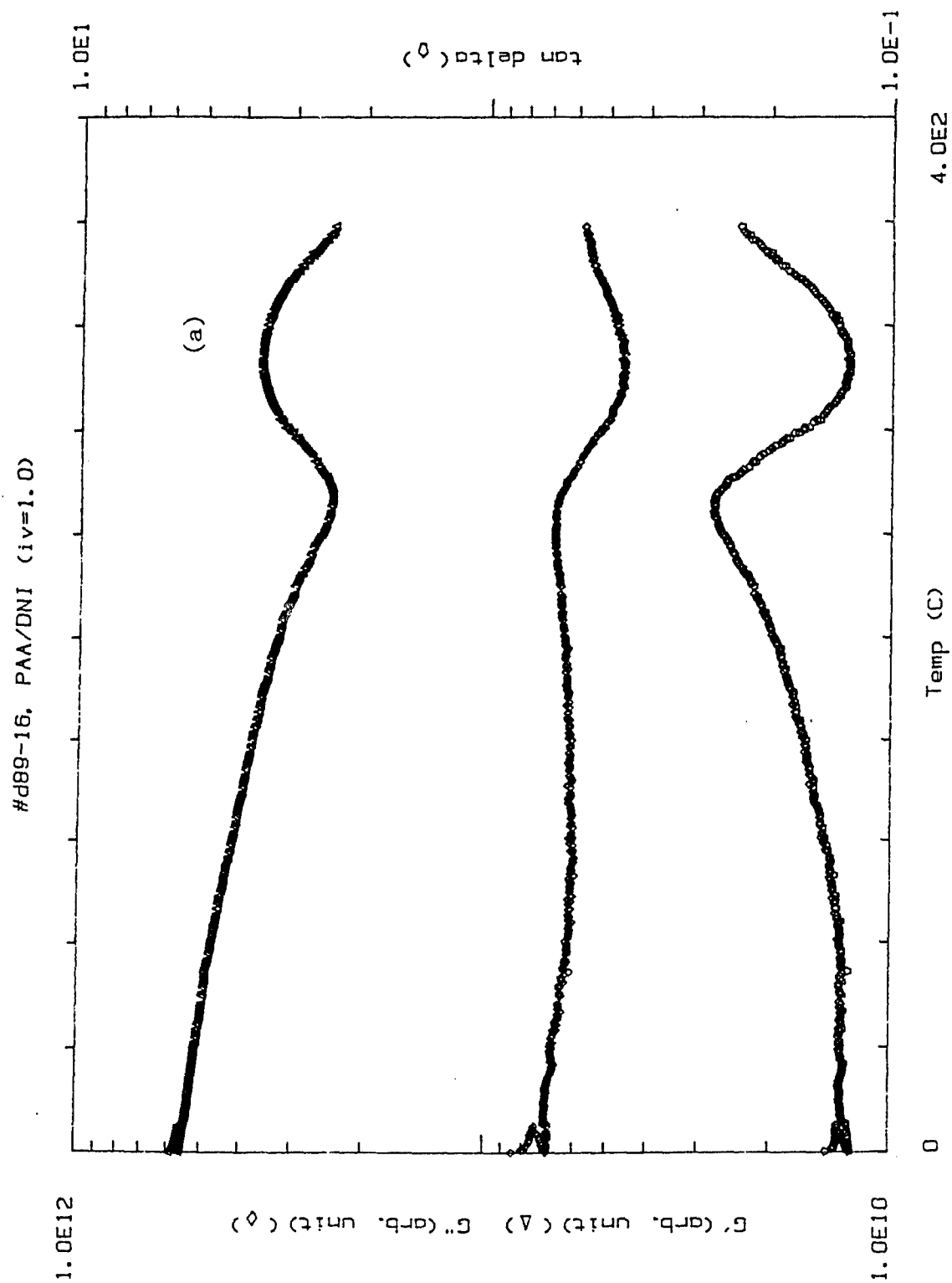


Fig.12. TICA spectra of PAA/DNI-3A for (a) temperature scan, and (b) isothermal scan at 240°C, and (c) isothermal scan at 280°C

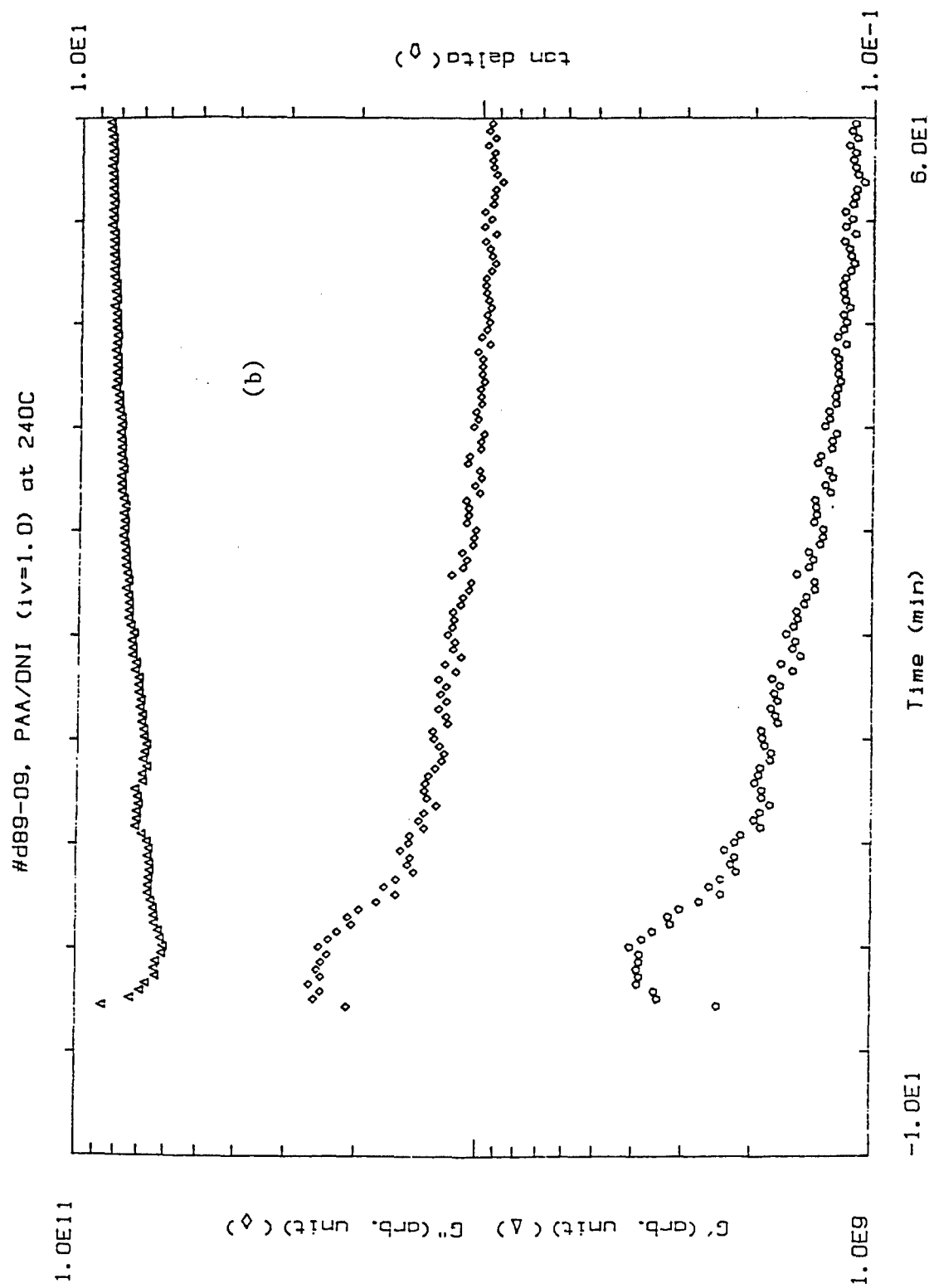


Fig.12. (continued)



#d89-06, PAA/DNI (iv=1.0) at 280C

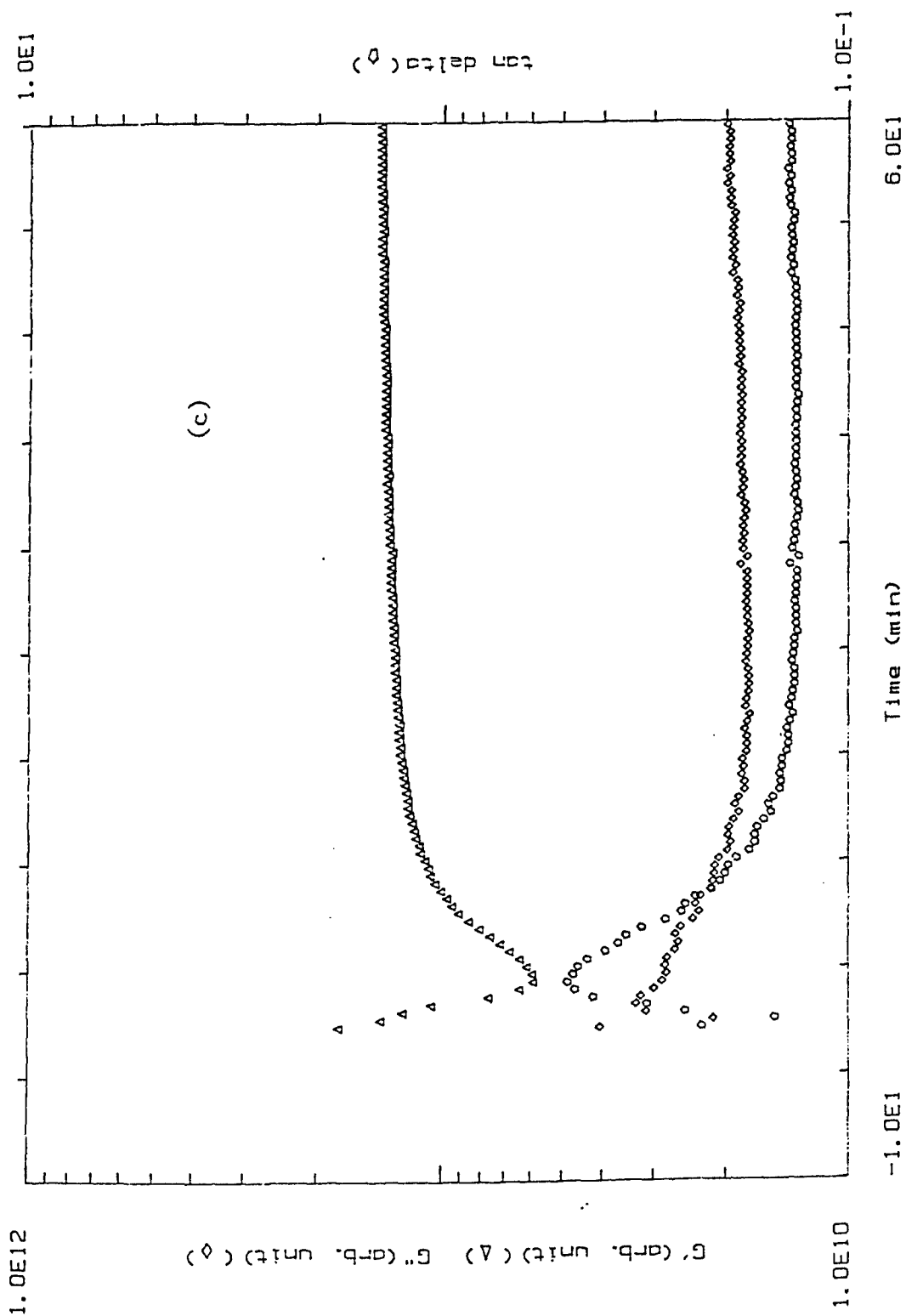
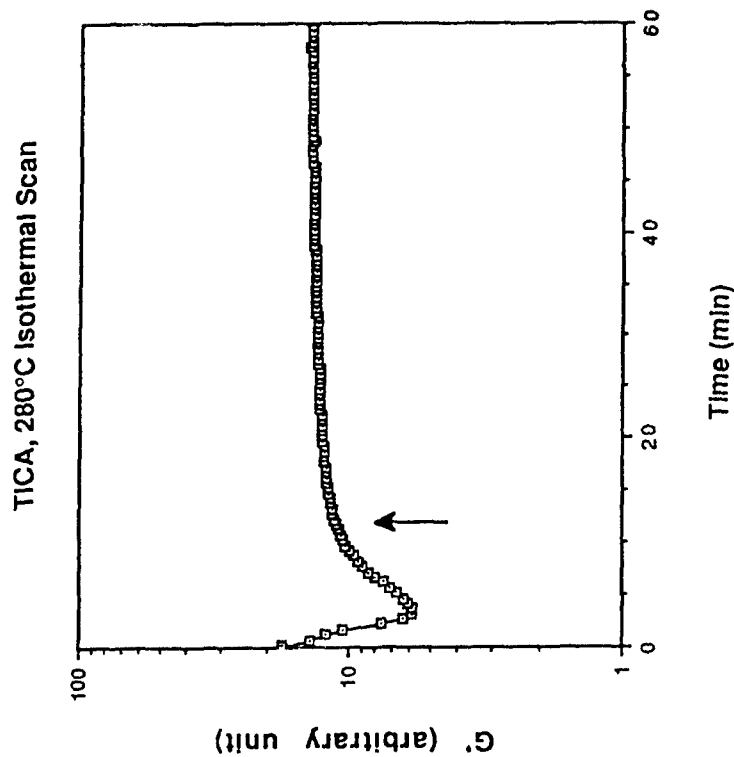


Fig.12. (continued)

To illustrate the relationship between the softening and the reaction rates, the TICA and FTIR data were replotted in Fig.13. It is very clear that the fast reaction is associated with the softening region. After the material vitrified at time  $t=12$  minutes, the reaction rate assumed the  $k_2$  value.

# Processing Consideration of In-Situ Rod Formation

(a) TICA rheology



(b) kinetics from IR

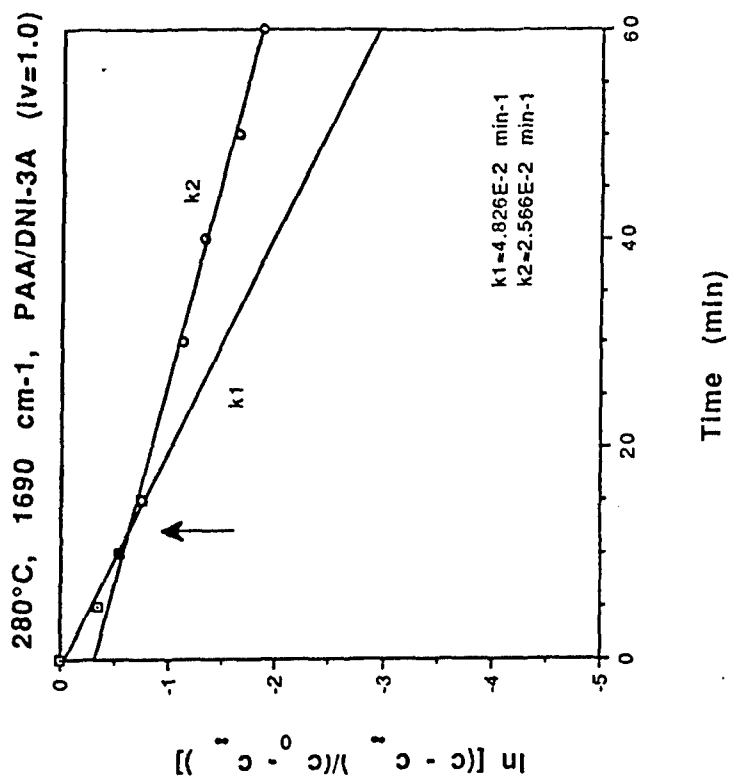


Fig.13. Relationship between softening and reaction rate for PAA/DNI-3A

## SECTION 5

### SUMMARY

The rod conversion kinetics of the PPA/DNI-3A system was studied using the FTIR. Analysis of the isothermal 280°C FTIR data showed a nice correlation between the disappearance of amic amide and the formation of imide, indicating a direct conversion without intermediate. The activation energy obtained for the poly(amic amide) was substantially higher than the literature value of amic esters. The isothermal results showed that the conversion proceeded initially according to a fast reaction rate  $k_1$  and slowed to a different reaction rate  $k_2$  later. The crossover point between  $k_1$  and  $k_2$  corresponds nicely with the vitrification time of the rheology measurement. This proves that the conversion rate and possibly the degree of conversion, is rheologically controlled.

This study defined the kinetic parameters of the rod conversion reaction at the beginning of the reaction. The effect of the crosslinking chemistry was not studied. The cracking of the nadic end group into cyclopentadiene presented a complication in the study of the crosslinking effect. The cyclopentadiene evolution temperature range overlapped with the rod conversion reaction range. Another crosslinking chemistry will be more suitable to study the crosslinking effect on rod conversion.

## REFERENCES

1. L.S. Tan and F.E. Arnold, "In Situ Molecular Composites I: Concept and Synthesis of Dialkylamines and N-Ethyl Benzylamines Containing Ethynyl, Phenylethynyl, Nadic and Benzocyclobutenyl Groups", *Polymer Preprints*, 32(1), (1991).
2. L.S. Tan and F.E. Arnold, "In Situ Molecular Composites II: Synthesis and Characterization of Poly(amic Dialkylamides) Impregnated with Thermosettable Secondary Amines", *Polymer Preprints*, 32(1), (1991).
3. L.S. Tan and F.E. Arnold, *Polymer Preprints*, 28(2), p316 (1987)
4. L.S. Tan and F.E. Arnold, "A Convenient Synthesis of High Molecular Weight Poly(amic Dialkyl Amide)", *Polym. Preprint*, p316 (1988)
5. C.Y-C Lee and I.J. Goldfarb, "Torsion Impregnated Cloth Analysis (TICA): A Forced Torsion Technique to Study Resins Supported by Inert Substrate", *Polym. Engr. & Sci.*, 21, p390 (1981).
6. T.T. Serafini, P.Delvigs and G.R. Lightsey, U.S. Patent 3,745,149 (1973)
7. M.J. Brekner and C. Feger, "Curing Studies of a Polyimide Precursor", *J. Polym. Sci., A*, 25, 2005 (1987). "Curing Studies of a Polyimide Precursor. II. Polyamic Acid", *ibid*, A, 25, 2479 (1987).
8. C. Feger, "Curing of Polyimides", *Polym. Eng. Sci.*, 29 (5), p347 (1989) 1b. T.L. St. Clair, M.K. Gerber and C.R. Gautreaux, "A comparison of the Polyimide isomers PMDA/ODA and ODPA/p-PDA", *ACS (PMSE)*, Spring, 1989, p.183.
9. P.D. Frayer, "The Interplay Between Solvent Loss and Thermal Cyclization in LARC-TPI", in "Polyimides -I" edited by K.L. Mittal, Plenum Press (1984)
10. E.L. Johnson, "The Effects of Reaction Temperature and Hydrolysis on Polyamic Acids and Polyimides", *J. Appl. Polym. Sci.*, 15, p.2825 (1971)
11. C-P Yang and S-S Wang, "Studies on the Imidization of N-Substituted Polymleamis Acids", *J. Polym Sci.* A27, p15 (1989)
12. J.A. Kreuz, A.L. Endrey, F.P. Gay, and C.E. Sroog, "Studies of Thermal Cyclizations of Polyamic Acids and Tertiary Amine Salts", *J. Polym Sci.*, A-1(4), p2607 (1966)
13. L.A. Laius, M.I. Bessonov, Ye. V. Kallistova, N.A. Adrova, and F.s. Florinskii, "Infrared Spectral Absorption Study of the Formation Kinetics of Polypyromellitimide (PPMI), *Vysokomol. soyed.* A9(10), p2185 (1967)
14. L.A. Lauis and M.I. Tsapovetsky, "Kinetics and Mechanism of Thermal Cyclization of Polyamic Acids", *Polymide I*, edited by K.L.Mittal, Plenum Press, NY, 1984

15. R.W. Lauver, "Kinetics of Imidization and Crosslinking in PMR Polyimide Resin", J. Polym. Sci., Poly. Chem. edition, 17, p2529 (1979).
16. F.A. Myers, "Cure Theology of PMR-15 Prepreg", Second International Technical Conference on Polyimides (1985)
17. R.W. Snyder and P.C. Painter, "Dynamic FT-IR Analysis of Cure Reactions and Kinetics of Polyimides", PMSE Proc. (Amer. Chem. Soc.), p57, 1988
18. J.D. Summers and J.E. McGrath, "Kinetic Studies of Homo- and Copolymer Solution Imidization", Polym. Preprints, 28(2), p230 (1987)
19. E.D. Wachsman and C.W. Frank, "Effect of Cure History on the Morphology of Polyimide: Fluorescence Spectroscopy as a Method for Determining the Degree of Cure", Polym. Matl. Sci. Eng. Proceeding (Amer. Chem. Soc.), p46, 1988
20. N.G. Gaylord and M. Martan, "Homopolymerization of Isomeric n-Phenyl-5-Norbornene-2,3-Dicarboximides, Model Compounds for Norbornene End-Capped Addition-Curing Polyimides", Polym. Preprint, 22, p11 (1981)
21. D.A Scola, in Processding of Second International Polyimide Conference, Society of Plastic Engineers, 1985, p247-252.
22. M.Navarre, "polyimide Thermal Analysis", in "Polyimides I" edited by K.L. Mittal, Plenum Press, 1984
23. E. Sacher, "A Reexamination of Polyimide Formation", J. Macromol. Sci.-Phys., B25(4), p405 (1986)
24. M.M. Koton et al, "Investigation of the Kinetics of Chemical Imidization", Polym. Sci. (USSR), 24, p791 (1982).
25. D.Garcia and T.T.Serafini, "FTIR Studies of PMR-15 Polyimides", J.Polym.Sci., B25, p2275 (1987).
26. P.R.Young and A.C. Chang, "FTIR Characterization of Thermally Cycled PMR-15 Composites", 33rd International SAMPE Symposium (1988).
27. C.A. Pryde, J Polym.Sci., "IR Studies of Polyimides. I. Effects of Chemical And Physical Changes During Cure", A(27), p711 (1989)
28. J.D. Summer et al., "Synthesis and Characteristics of Novel Poly(imide Siloxane) Segmented Copolymers, Polymer Preprints, 27, (1986)
29. J.D. Summers, Et al., " Synthesis and solution Imidization Studies of Soluble Poly(imide siloxane) Segmented Copolymers", 32nd Intern. SAMPE Symp. (1987)
30. G.Socrates, "Infrared Characteristic Group Frequencies", Chap. 10, John-Wiley & Sons, NY 1980.

## **APPENDIX A**

**Illustrated examples for kinetic data  
calulation from Sections 3(c) and 3(d)**

Example 1 For a first order reaction,  $[c]_t = [c]_0 \exp(-t/100)$  then  $k=0.01$ , the  $[c]$  values at different time  $t$  are listed in the following table.

time (min)	$[c]_t/[c]_0$
0	1.00
5	0.95123
10	0.90484
15	0.86071
...	
120	0.30119
180	0.16530

If the data were analyzed by assuming  $[c]_t$  at  $t=120$  min to be zero ( $[c]_{120}=0$ ) and apply equation (10) to get the  $k$  value the error is about 70% ( $k=0.017$ ), if  $[c]_{180}$  is assumed to be zero the error is reduced to 50% ( $k=0.015$ ). Because of other complication in solid state reaction like diffusion controlled quenching of the reaction, it is difficult to determine if  $[c]_t$  is indeed zero. That is the motive to develop the approach for evaluating the  $k$  values, in which whether  $t$  is equal to infinity or not is not involved at all.

The same example is used to demonstrate the application of this approach as follows.



### Example 2.

For the same first order reaction  $[c]_t = [c]_0 \exp(-t/100)$ , assume  $a_c b = 1$ . Then

$$A_c(t) = a_c b [c]_t = [c]_t$$

and

$$\Delta A(t_1, t_2) = \Delta A_c(t_1, t_2) = [c]_{t_1} - [c]_{t_2} = \Delta[c]$$

The concentration, concentration difference and its logarithm values are listed in the following table.

time (min)	$[c]_t/[c]_0$	$\Delta[c]_t/[c]_0$	$\ln \Delta[c]_t/[c]_0$
0	1.00	0.049	-3.021
5	0.95123	0.046	-3.071
10	0.90484	0.044	-3.121
15	0.86071		
...			
120	0.30119		
180	0.16530		

After plotting  $(\ln \Delta[c]_t/[c]_0)$  or  $(\ln \Delta A(t_1, t_2))$  verse time  $t_1$ , the slope was found to be exactly equal to the true  $k$  value, 0.01.

Two things have to be emphasize. Firstly, it is plotted of  $(\ln \Delta[c]_t/[c]_0)$  or  $(\ln \Delta A(t_1, t_2))$  verse  $t_1$ , not verse other  $t$ . Secondly, it has to be equally spaced data used. Non equally spaced data do not fit equation (12). This technique is very useful for analyzing FTIR spectra. No infrared absorbance due to the unidentified background or the initial product is involved here. With the data treatment shown in this approach the correct kinetic data  $k$  can then be obtained.

## **APPENDIX B**

### **The Report of TGA/MS Results of PAA/DNI-3A and DNI-3A Systems from SRL**



# SYSTEMS RESEARCH LABORATORIES

2800 INDIAN RIPPLE RD., DAYTON, OH 45440-3696 • (513) 426-6000

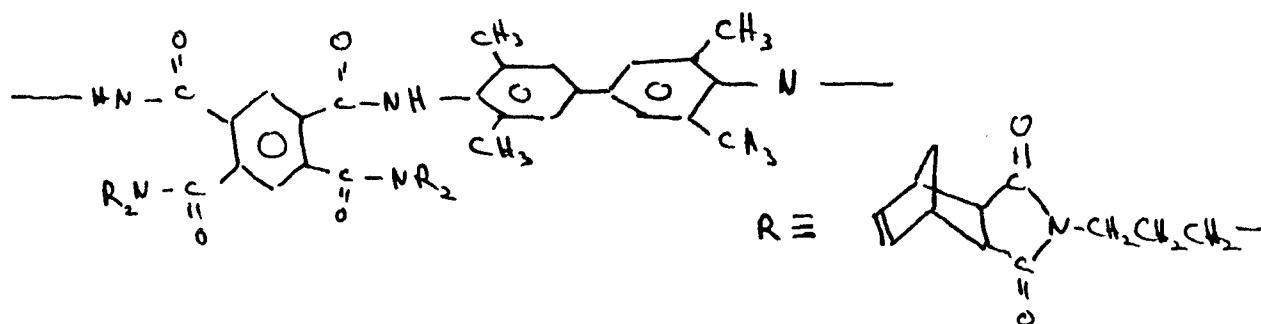
A DIVISION OF **ARVIN/CALSPAN**

8 August 1989

In Reply Reference: 5556

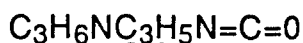
Wright Research and Development Center  
Materials Laboratory  
WRDC/MLBP (Attn: Lisa R. Denny)  
Wright-Patterson Air Force Base, OH 45433-6533

SUBJECT: Analysis of Sample LST-70359-44A



1. Initial Weight 4.3 mg  
Weight Loss (950°C) 2.8 mg (65%)
2. The temperature dependence of the total-ionization current is shown in Fig. 93. The behavior of  $dW/dT$  provides no information due to noise in the data. This is the fifth sample in this series where  $dW/dT$  data are poor (c.f., LST-70357-19A, LST-70359-5A, -13A, -13B). One possible explanation is swinging of the sample which is induced by the rapid loss of C<sub>5</sub>H<sub>6</sub>. The overall weight loss in this sample falls in the range (51 - 68%) established from the previous three samples.  
  
Two major maxima in the total-ionization profile occur at 230 and 370 °C; these are essentially as observed for Sample LST-70357-19A.
3. At temperatures below 230°C, only traces of products are observed. Three profiles can be discerned; however, the low abundance of these products precludes assignment. The peak in the total-ionization current at 230°C arises from the release of C<sub>5</sub>H<sub>6</sub> as the product of the retro-Diels Alder reaction. No other products are released in this temperature region.

4. The next volatile product arises from the imidization process. The rate of its production maximizes at 370°C and accounts for the second peak in the total-ionization spectrum. Although it is not possible to make positive identification of the structure, it can be said that it is a complex secondary amine. The highest mass ion observed is at m/e 189; the largest major ion is at m/e 138 and is tentatively assigned as

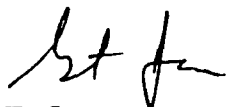


Since no other volatiles of any magnitude are seen following the retro-Diels Alder reaction prior to the imidization, it is possible that the amine cyclizes prior to undergoing the imidization. No molecular ion is observed corresponding to the nominal mass of the diamine expected from the retro-Diels Alder reaction. Since all ions in this region have the same temperature dependence, it is concluded that a single secondary amine is being observed which is not degraded thermally but by electron impact during detection.

5. Other identified products (thermal degradation) include CO, CH<sub>4</sub>, H<sub>2</sub>, HCN, and tetramethyl-substituted biphenyl.
6. The temperature dependence of the identified products is shown in Figs. 94 and 95.

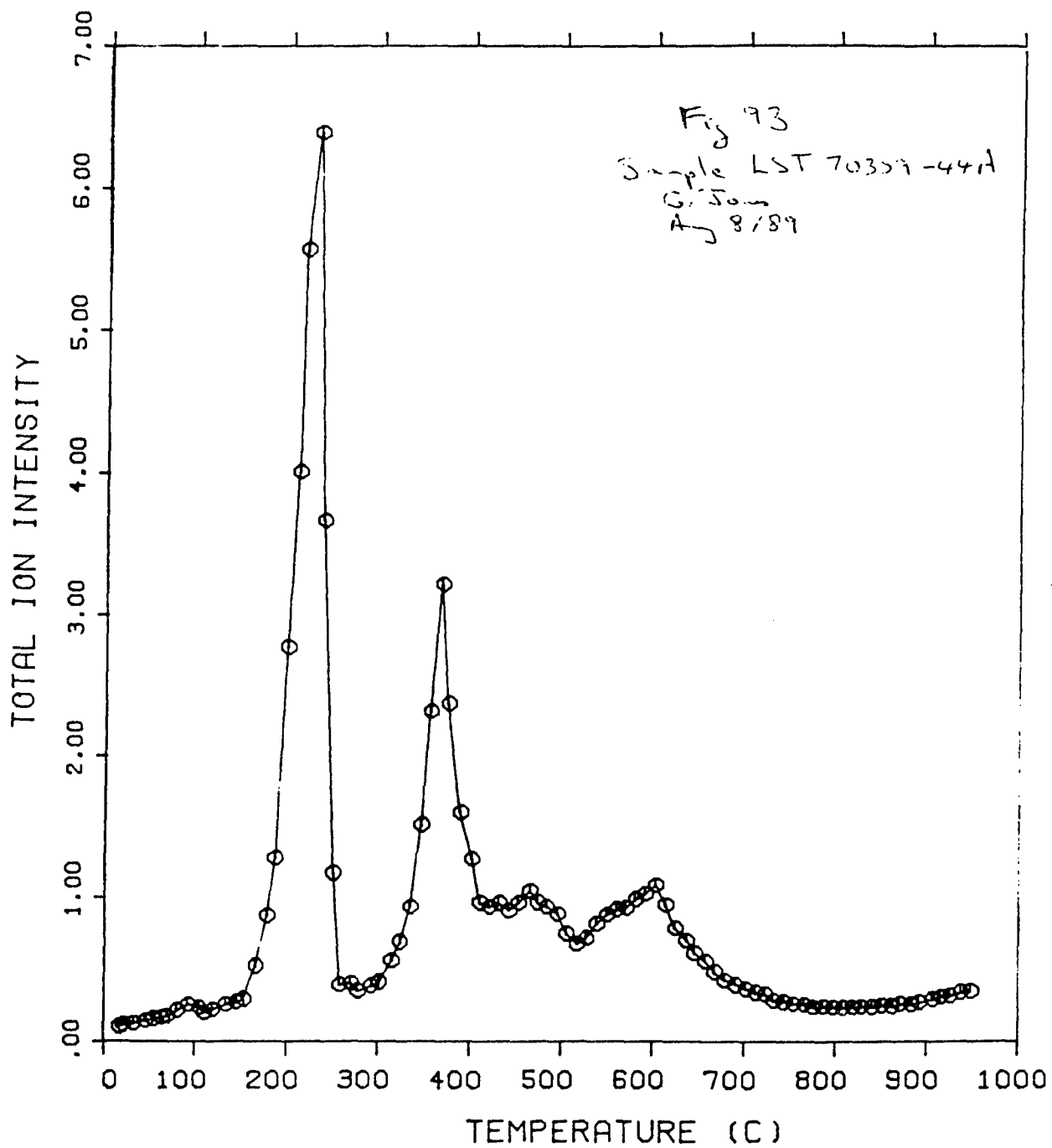
Very truly yours,

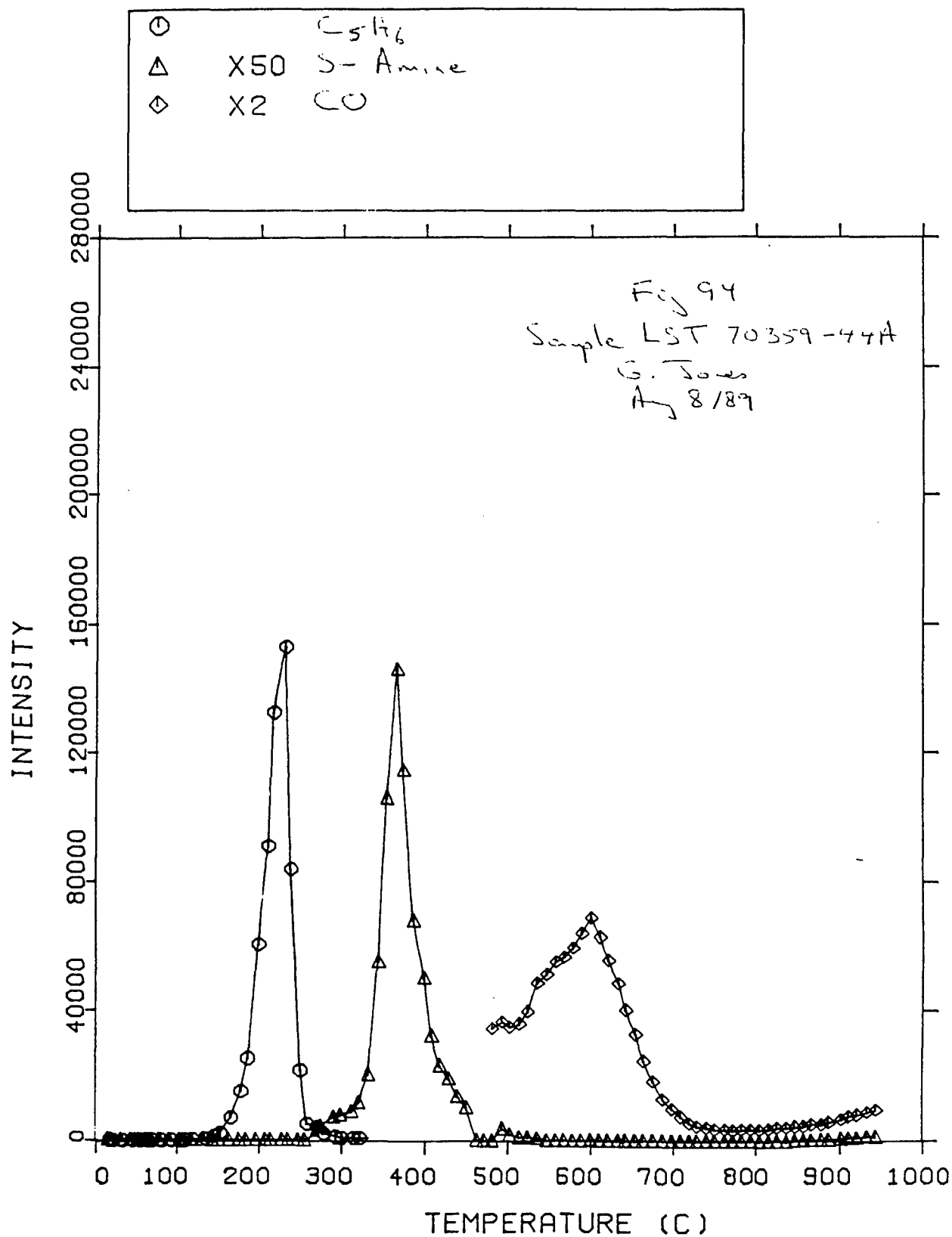
SYSTEMS RESEARCH LABORATORIES, INC.  
*A Division of Arvin/Calspan*

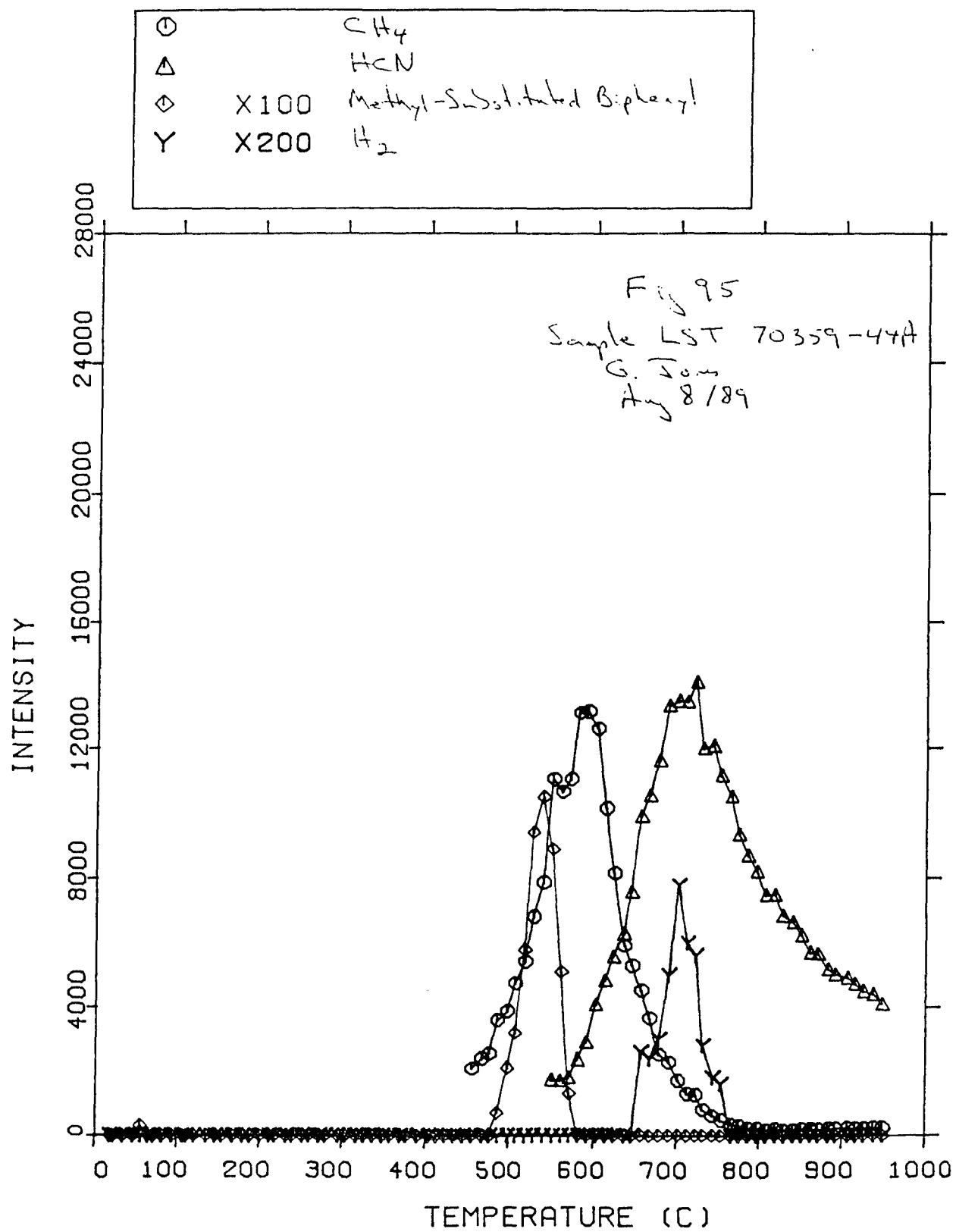


E. Grant Jones, Ph.D.  
Senior Chemist  
Research Applications Division

EGJ:mw









# SYSTEMS RESEARCH LABORATORIES

2800 INDIAN RIPPLE RD., DAYTON, OH 45440-3696 • (513) 426-6000

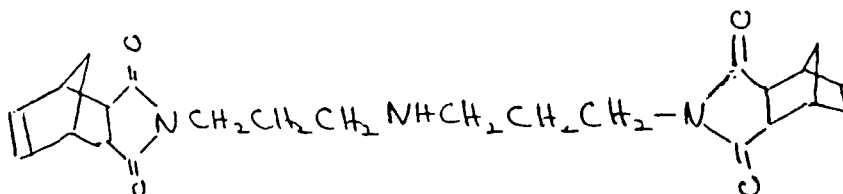
A DIVISION OF **ARVIN/CALSPAN**

15 August 1989

In Reply Reference: 5556

Wright Research and Development Center  
Materials Laboratory  
WRDC/MLBP (Attn: Lisa R. Denny)  
Wright-Patterson Air Force Base, OH 45433-6533

SUBJECT: Analysis of Sample LST-70357-14A



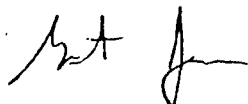
1. Initial Weight      5.8 mg  
Weight Loss      5.7 mg      (98%)
2. The temperature dependence of  $dW/dT$  and total-ionization current is shown in Fig. 101. The extent of weight loss and the profiles in Fig. 101 indicate that the entire sample is consumed either by degrading to produce volatiles or by sublimation of the original sample prior to thermal degradation.
3. The expected major low-temperature product,  $C_5H_6$  from the retro-Diels Alder reaction, is several times smaller than was observed in Sample LST-70359-44A. When it is realized that the current sample has the potential to release much more  $C_5H_6$ , it becomes apparent that sublimation of the original sample is competing with  $C_5H_6$  production and, in fact, dominates. The temperature dependence of  $C_5H_6$ , shown in Fig. 102, displays a maximum at  $220^\circ C$  which is about 10 deg. below the corresponding maximum from Sample LST-70359-44A. This illustrates the truncation of the retro-Diels Alder reaction due to sample loss. This process appears as a high-temperature satellite maximum in the total-ionization profile (c.f., Fig. 101).



4. The major volatile products observed from this sample are unrelated to the sample per se. The largest product is unreacted reagent  $C_9H_8O_3$ , accounting for the large peak in the total-ionization profile. The low-temperature region around 90 and 140°C is dominated by the solvent chloroform  $CHCl_3$ . This observation is surprising since the solvent reported for the original preparation was  $CH_3Cl$ .
5. At 230°C approximately 90% of the original sample weight has been lost. Analysis of volatiles at higher temperature is questionable. The profile of m/e 138 is shown in Fig. 103; this was previously ascribed (Sample No. LST-70359-44A) to the s-amine released during cyclization.
6. Over the same temperature region, a broad release occurs, accounting for the maximum in the total-ionization and dW/dT temperature profiles around 420°C. Possibly significant is the fact that this unidentified product was also observed in the companion sample (unidentified) over a narrower range.
7. It should be pointed out that for small non-polymeric systems where sublimation commonly occurs, it is important that reagents and other contaminants be removed because of their increased significance compared to the products released in reduced abundance due to competition with sublimation, i.e., a cleaner sample may improve the chances of identifying the cured products.

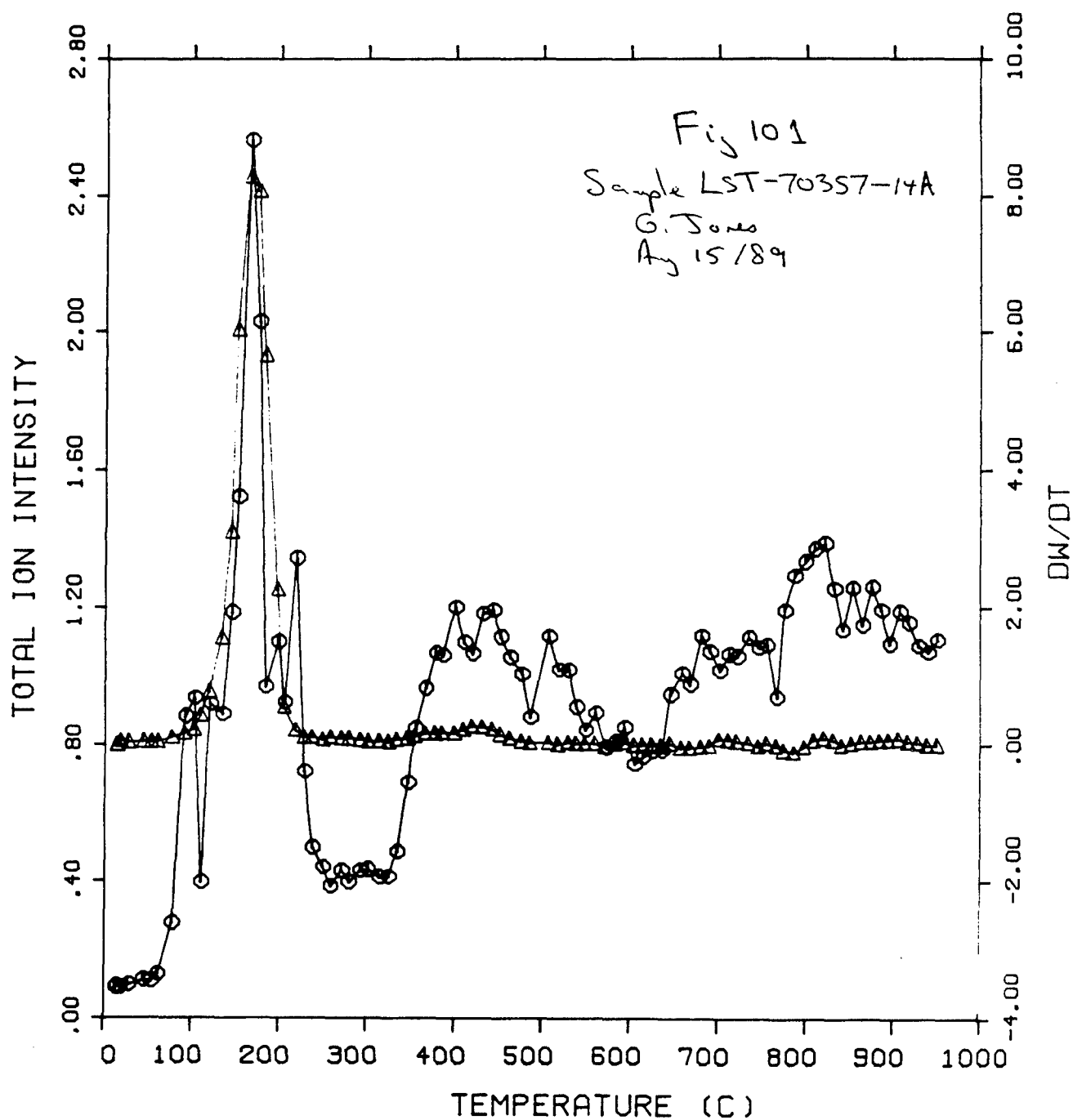
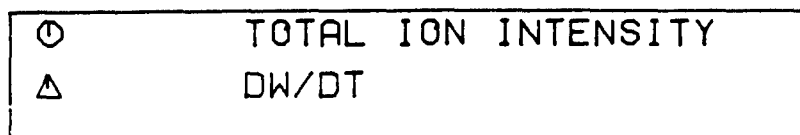
Very truly yours,

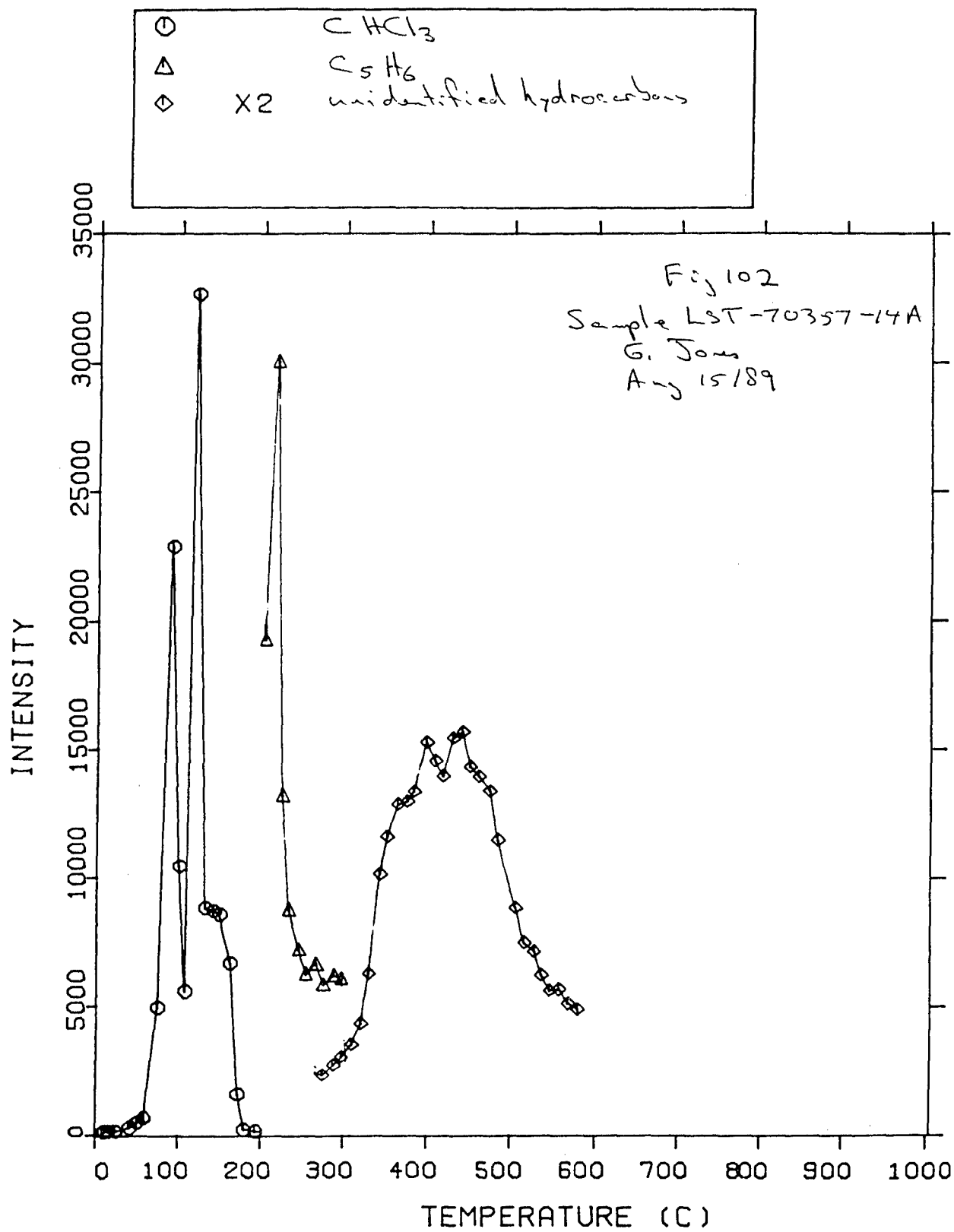
SYSTEMS RESEARCH LABORATORIES, INC.  
*A Division of Arvin/Calspan*

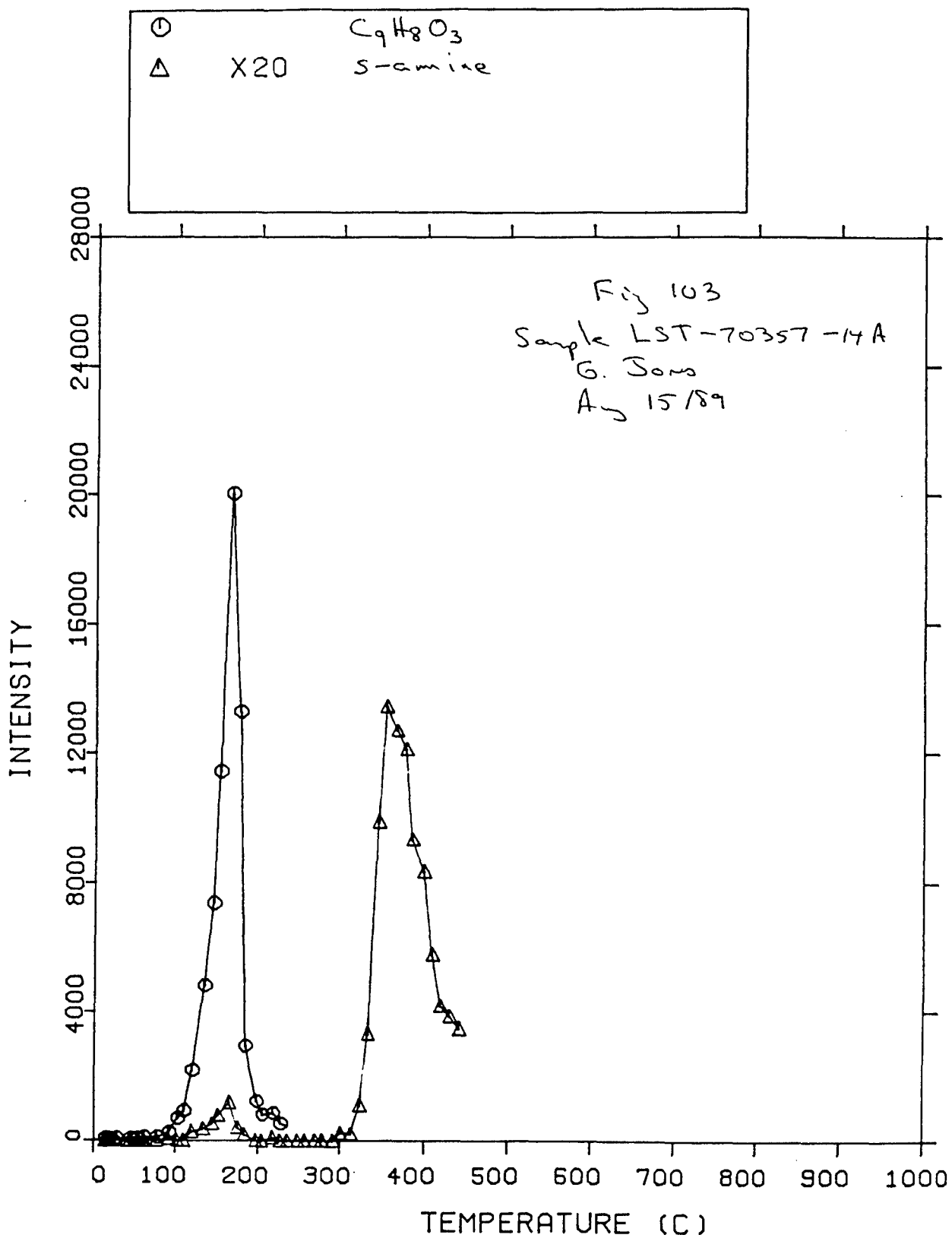


E. Grant Jones, Ph.D.  
Senior Chemist  
Research Applications Division

EGJ:mw



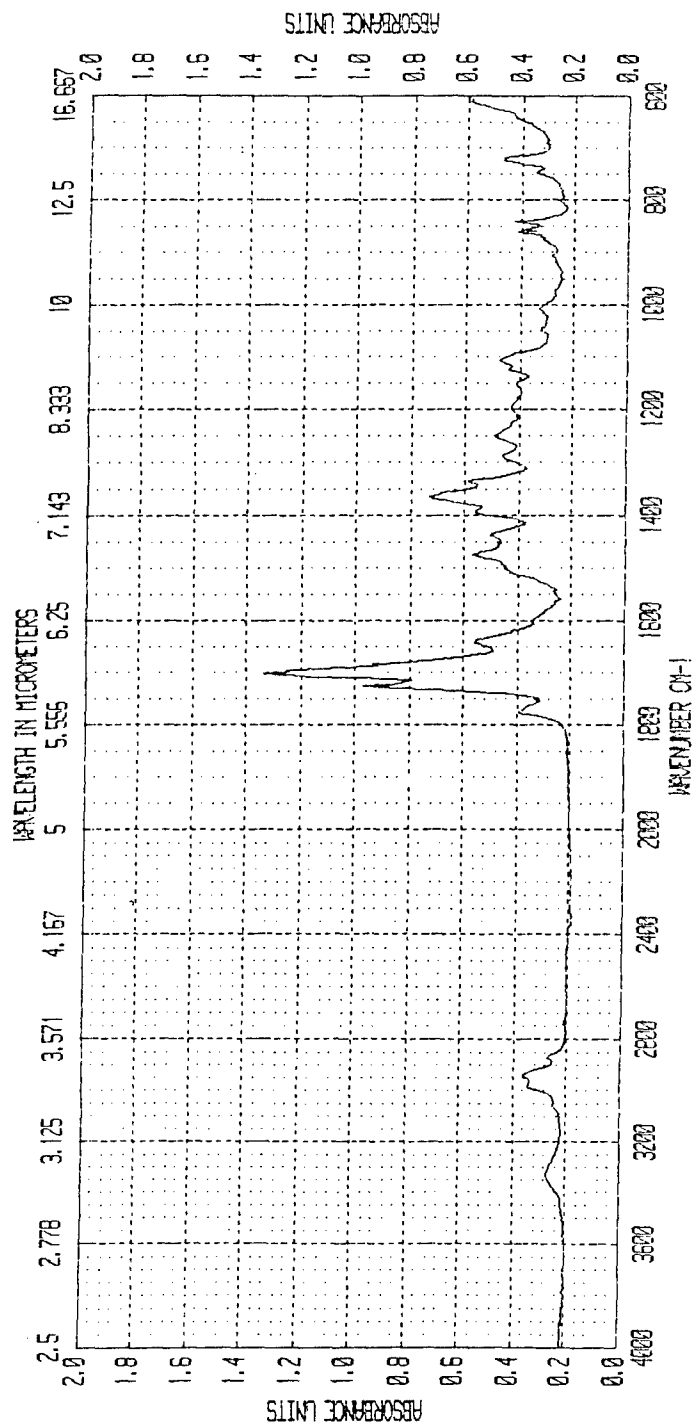




## APPENDIX C

### Absorption Spectra from FTIR for PAA/DNL-3A

# BECKMAN

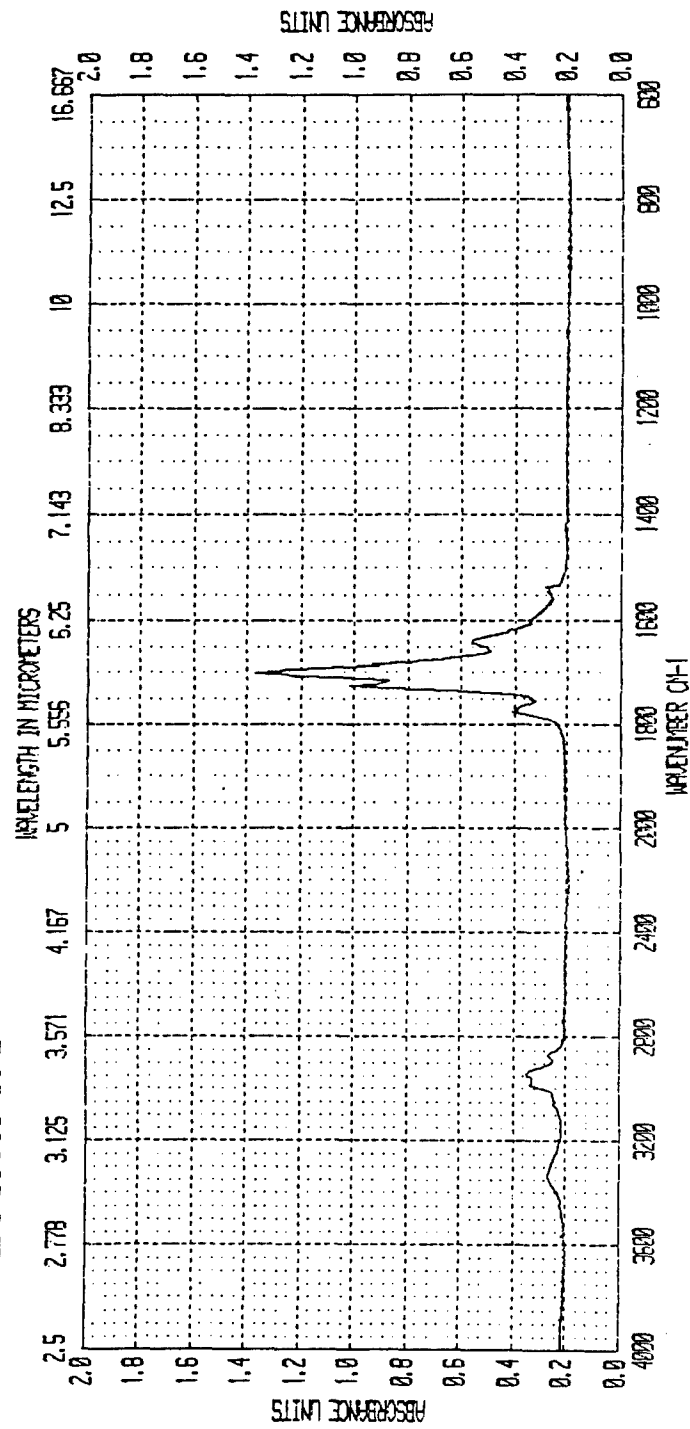


t=0 min. @240°C

Scan Name	Resolu	Apodized	Start	End	Scan Time	First Y
240/0	4	no	4000.93	401.12	30 scans	0.2135
At 240 TIME 0						

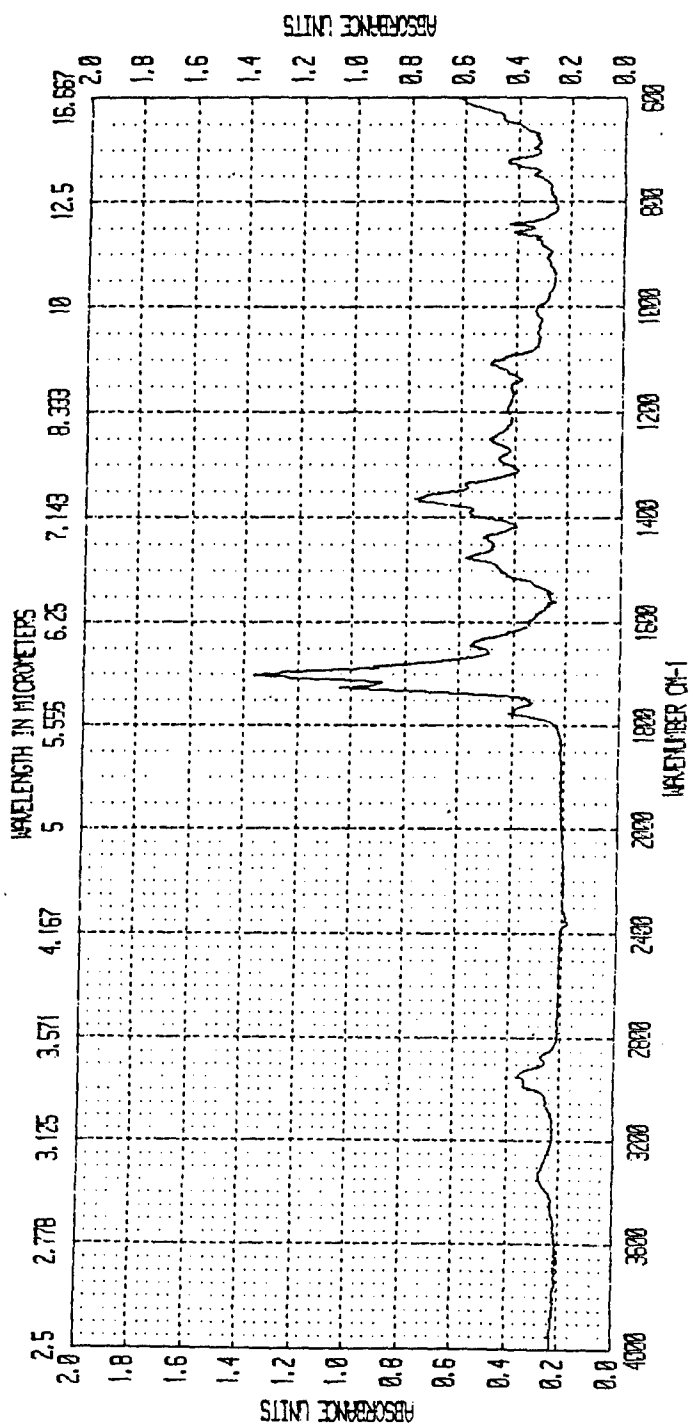
Scan Name	240/1.0
Resolu	4
Apodized	no
Start	4000.93
End	401.12
Scan Time	30 scans
First y	0.2145

# BECKMAN



t=10 min. @240 °C

# BECKMAN



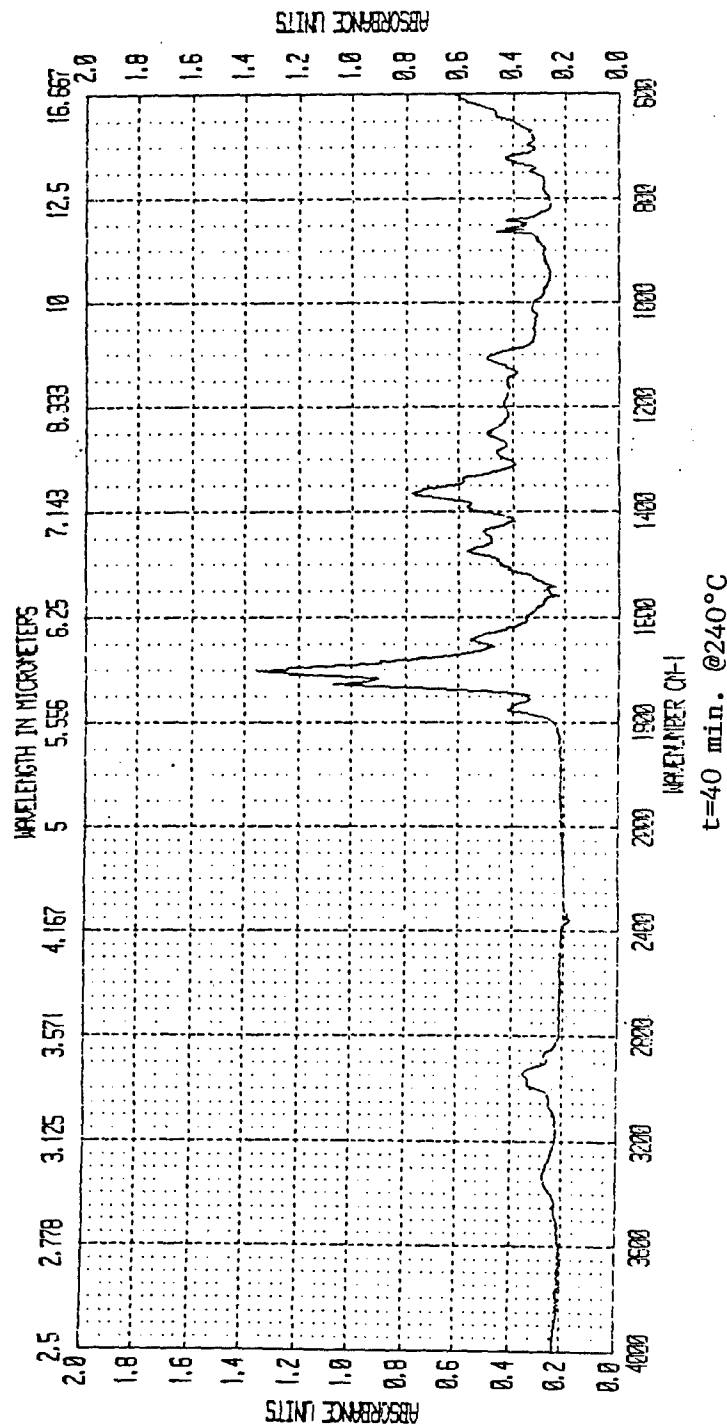
t=20 min. @240°C

Scan Name	Resolu	Hoodled	Start	End	Scan Time	First y
240/20	4	AT 240C FOR 20 MIN	4000.93	401.12	30 scans	0.2281



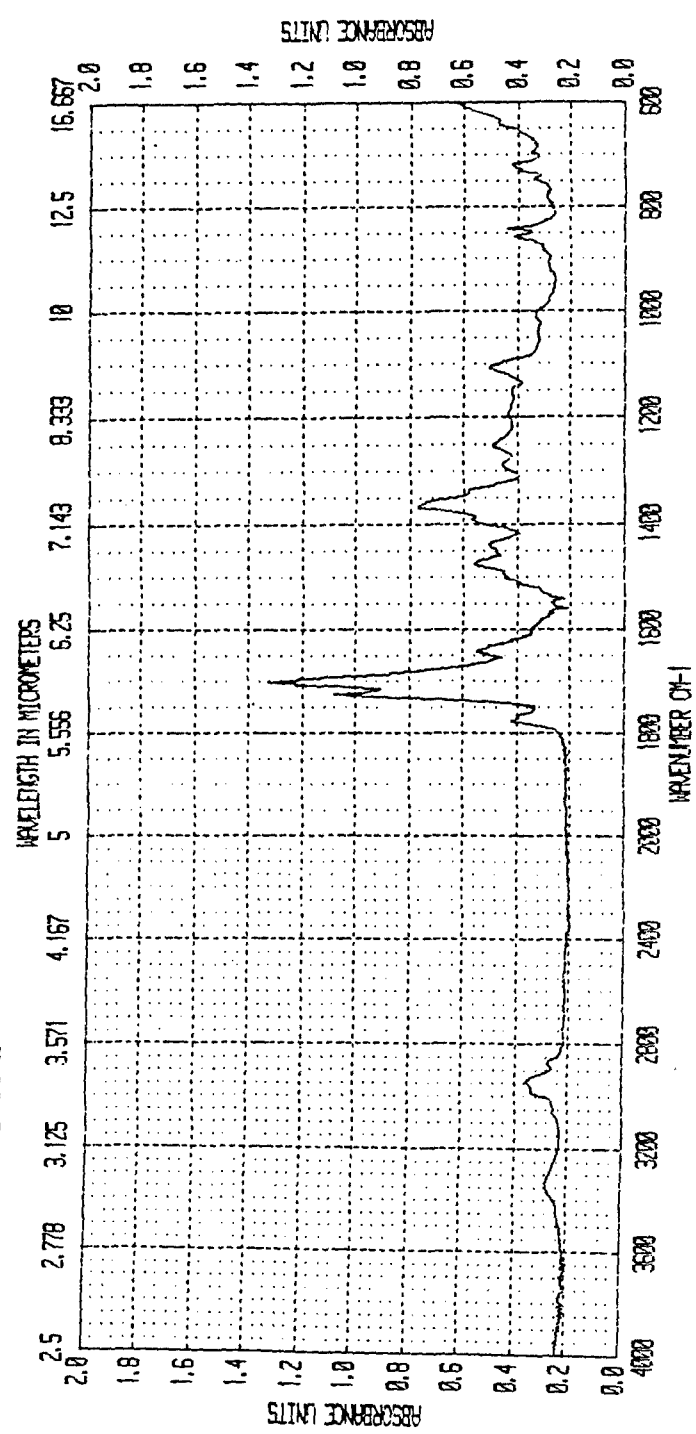
Scan Name	Resolu	Apodized	Start	End	Scan Time	First Y
240/40	4	no	4000.93	401.12	30 scans	0.2277

# BECKMAN



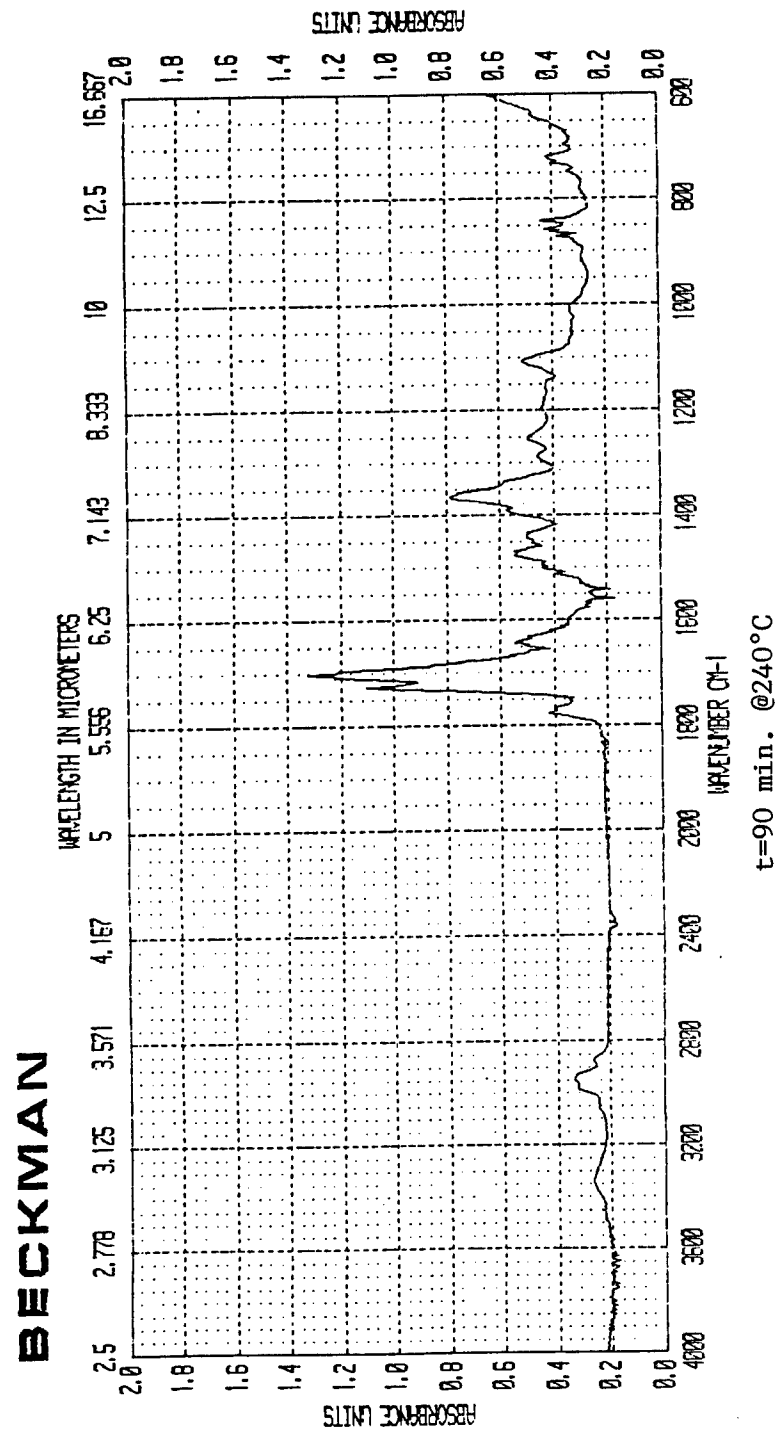
Scan Name	240/60
Resolution	4
Apodized	AT 240C FOR 60 MIN
Start	4000.93
End	401.12
Scan time	30 scans
First Y	0.2922

BECKMAN

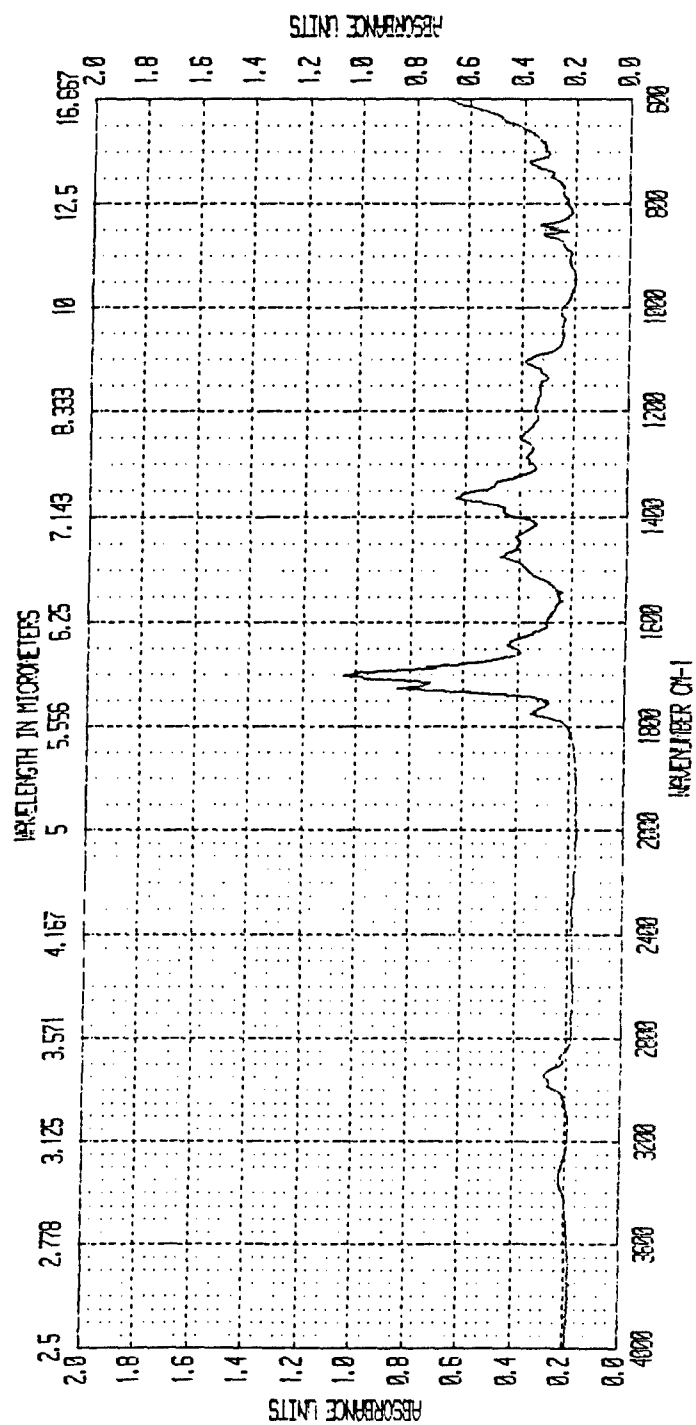


t=60 min. @240°C

Scan Name	240/50
Resolu	4
Apodized	AT 240C FOR 90 MIN
Start	4000.93
End	401.12
Scan Time	30 scans
First Y	0.2196



**BECKMAN**

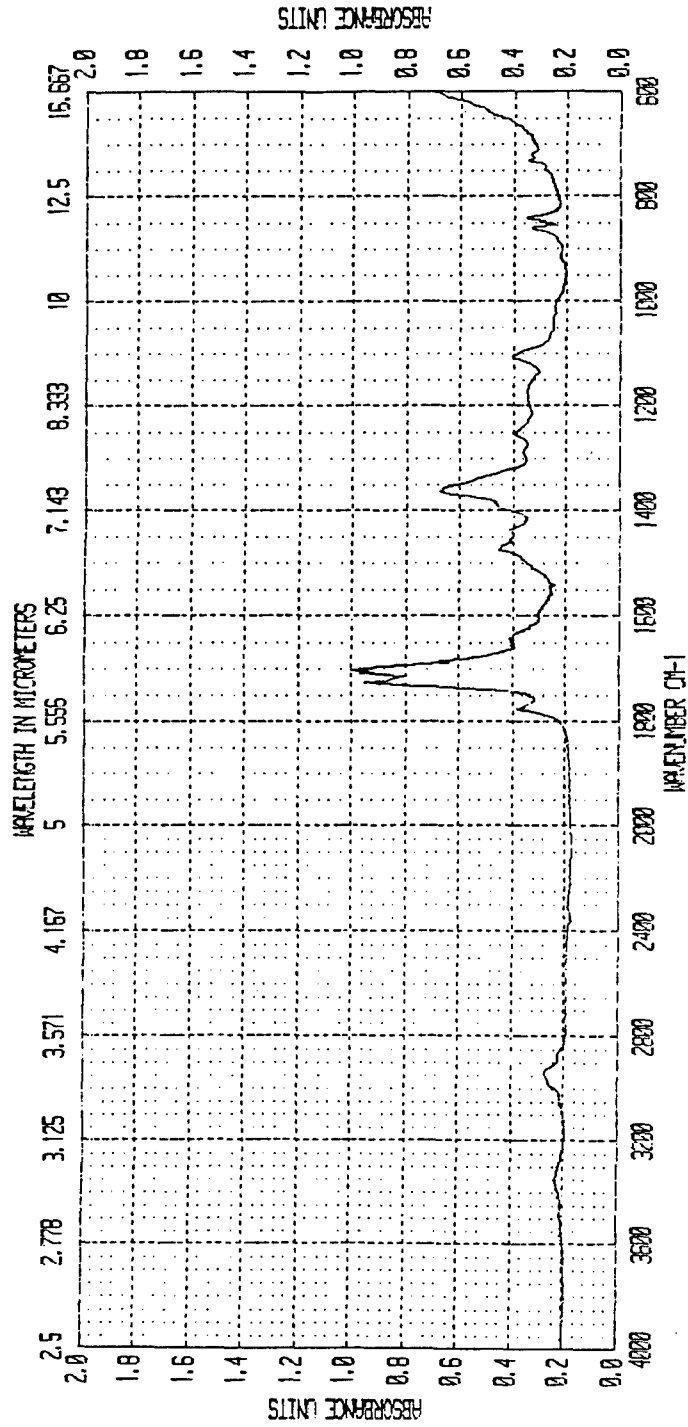


t=0 min @260°C

Scan Name	Resolu	Apodized	Start	End	Scan Time	First Y
260/0	4	no	4000.93	401.12	30 scans	0.1927
2600 0 TIME						

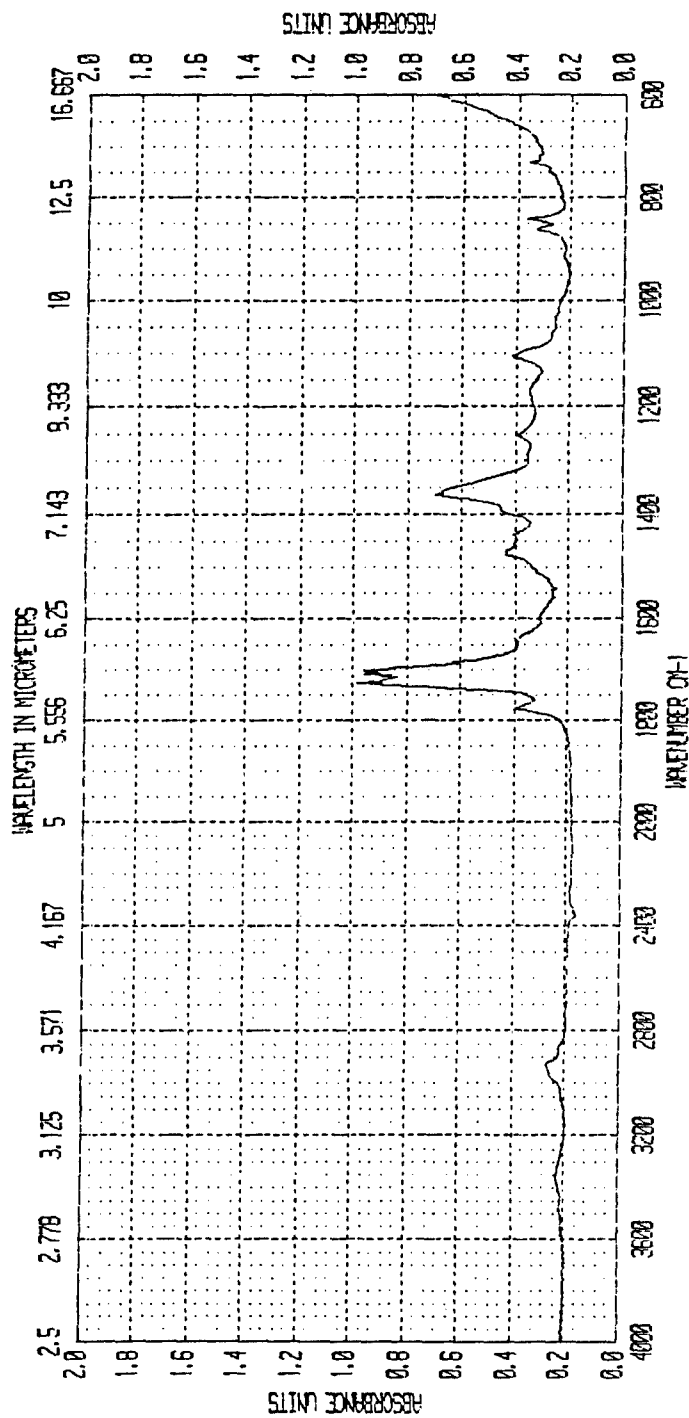
Scan Name	260/5
Resolu	4
Apodized	260C FOR 5 MIN
start	4000.93
end	401.12
Scan time	30 scans
First Y	0.2029

# BECKMAN



t=5 min. @260°C

# BECKMAN

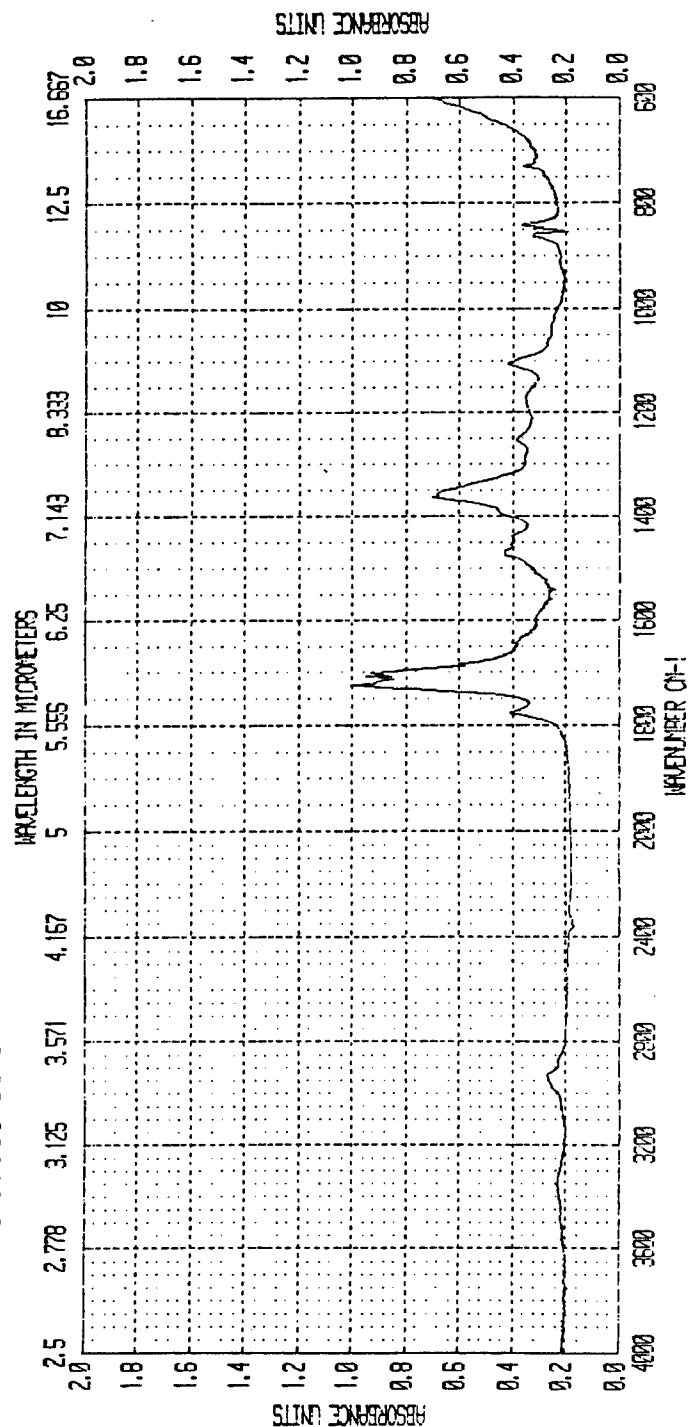


t=10 min. @260°C

Scan Name	260/10
Resolution	4
Apodized	no
Scale	4000.93
Gain	401.12
Scan Time	30 scans
First Y	0.2075

Scan Name	260715
Resolution	4
Modulated	no
Start	4000.93
End	401.12
Scan Time	30 scans
First Y	0.2103

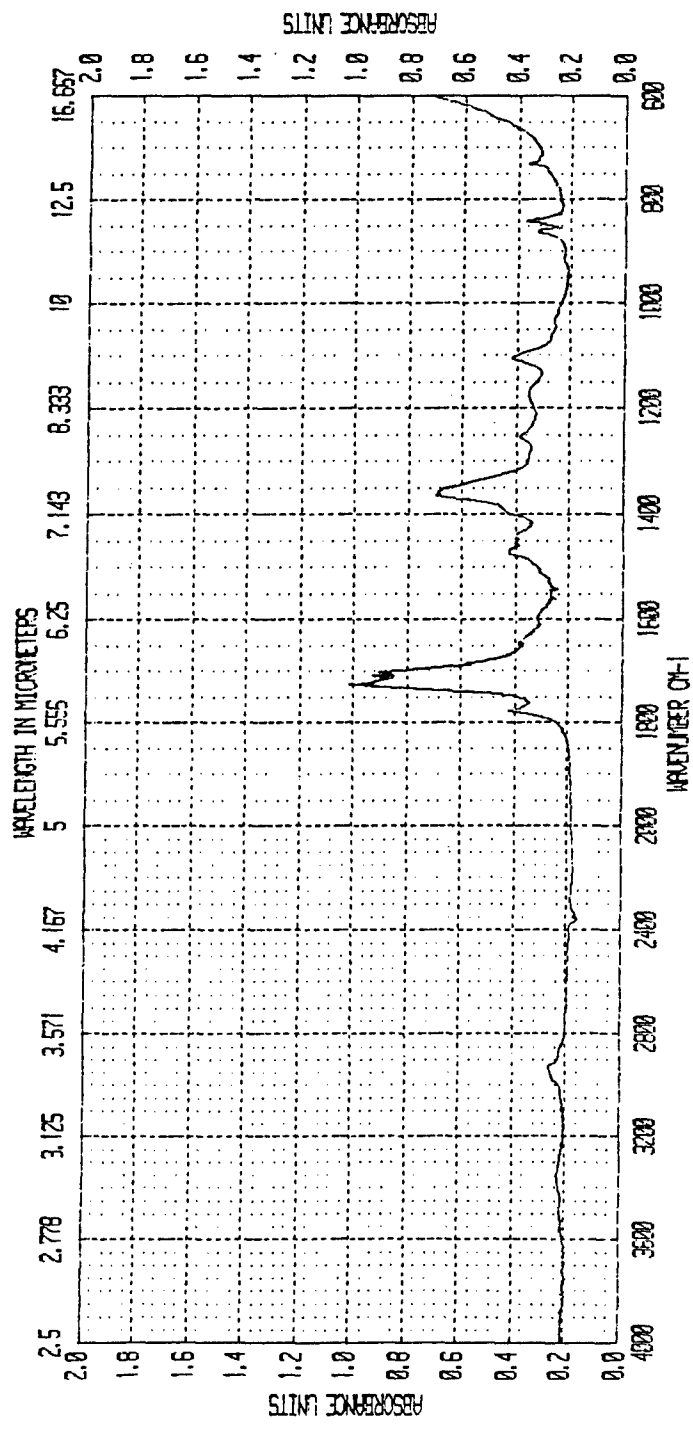
**BECKMAN**



t=15 min. @260°C

Scan Name	260/20
Resolu	4
Modified	no
Start	4000.93
End	401.12
Scan time	30 scans
First Y	0.2129

# BECKMAN

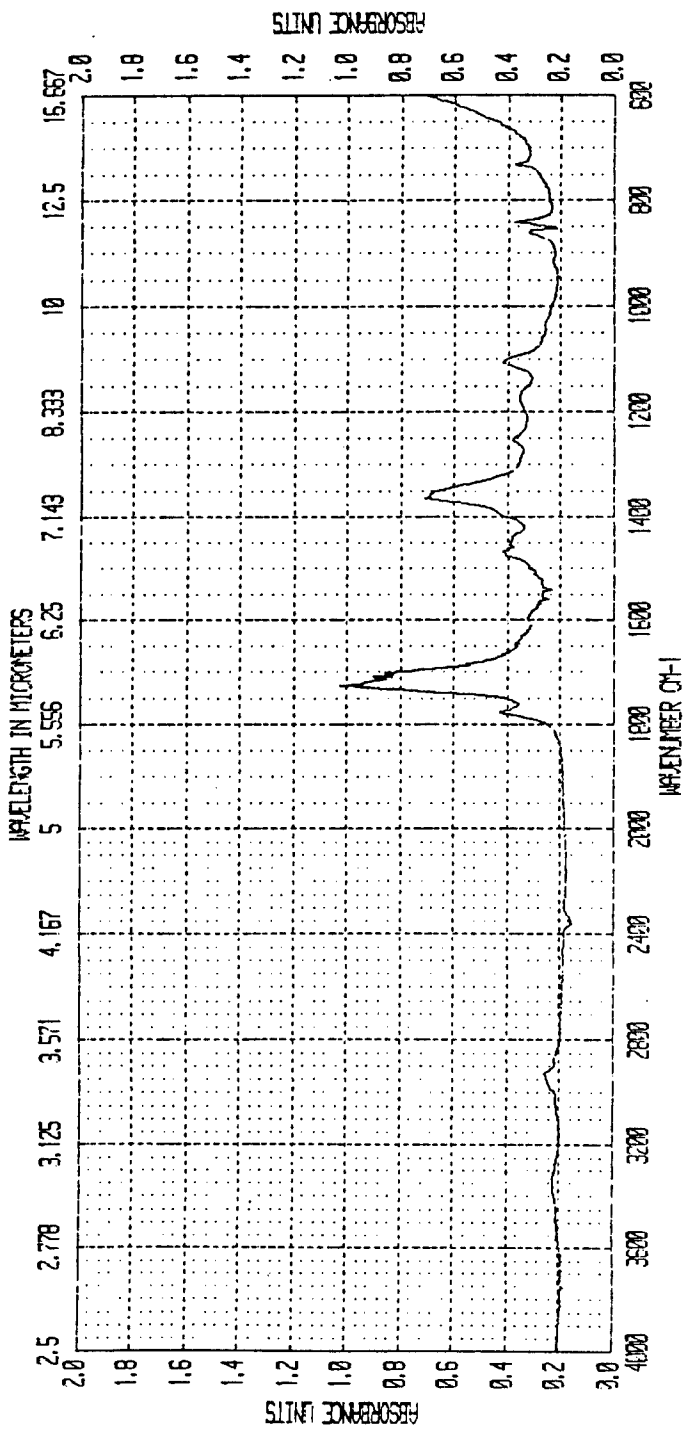


t=20 min. @260°C



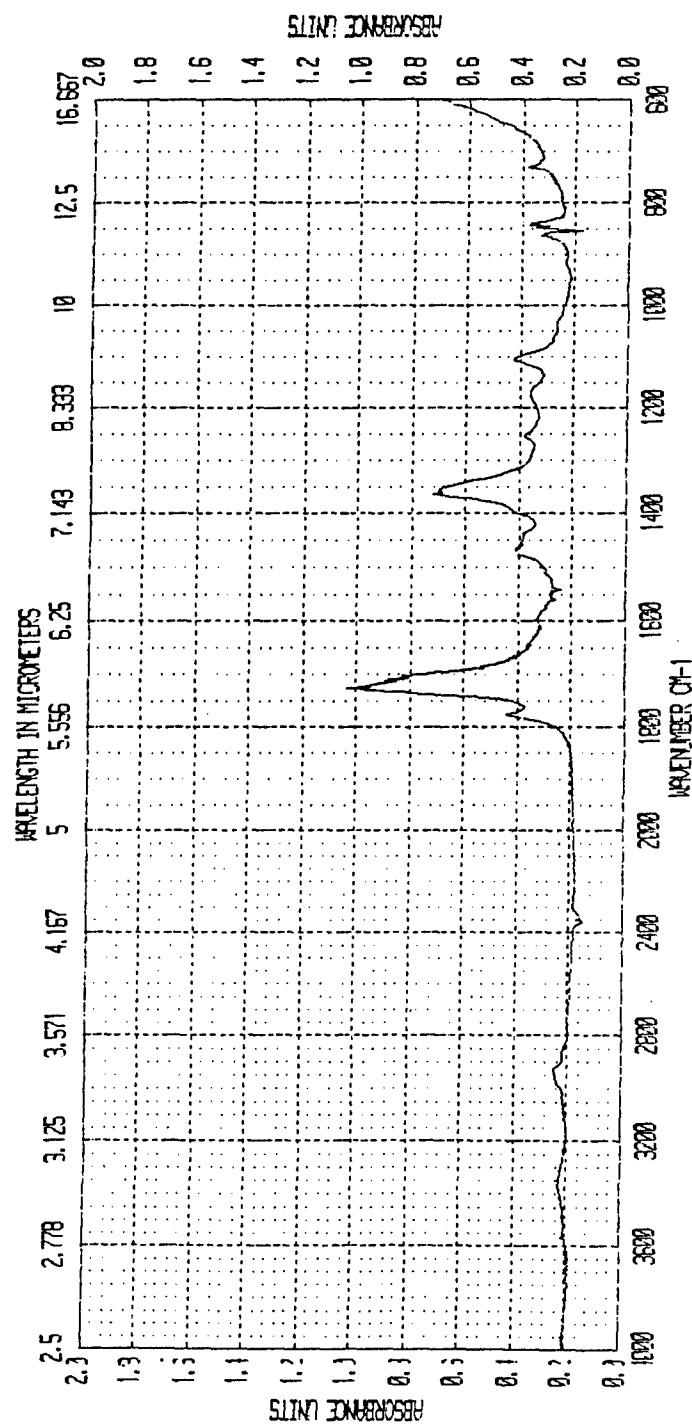
Scan Name	260/30
Resolu	4
Applied	260C FOR 30 MIN
start	4000.93
end	401.12
Scan time	30 scans
First Y	0.2055

# BECKMAN



t=30 min. @260°C

# BECKMAN

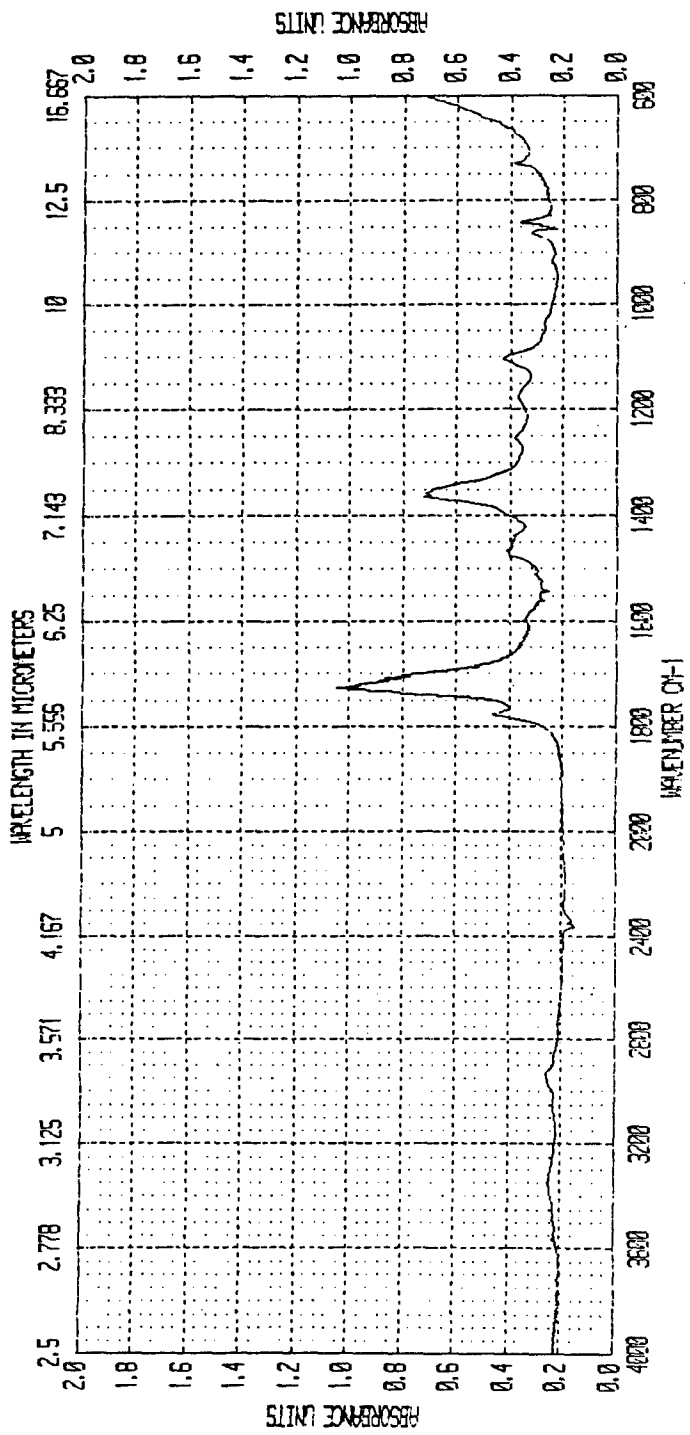


t=40 min. @260°C

Scan Name	260/40
Resolution	4
Wavelength	2600 FOR 40 MIN
Scan Time	4000.93
Scan Length	401.12
Scan Time	30 scans
Scan Time	0.2083

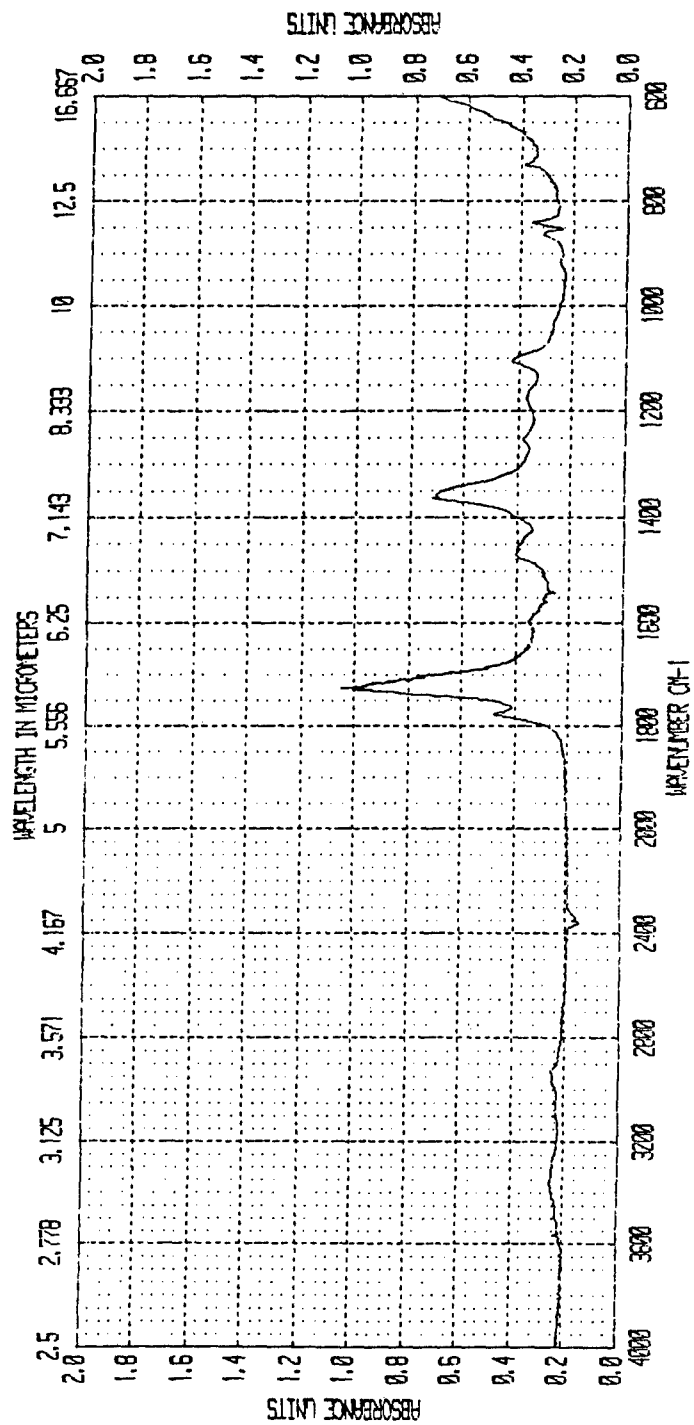
Scan Name	260/60
Resolution	4
Apodized	no
Start	4000.33
End	401.12
Scan time	30 scans
First Y	0.2199

# BECKMAN



t=60 min. @260°C

# BECKMAN

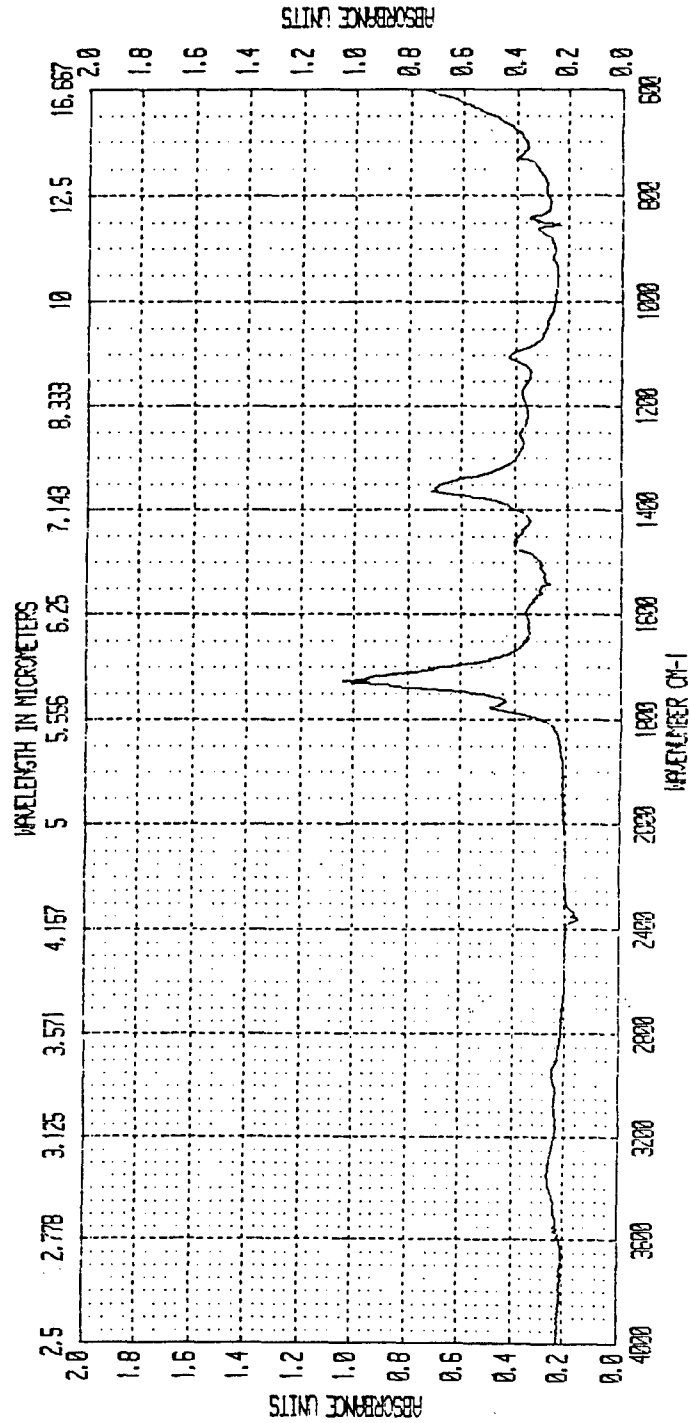


t=90 min. @260°C

Scan Name	260/90
Resolution	4
Apodized	no
Start	4000.93
End	401.12
Scan Time	30 scans
First Y	0.2188

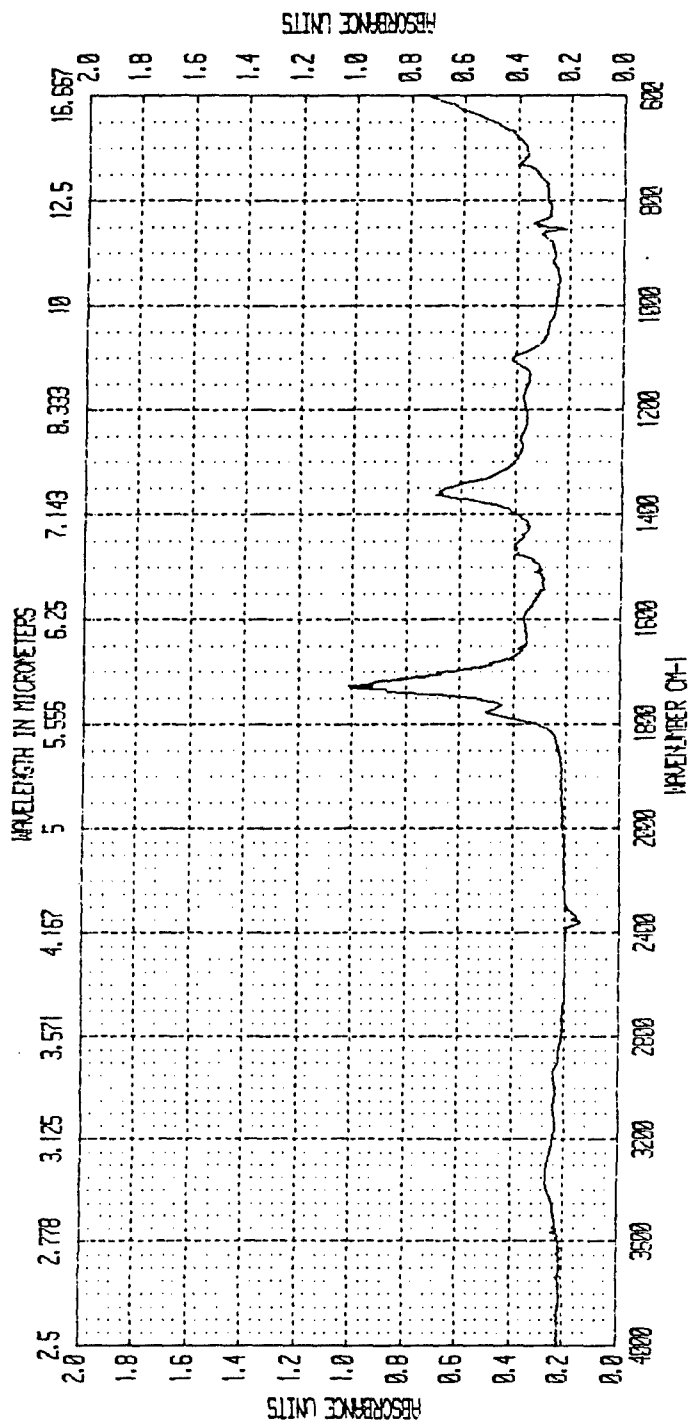
Scan Name	Resolu	Hpodized	Start	End	Scan Time	First Y
260/150	4	no	4000.93	401.12	30 scans	0.2240
260C FOR 150 MIN						

# BECKMAN



t=150 min. @260°C

# BECKMAN

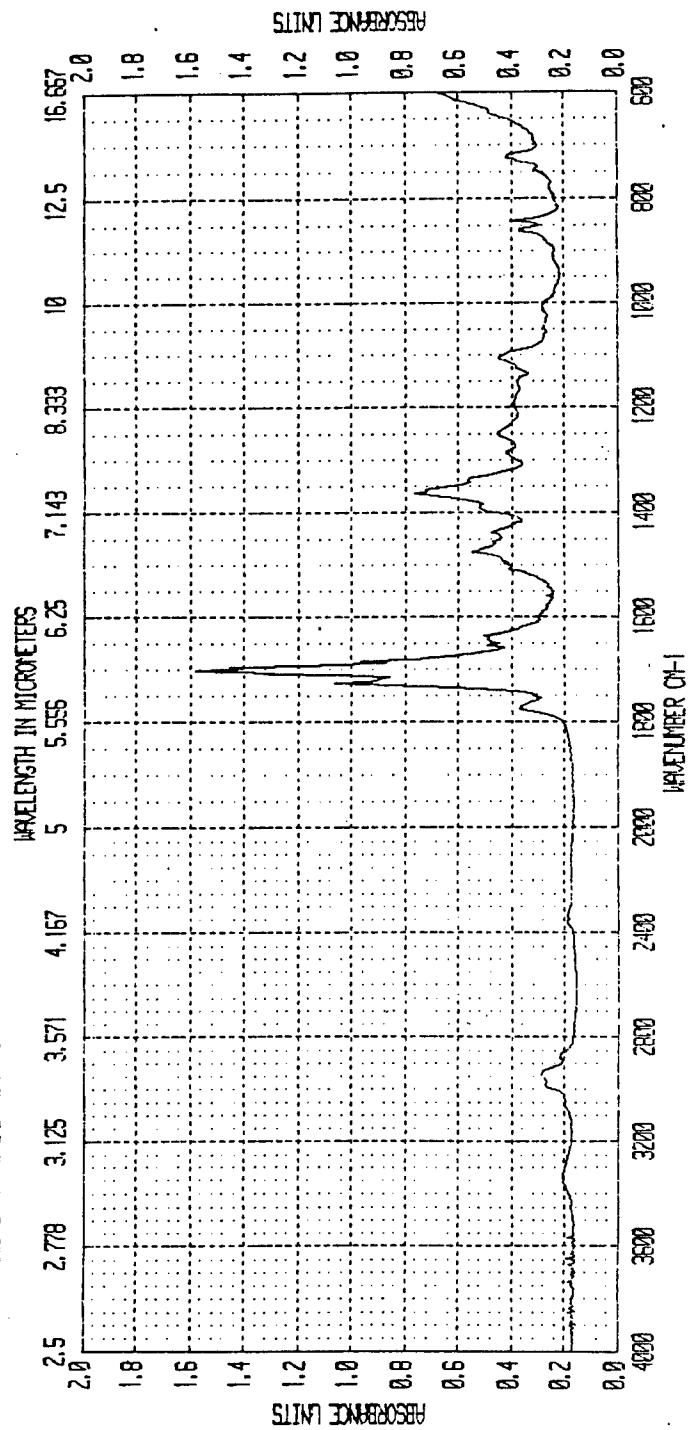


t=240 min. @260°C

Scan Name	Result	Apodized	Start	End	Scan Time	First Y
260/240		no	4000.93	401.12	30 scans	0.2211
260C FOR 240 MIN						

Scan Name	280/0
Resolu	4
Apodized	no
Start	4000.93
End	401.12
Scan Time	9 seconds
First Y	0.1706

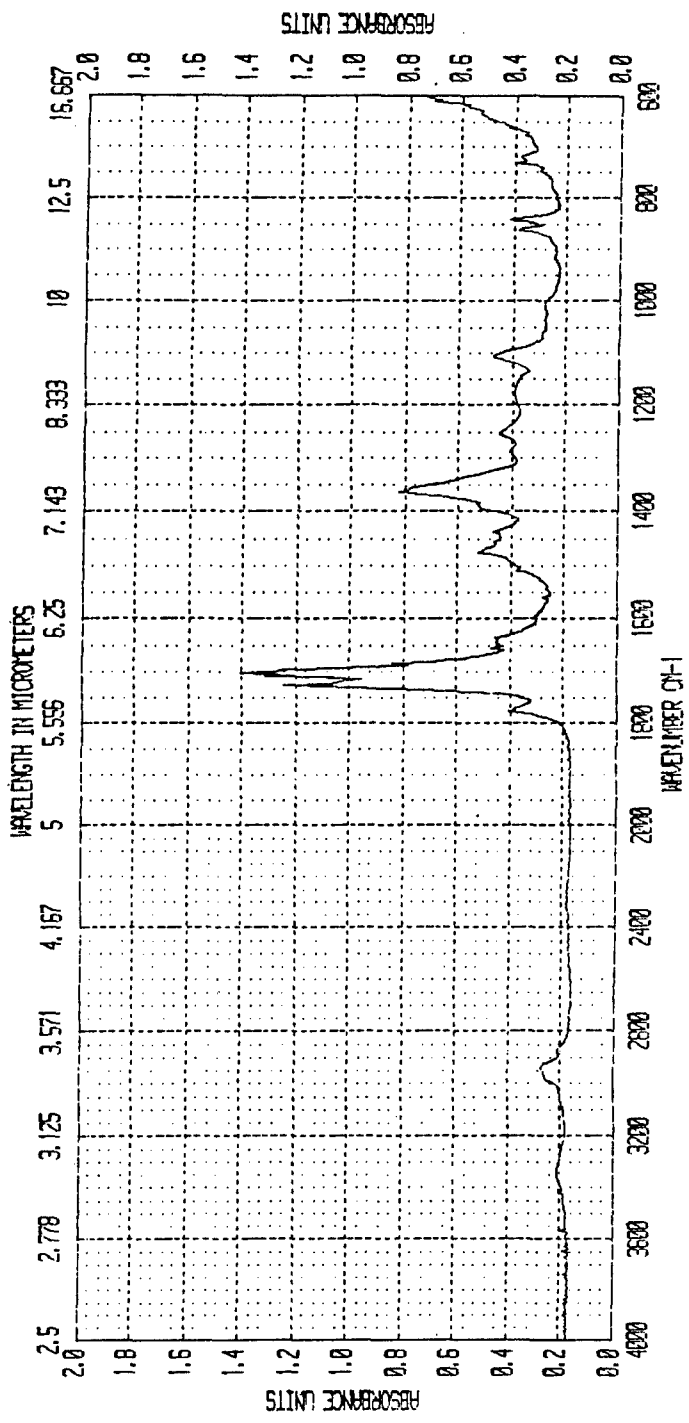
# BECKMAN



t=0 min. @280°C

Scan Name	280/5
Resolu	4
Apodized	no
Start	4000.93
End	401.12
Scan Time	10 seconds
First Y	0.1721

# BECKMAN

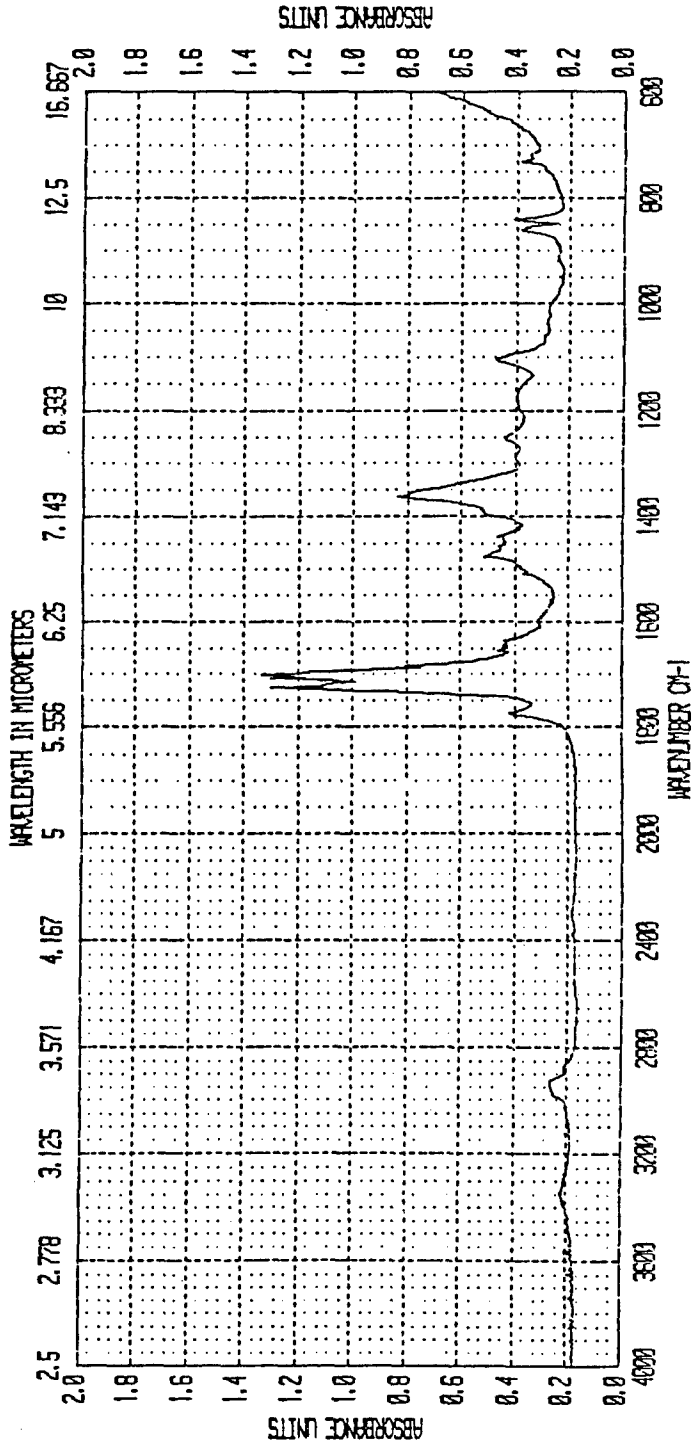


t=5 min. @280°C



Scan Name	280710
Resolution	4
Apodized	no
Start	4000.93
End	401.12
Scan Time	11 seconds
First Y	0.1752

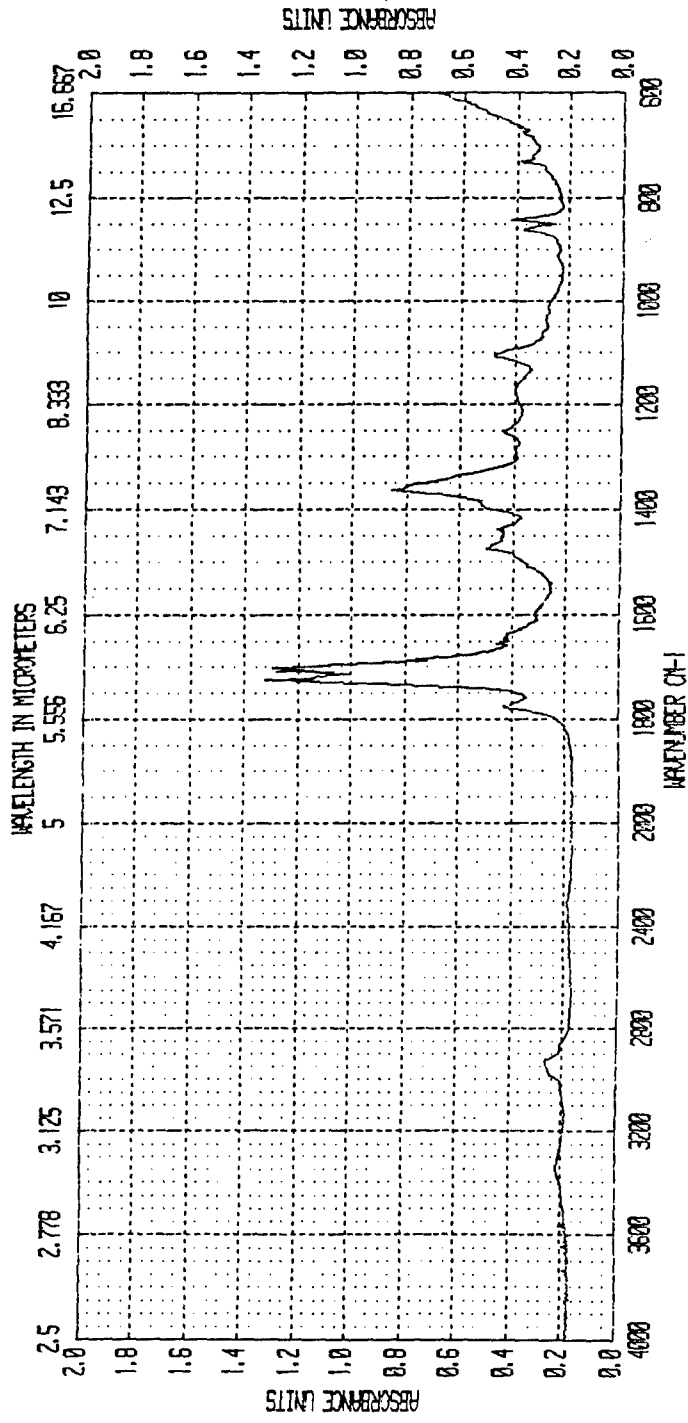
# BECKMAN



t=10 min. @280°C

Scan Name	2807.15	4	280C FOR 15 MIN	4000.93	401.12	10 seconds	0.1770
Resolu							
Apodized							
Start							
End							
Scan Time							
First y							

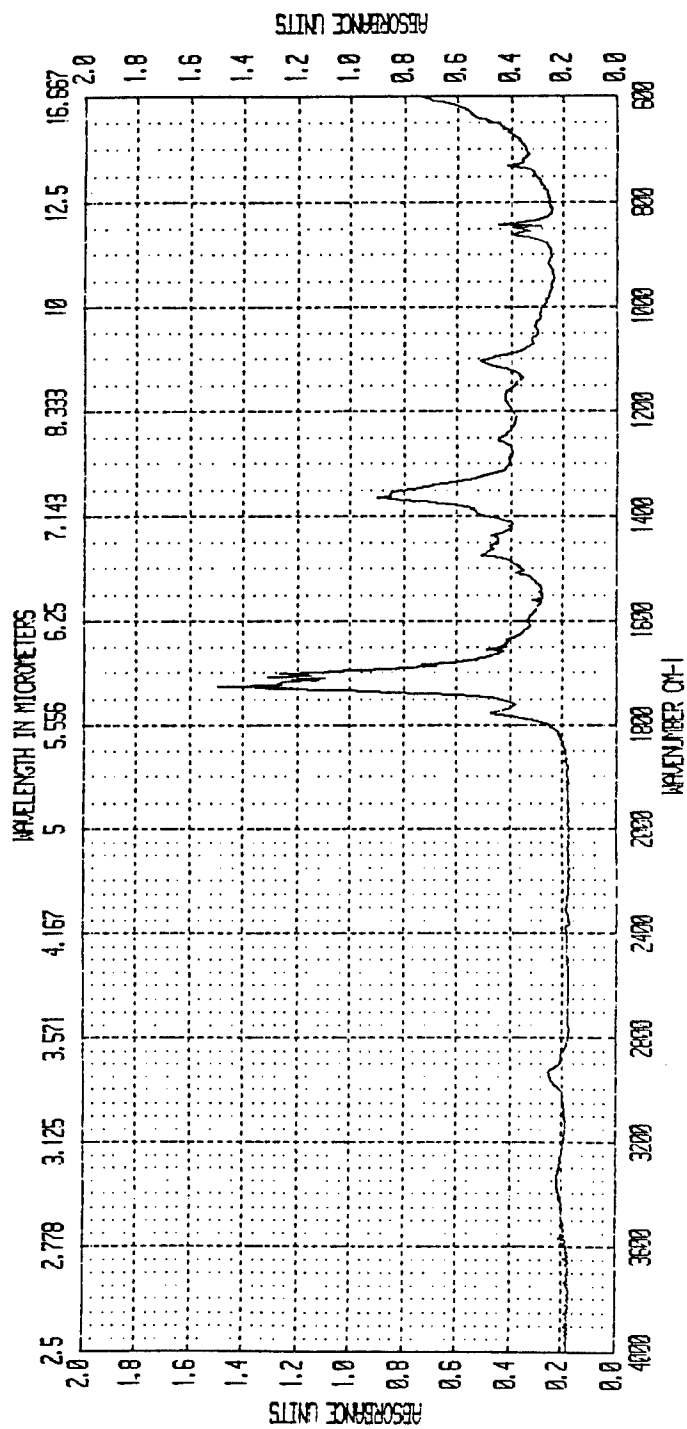
# BECKMAN



t=15 min. @280°C

Scan Name	280/J0
Resolu	4
Apodized	no
Start	4000.93
End	401.12
Scan time	10 seconds
First Y	0.1810

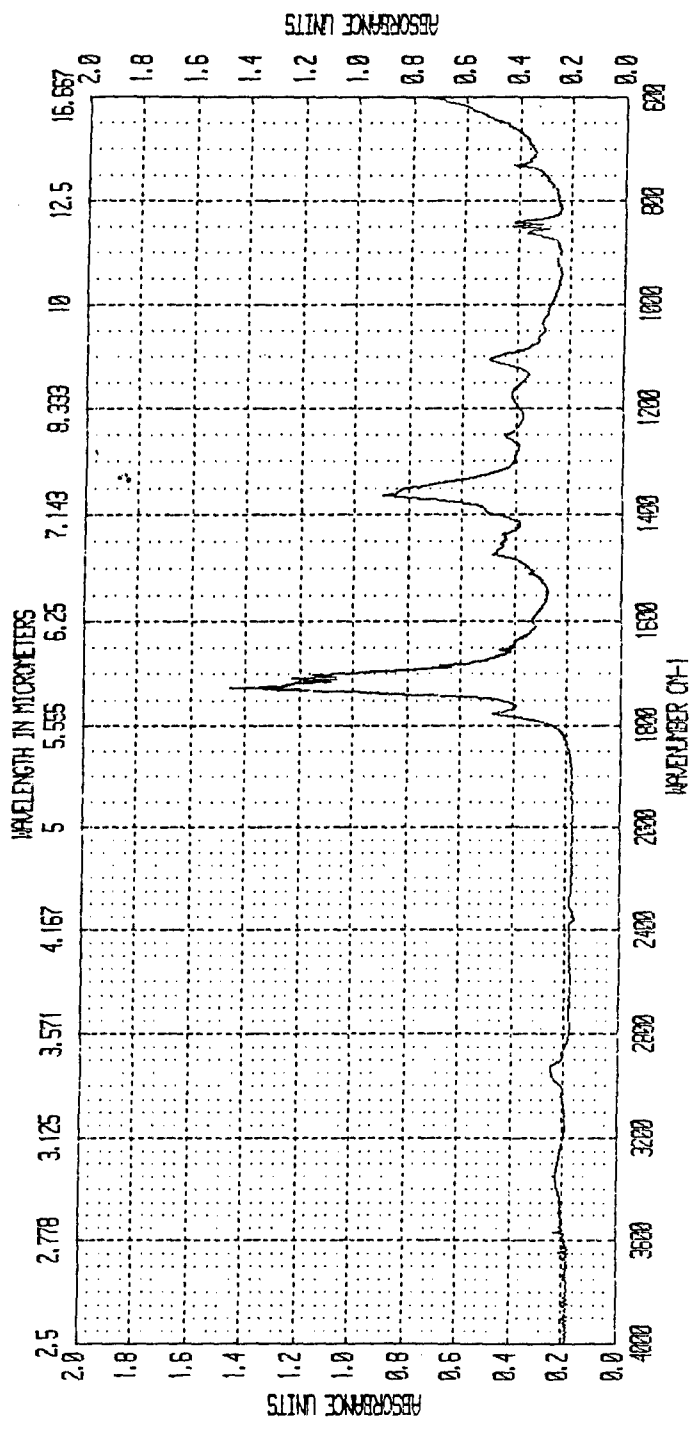
# BECKMAN



t=30 min. @280°C

Scan Name	280/40
Resolu	4
Apodized	no
Start	4000.93
End	401.12
Scan Time	11 seconds
First Y	0.1863

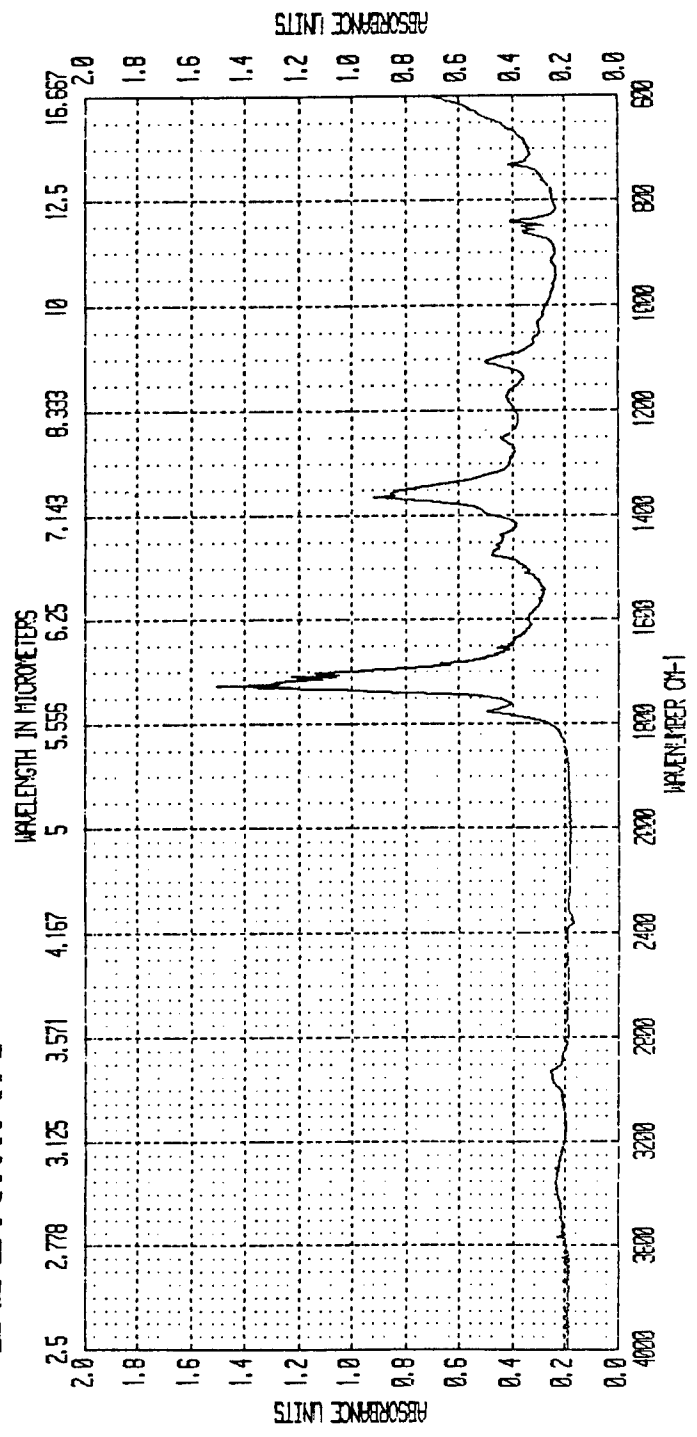
# BECKMAN



t=40 min. @280°C

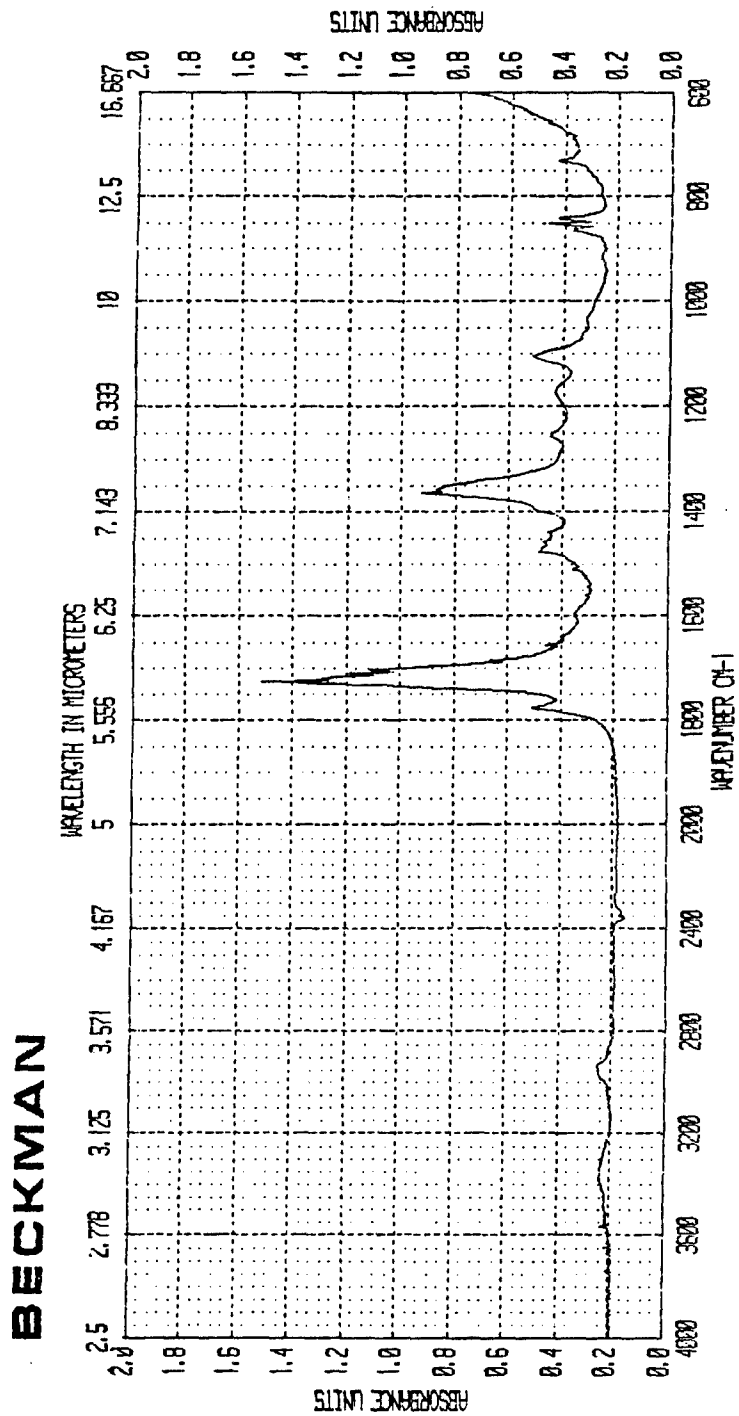
Scan Name	280/50
Resolu	4
Apodized	no
Start	4000.93
End	401.12
Scan Time	30 seconds
First Y	0.1388

# BECKMAN



t=50 min. @280°C

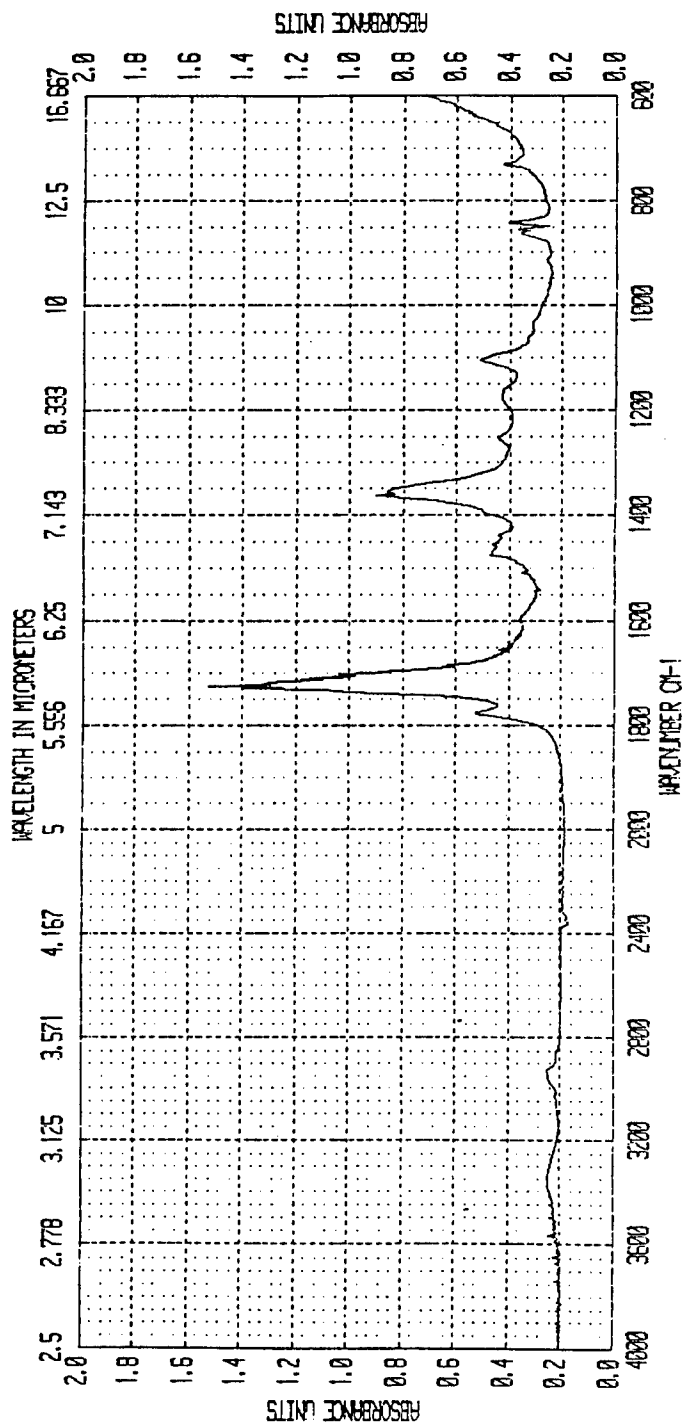
Scan Name	Resolu	Apodized	Start	End	Scan Time	First Y
280/60	4	2800 FOR 60 MIN	4000.93	401.12	11 seconds	0.1965



t=60 min. @280°C

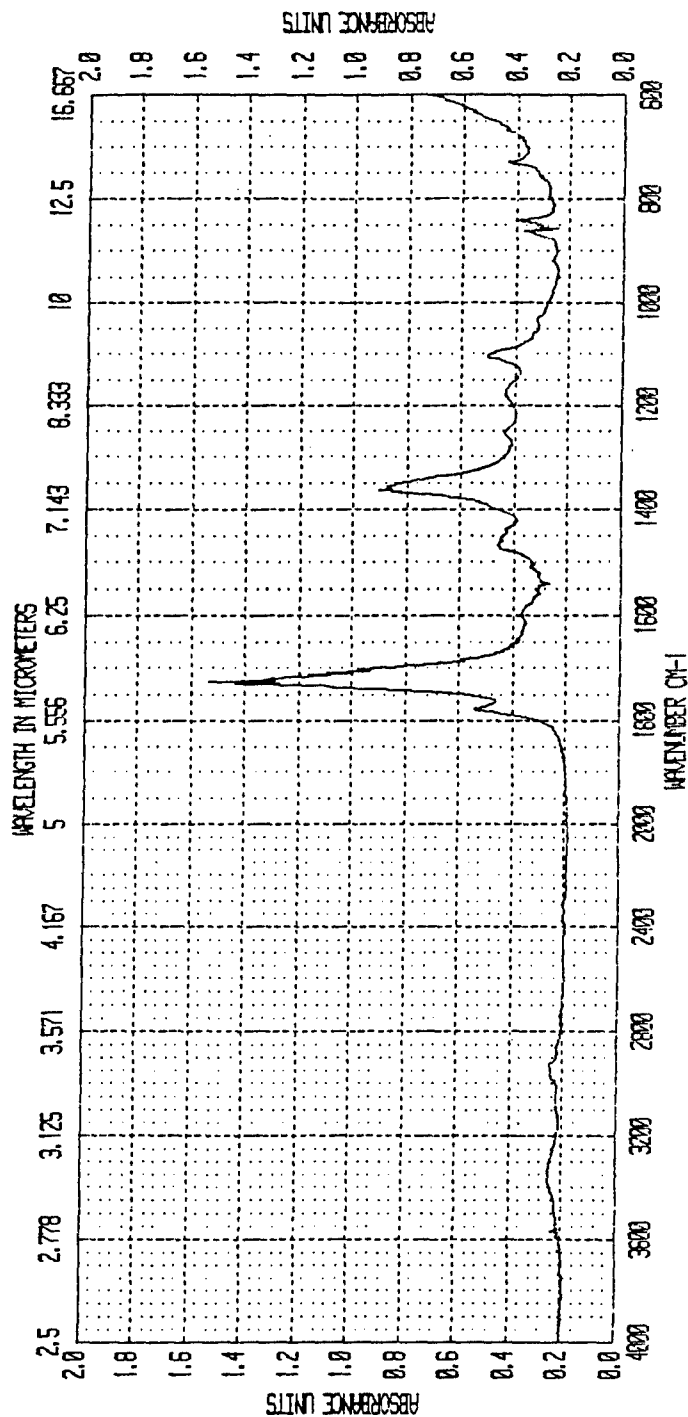
Scan Name	280/90
Resolu	4
Apodized	no
Start	4000.93
End	401.12
Scan Time	9 seconds
First Y	0.2016

**BECKMAN**



t=90 min. @280°C

# BECKMAN



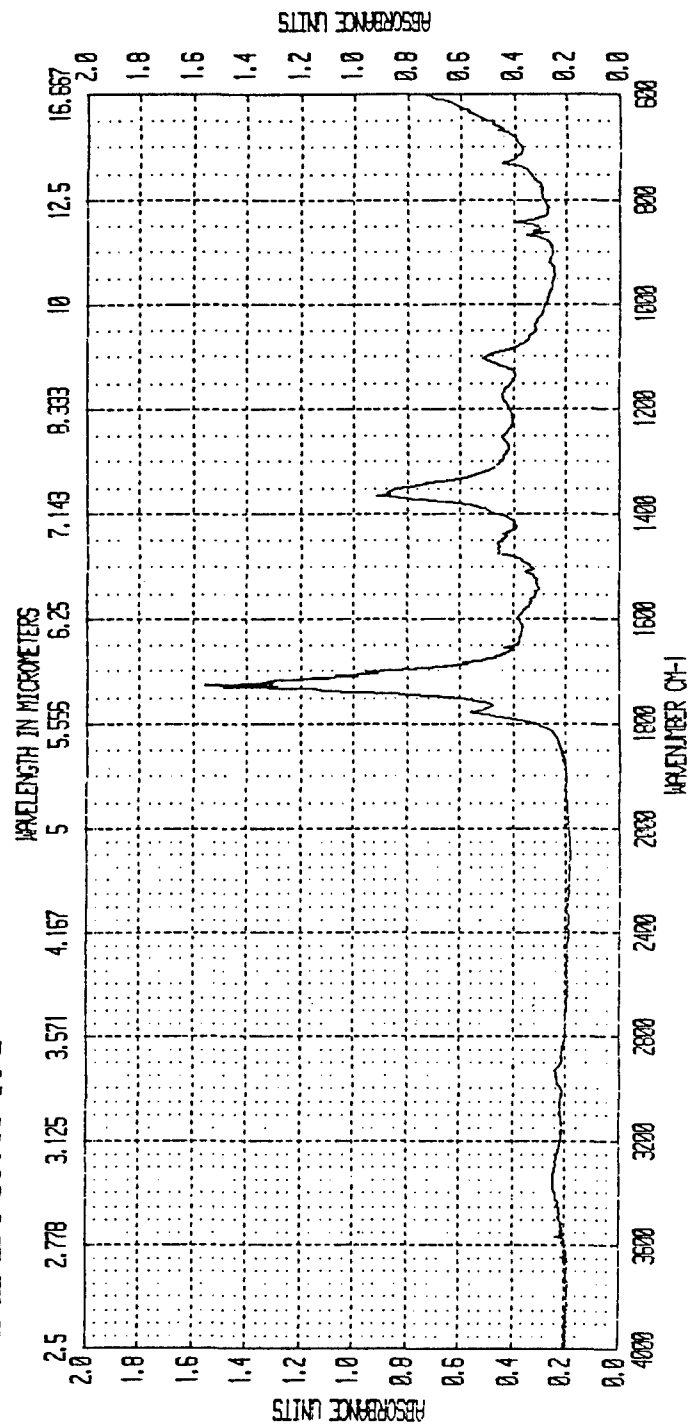
t=130 min. @280°C

Scan Name	280/130	4	280C FOR 130 MIN	4000.93	401.12	10 seconds	0.2011
Resolu				Start	End	Scan Time	First Y
Apodized							



Scan Name	280/180
Resolu	4
Apodized	no
Start	4000.93
End	401.12
Scan Time	10 seconds
First Y	0.1950

# BECKMAN



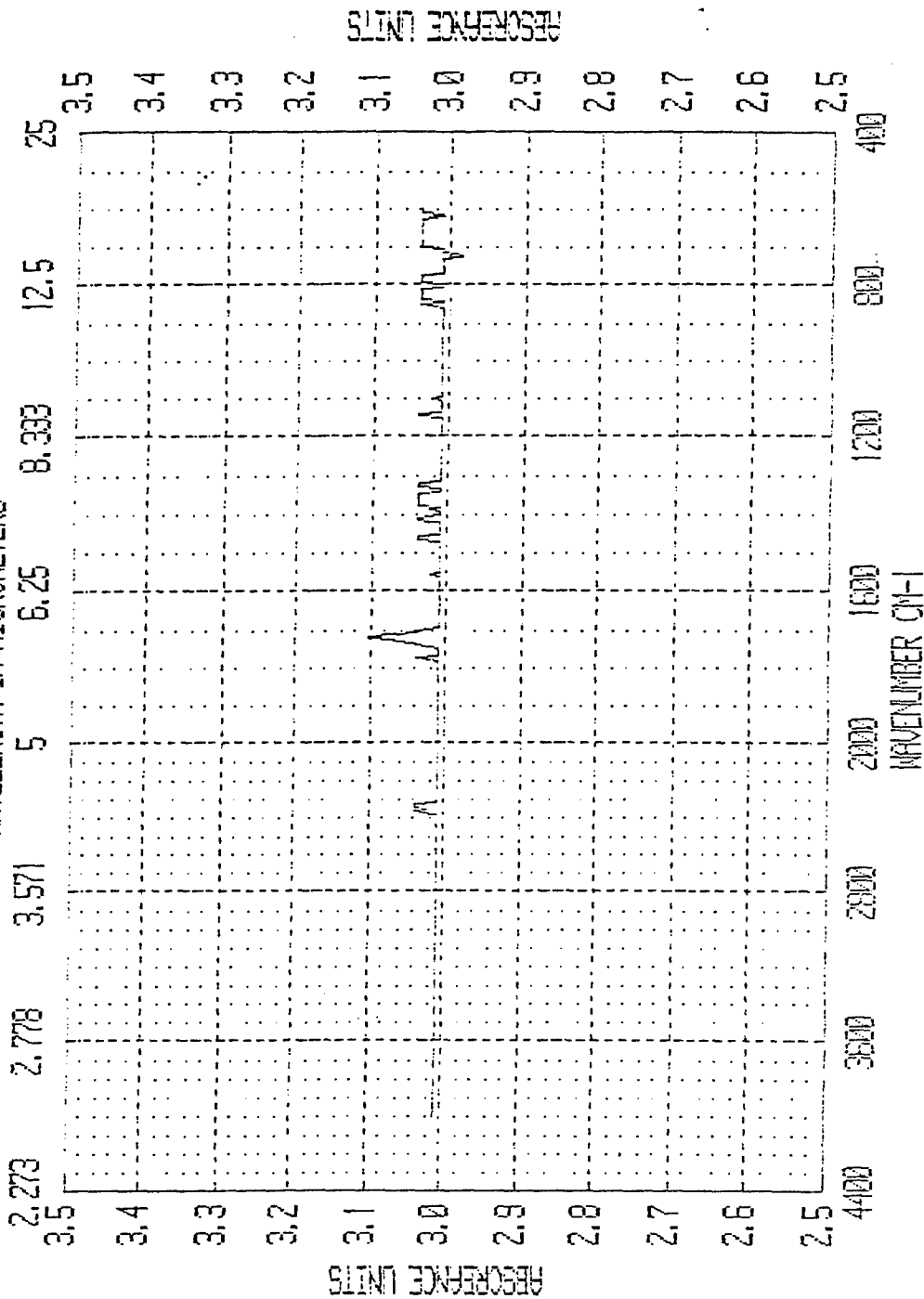
t=180 min. @280°C

## **APPENDIX D**

### **Subtraction Spectra from FTIR for PAA/DNI-3A**

# BECKMAN

WAVELENGTH IN MICROMETERS

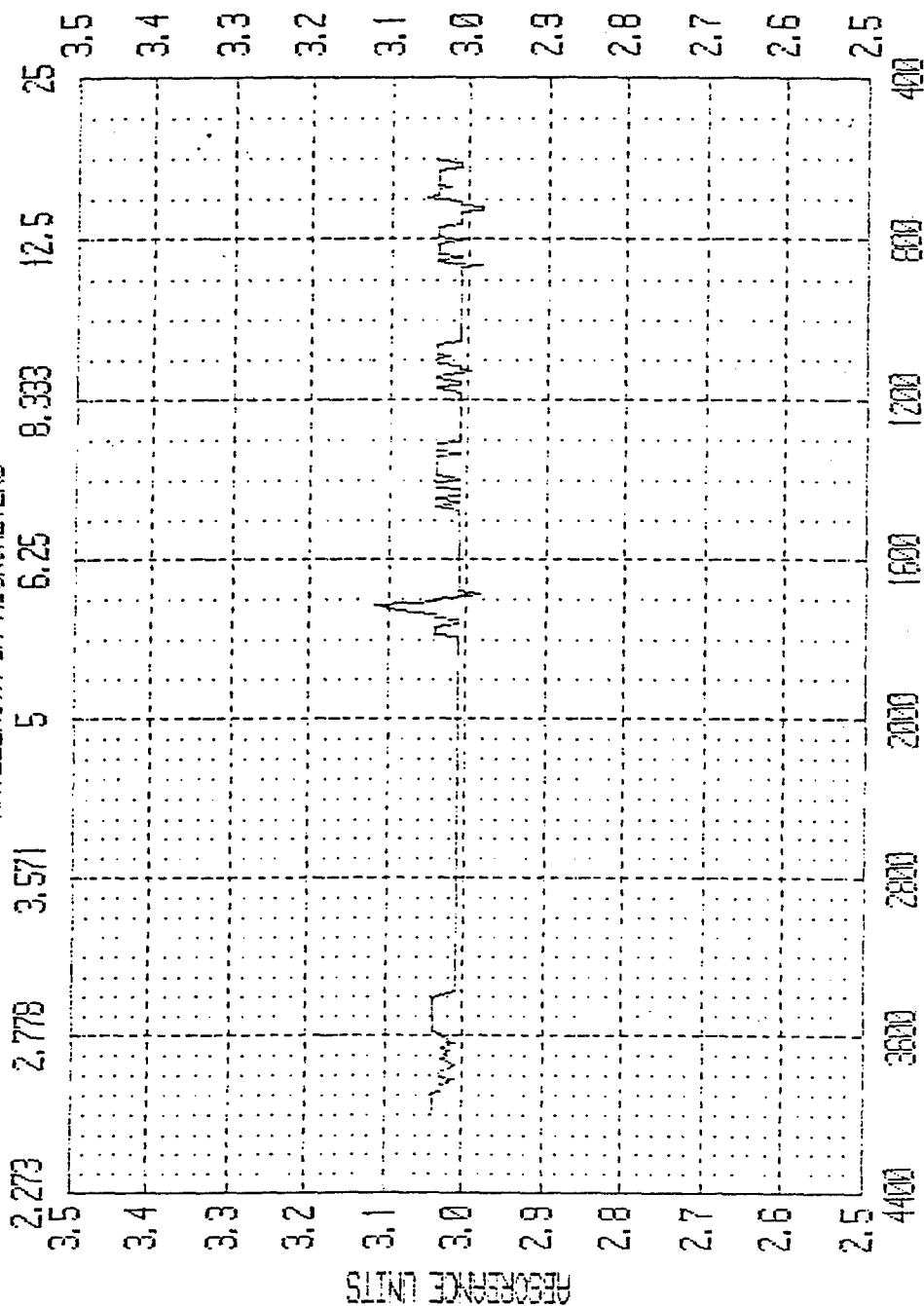


t=10 - 0 min. @240°C

Scan Name	Result	Apodized	Start	End	Scan Time	First Y
4	3598.36	no	401.12	30 scans	3.0103	
No additional information						
40% - 200%						
RESULT						

# PERKINELMER

WAVELENGTH IN MICROMETERS

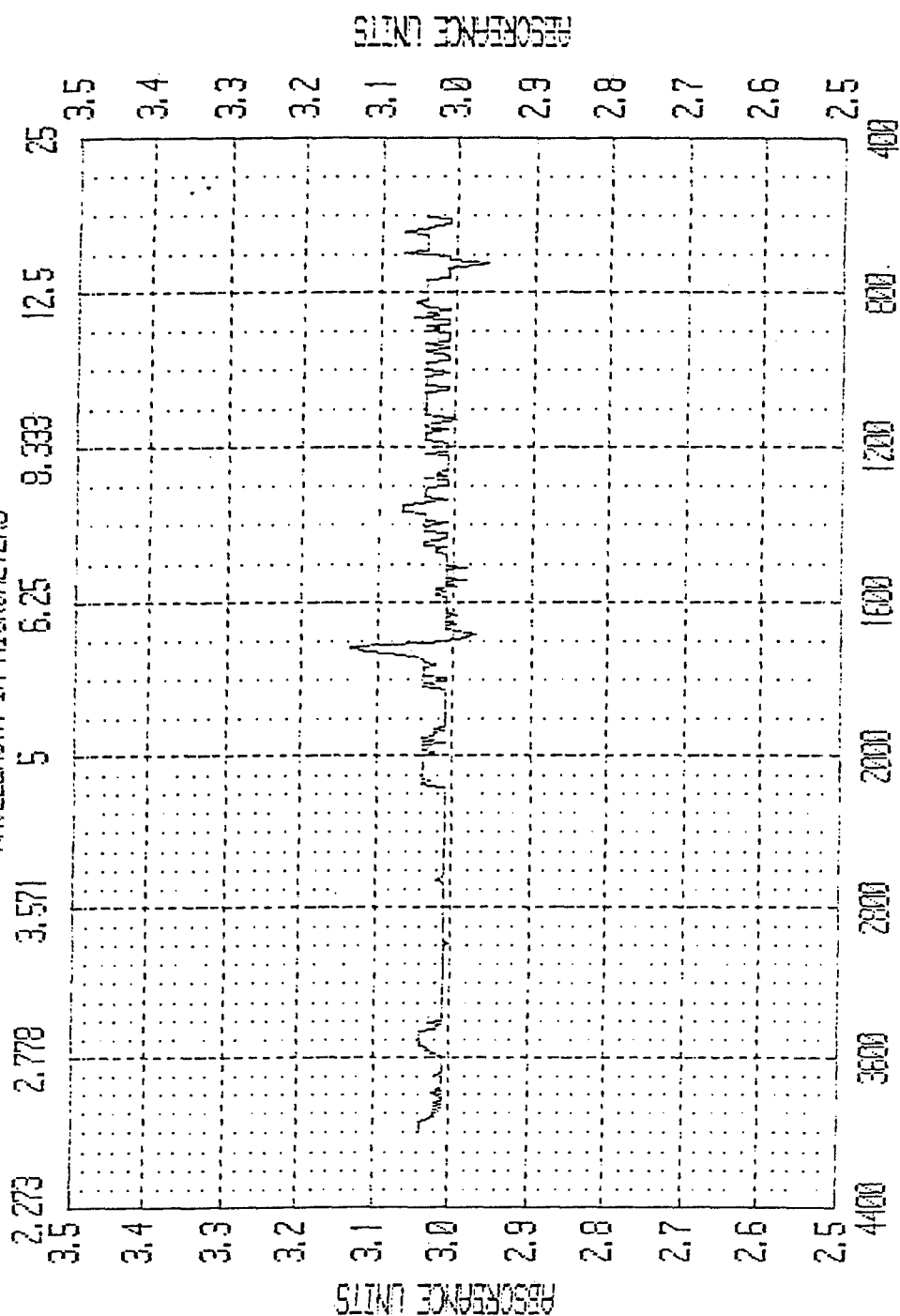


t=20 - 0 min. @240°C

Scan Name	Resolu	Apodized	Start	End	Scan Time	First Y
RESULT	4	no	3598.36	401.12	30 scans	3.0384
No additional Information						
240/20 - 240%						

# BECKMAN

WAVELENGTH IN MICROMETERS



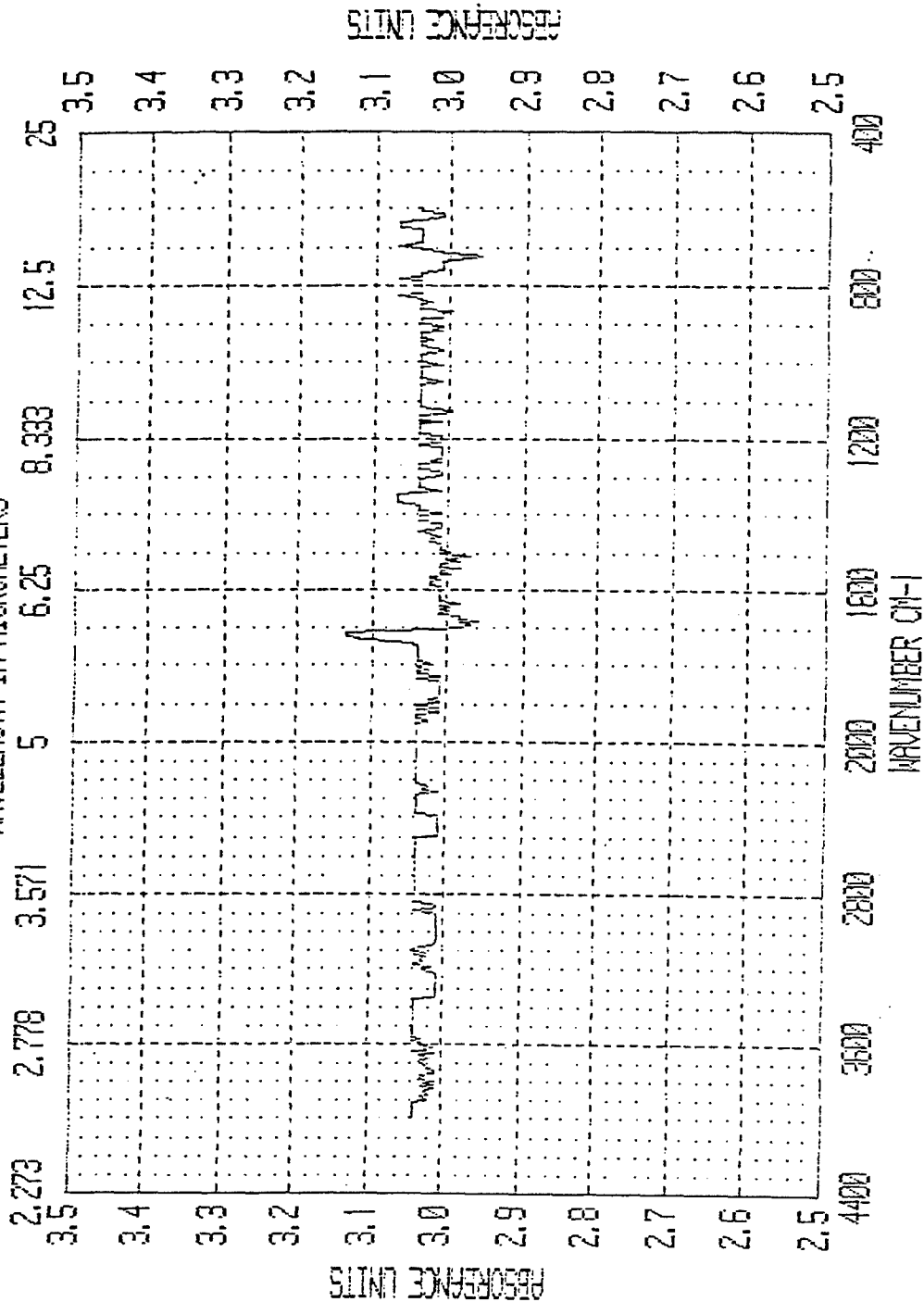
WAVELENGTH CN-1

t=40 - 0 min. @240°C

Scan Name	Resolu	Apodized	Start	End	Scan Time	First Y
RESULT	4	no	3998.36	401.12	30 scans	3.0384
No additional information						
240/40 - 200%						

# BECKMAN

WAVELENGTH IN MICROMETERS

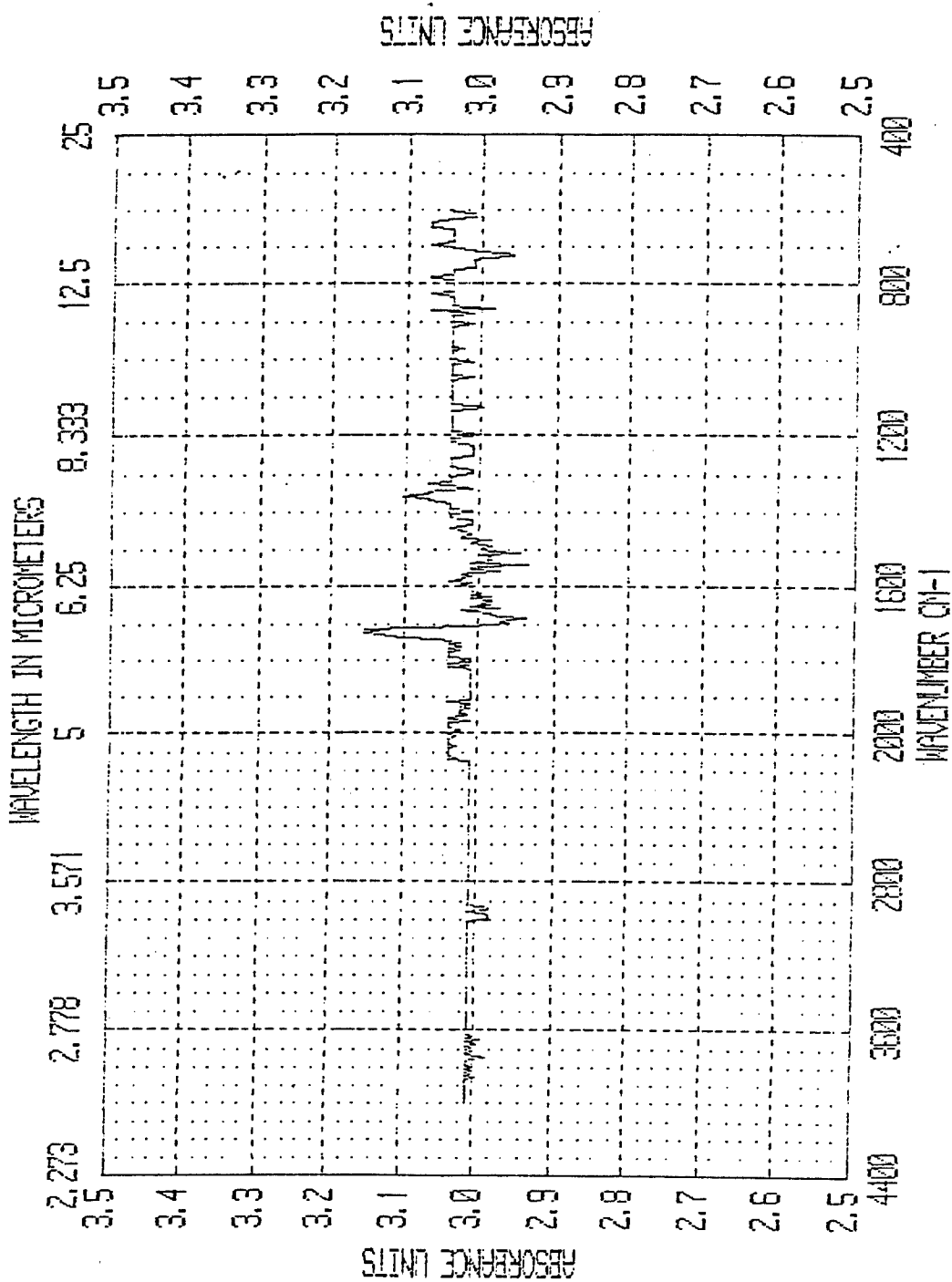


t=60 - 0 min. @240°C

Scan Name	Result	Apodized	Start	End	Scan Time	First y
4	3998.36	no	401.12	30 scans	3.0384	
No additional information						
240/60 - 240						

Scan Name	Result	Apodized	Start	End	Scan Time	First Y
RESUL1	4	no	3998.36	401.12	30 scans	3.0103
No additional information						
2401% - 240%						

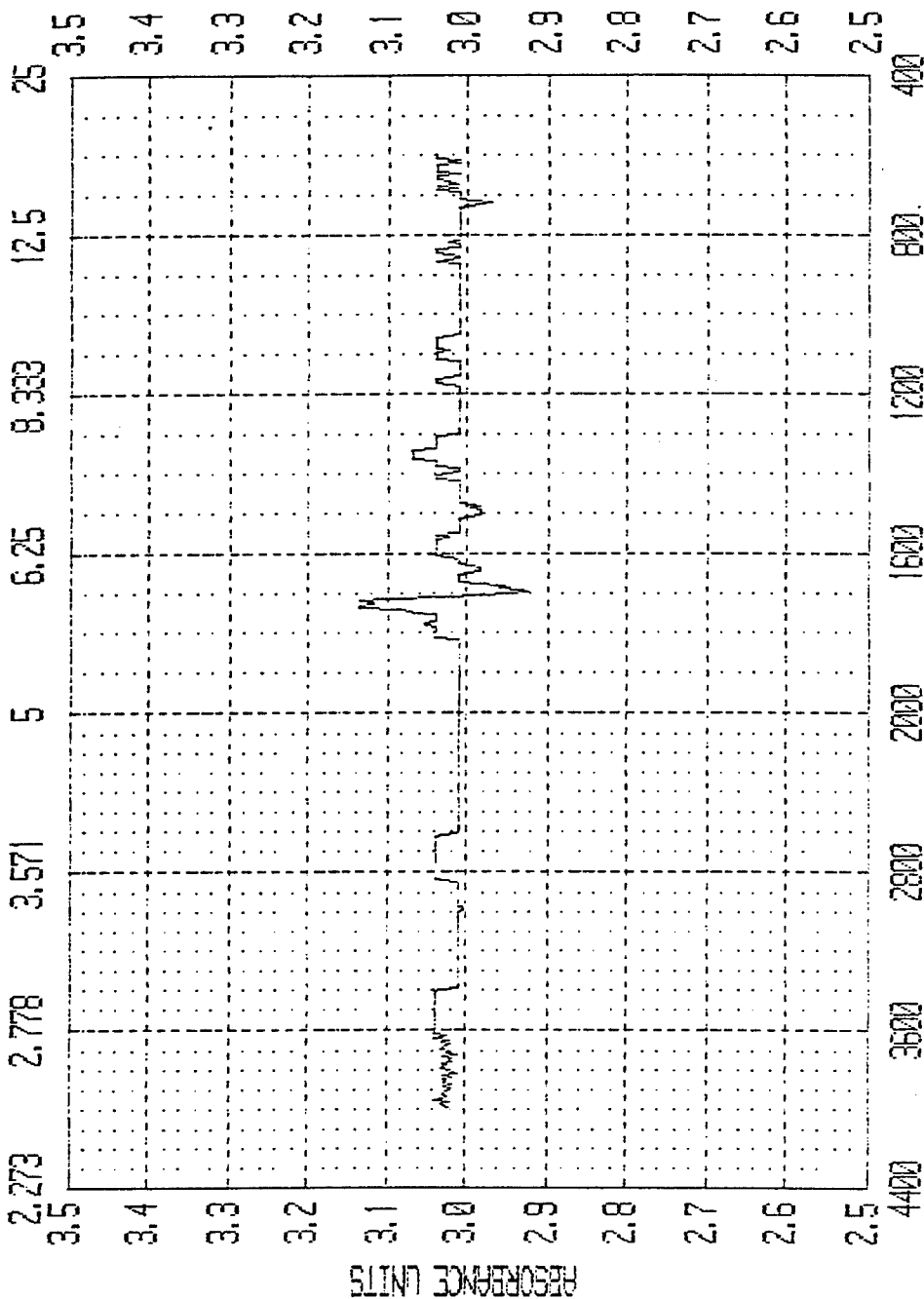
# BECKMAN



t=90 - 0 min. @240°C

# BECKMAN

WAVELENGTH IN MICROMETERS

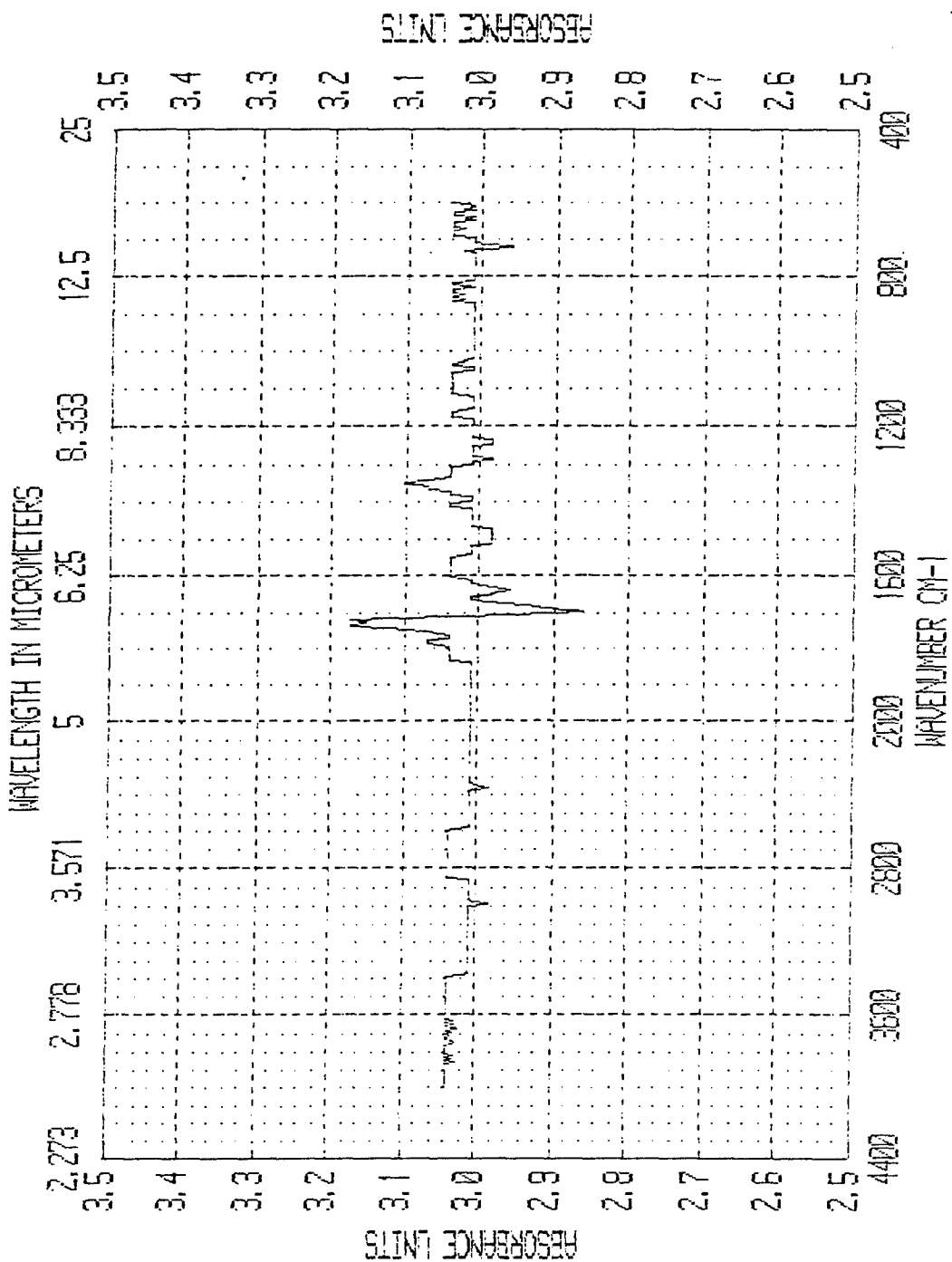


t=5 - 0 min. @260°C

Scan Name	Result	Apodized	Start	End	Scan Time	First Y
4	no	3998.36	401.12	30 scans	3.0103	
No additional information						
260/5 - 200%						



# BECKMAN

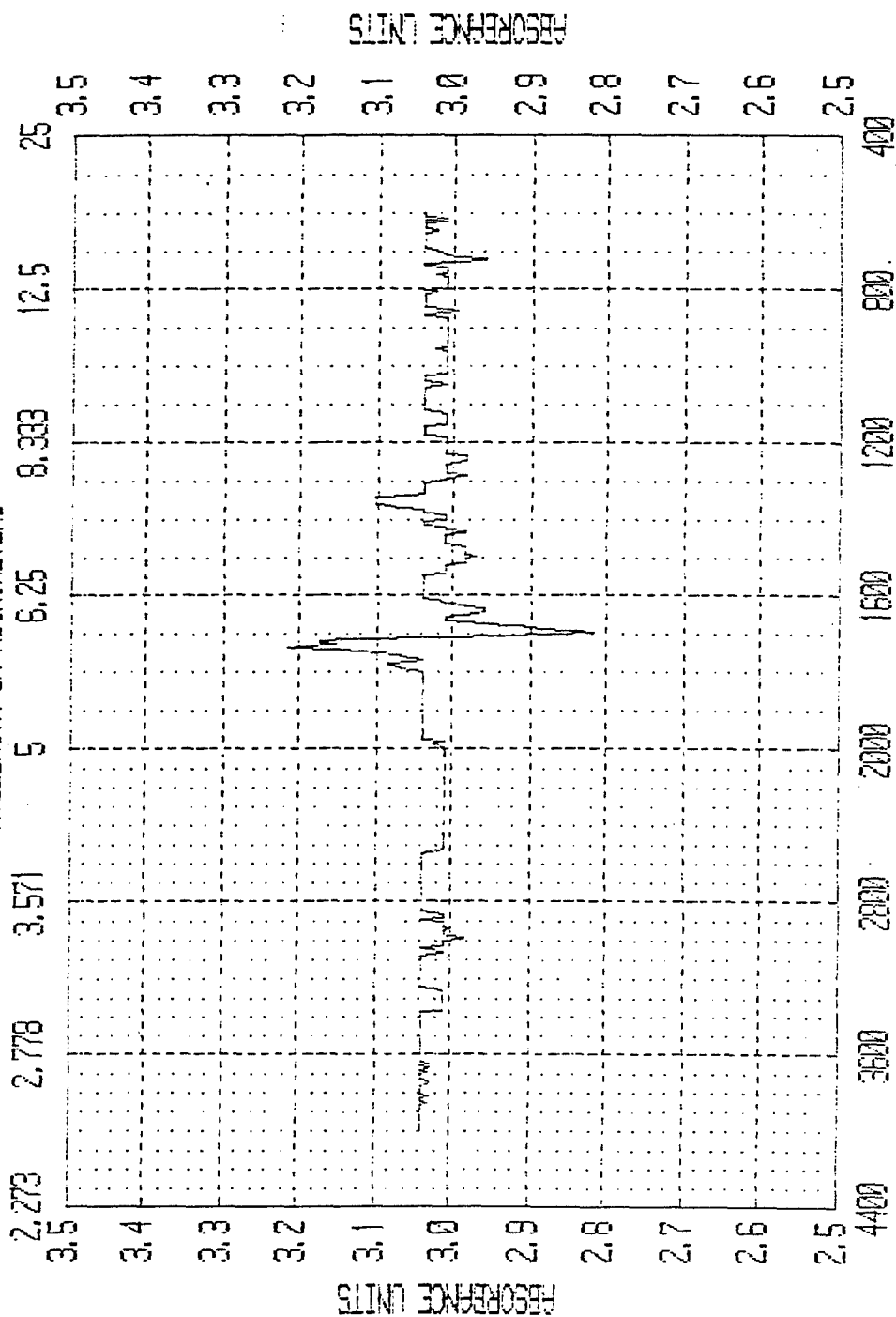


t=10 - 0 min. @260°C

Scan Name	Result	Apodized	Start	End	Scan Time	First Y
4	3598.36	no	401.12	30 scans	3.0324	
No additional information						
200/10 - 760/10						

# BECKMAN

WAVELENGTH IN MICROMETERS

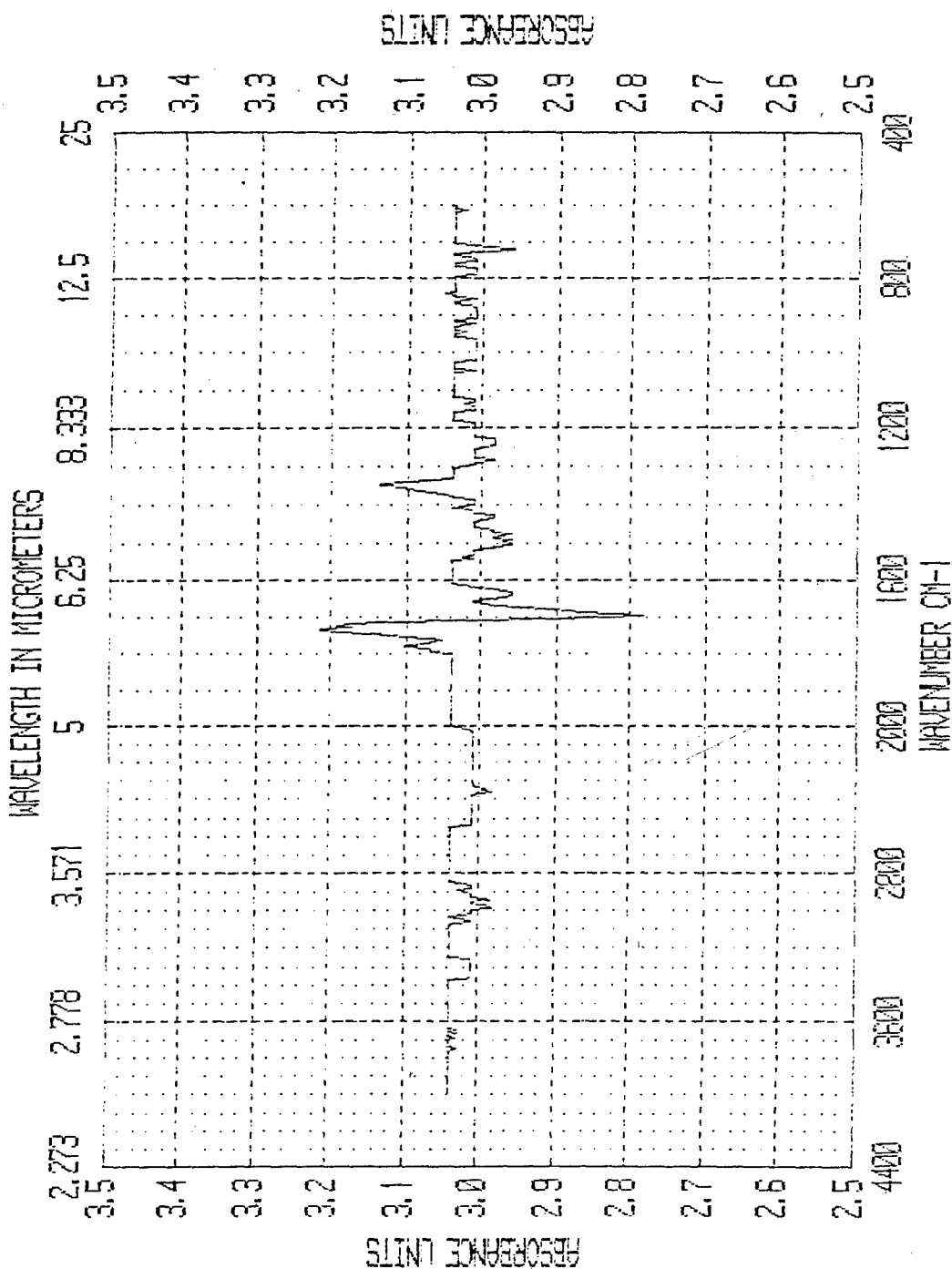


WAVENUMBER CM-1

t=15 - 0 min. @260°C

Scan Name	Result	Apodized	Start	End	Scan Time	First Y
4	No additional information	3958.36	401.12	30 scans	3.0384	
						260/15 - 260°

# BECKMAN

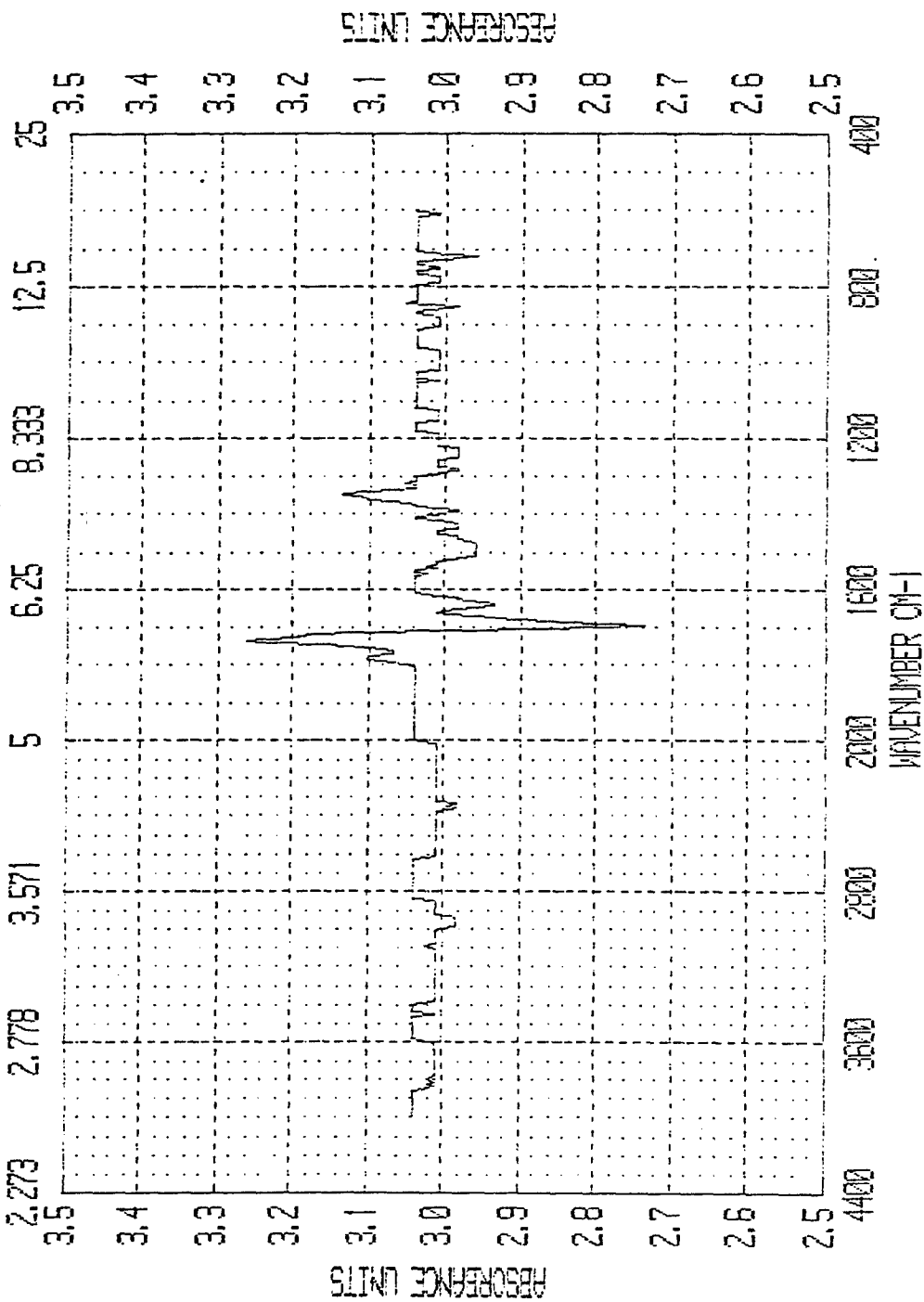


t=20 - 0 min. @260°C

Scan Name	Result	Apodized	Start	End	Scan Time	First Y
4	3998.36	no	401.12	30 scans	3.0384	
No additional information						
260°C - 26%						

# BECKMAN

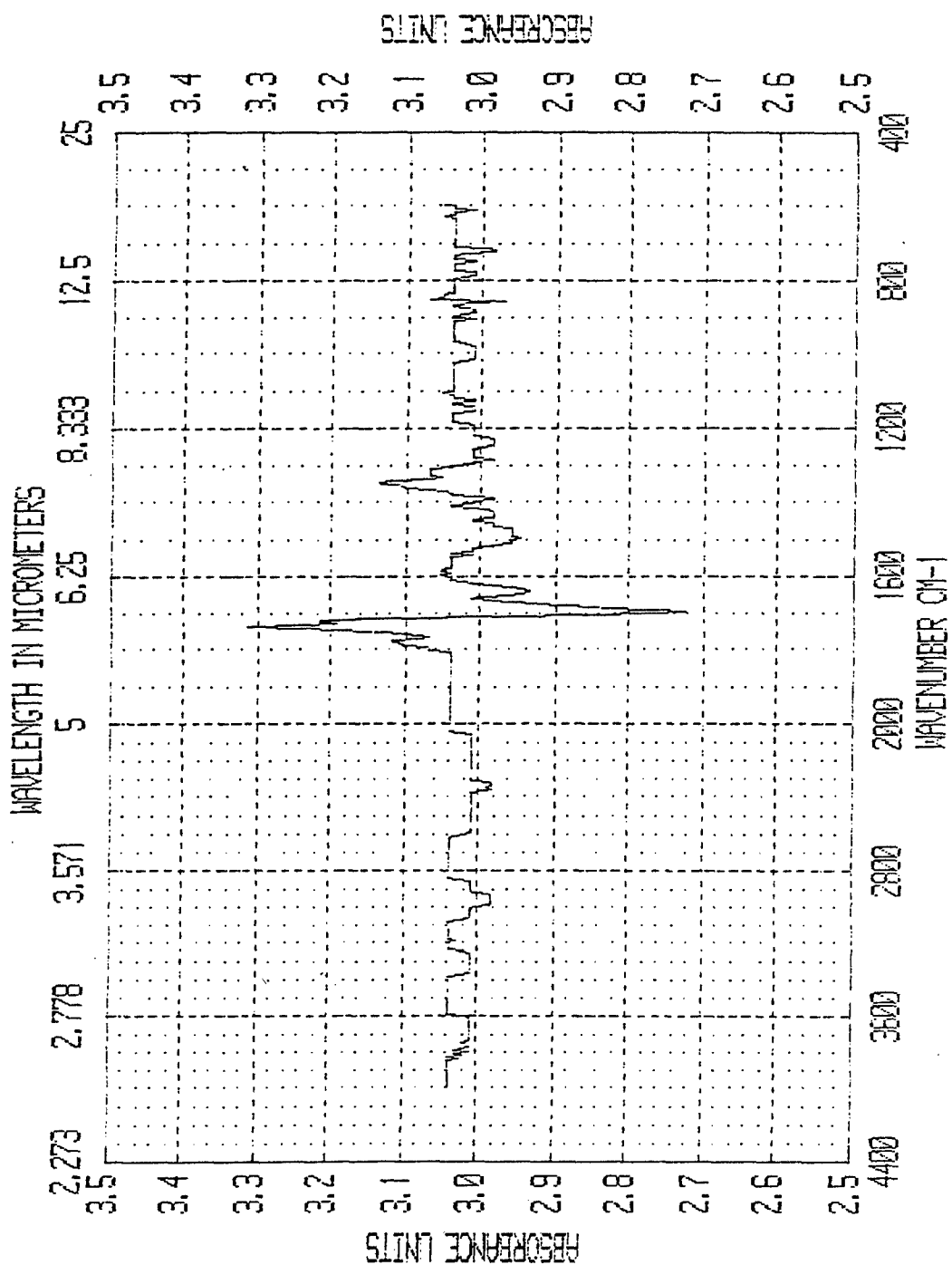
WAVELENGTH IN MICROMETERS



t=30 -0 min. @260°C

Scan Name	Result	Apodized	Start	End	Scan Time	First Y
4	no		3598.36	401.12	30 scans	3.0384
No additional information						
20% - 20%						

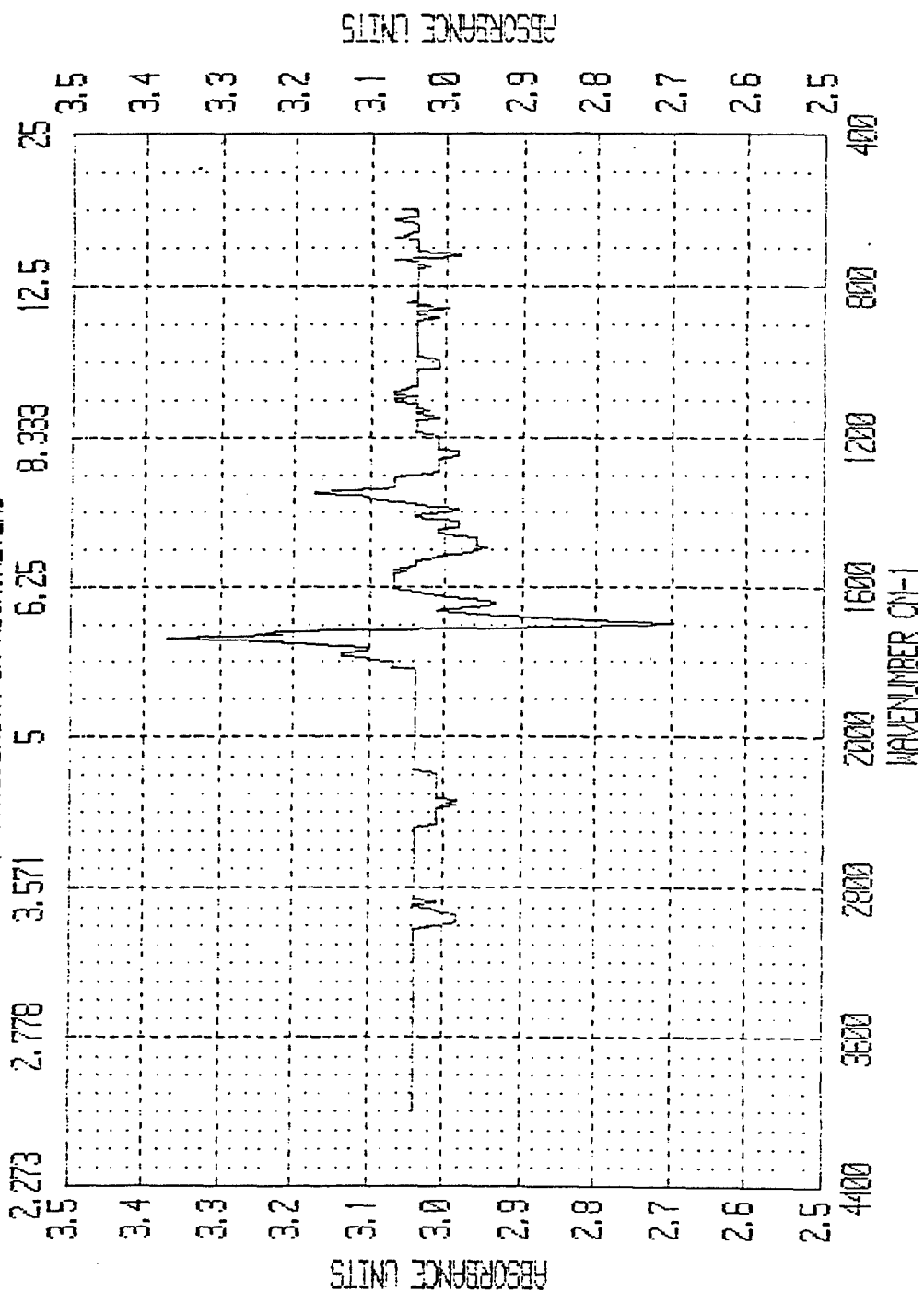
# BECKMAN



Scan Name	Result	4	No additional information	3998.36	Start	End	401.12	30 scans	3.0384	First Y
Resolu	Apodized	no								
2% to - 20%										

# BECKMAN

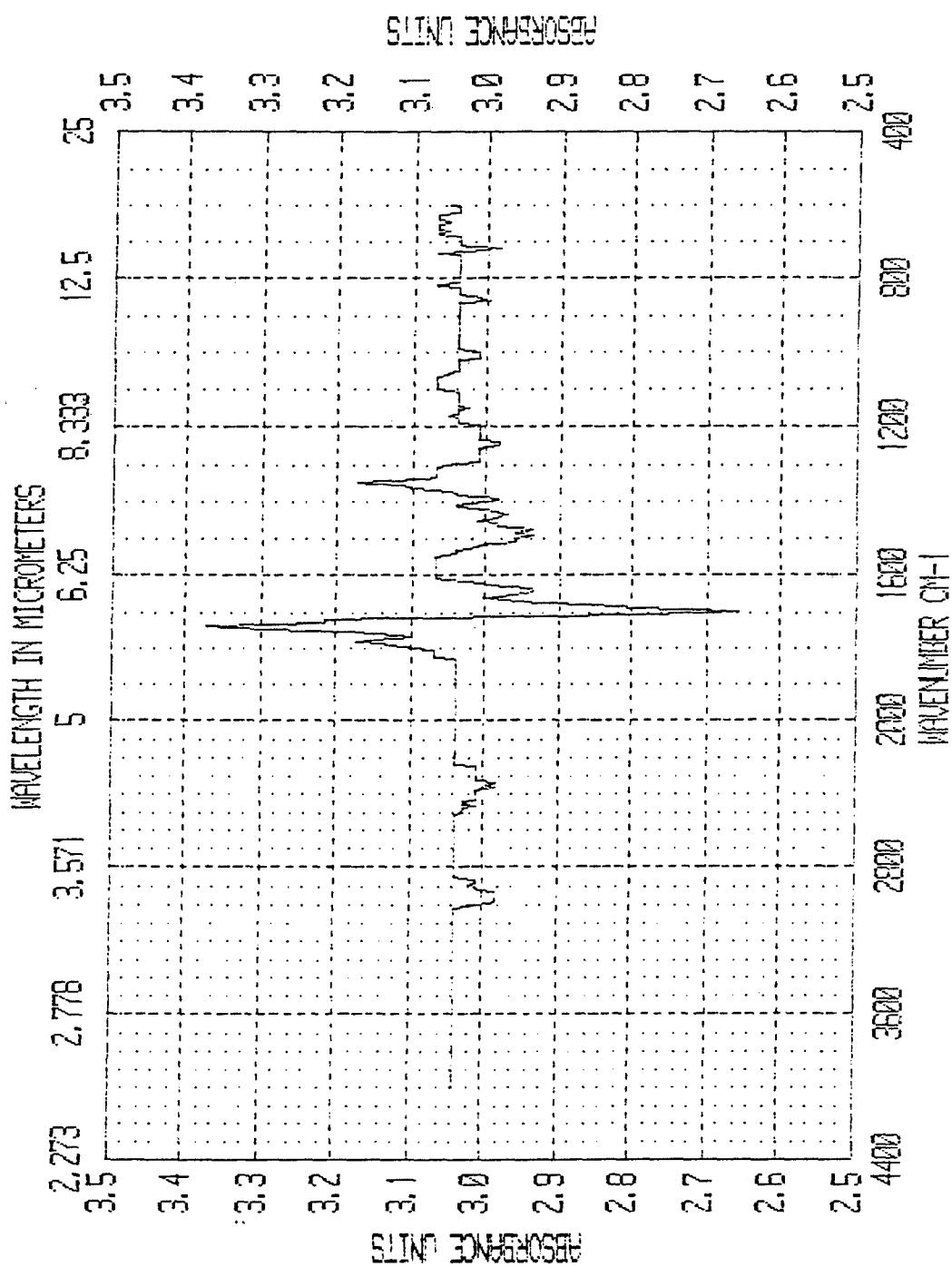
WAVELENGTH IN MICROMETERS



t=60 - 0 min. @260°C

Scan Name	Result	Apodized	Start	End	Scan Time	First Y
4	3998.36	no	401.12	30 scans	3.0384	
No additional information						
2%/60 - 260%						

# BECKMAN

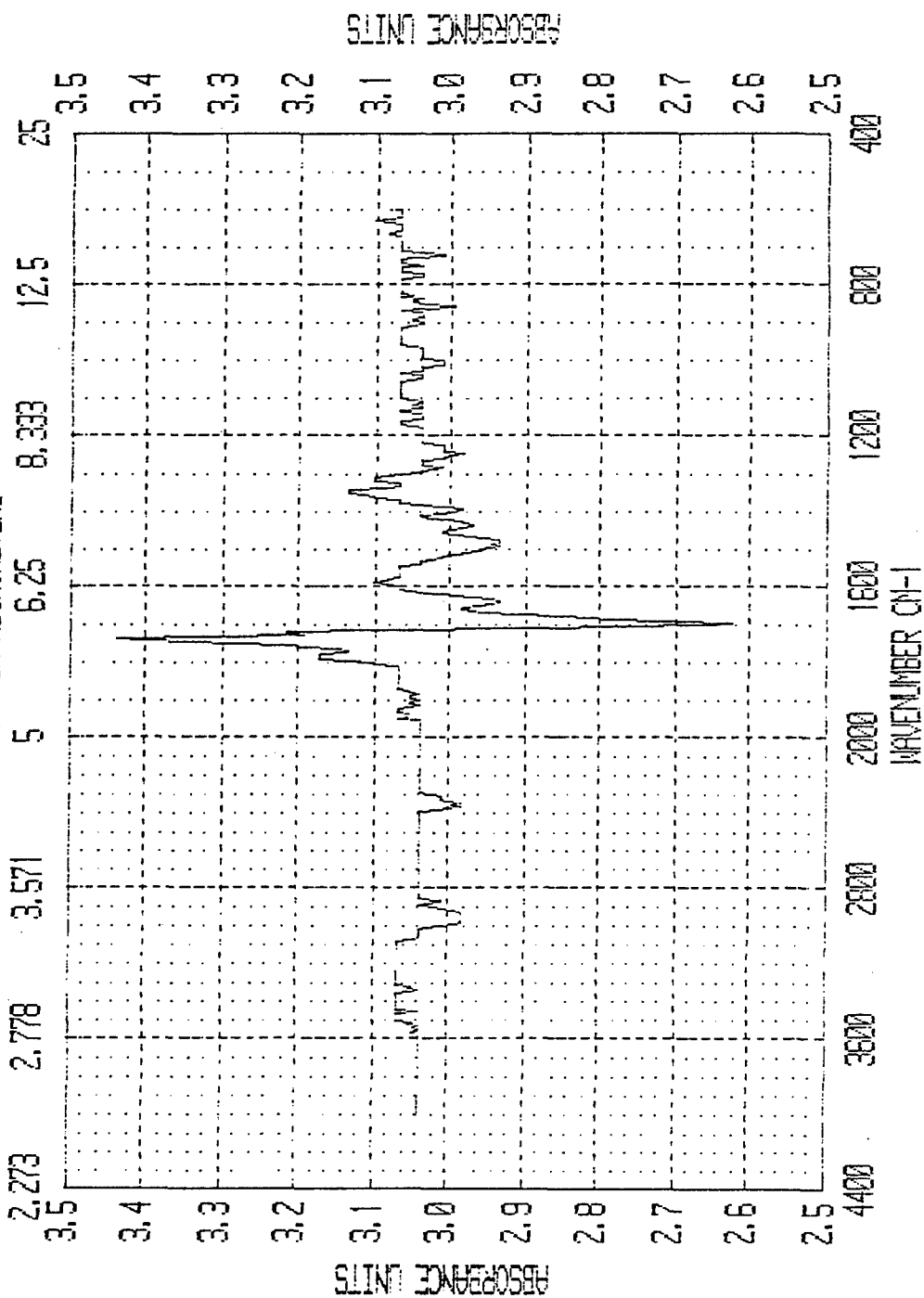


t=90 - 0 min. @260°C

Scan Name	Result	Apodized	Start	End	Scan Time	First
	4	no	3998.36	401.12	30 scans	3.0384
No additional information						
260/90 - 260%						

# BECKMAN

WAVELENGTH IN MICROMETERS

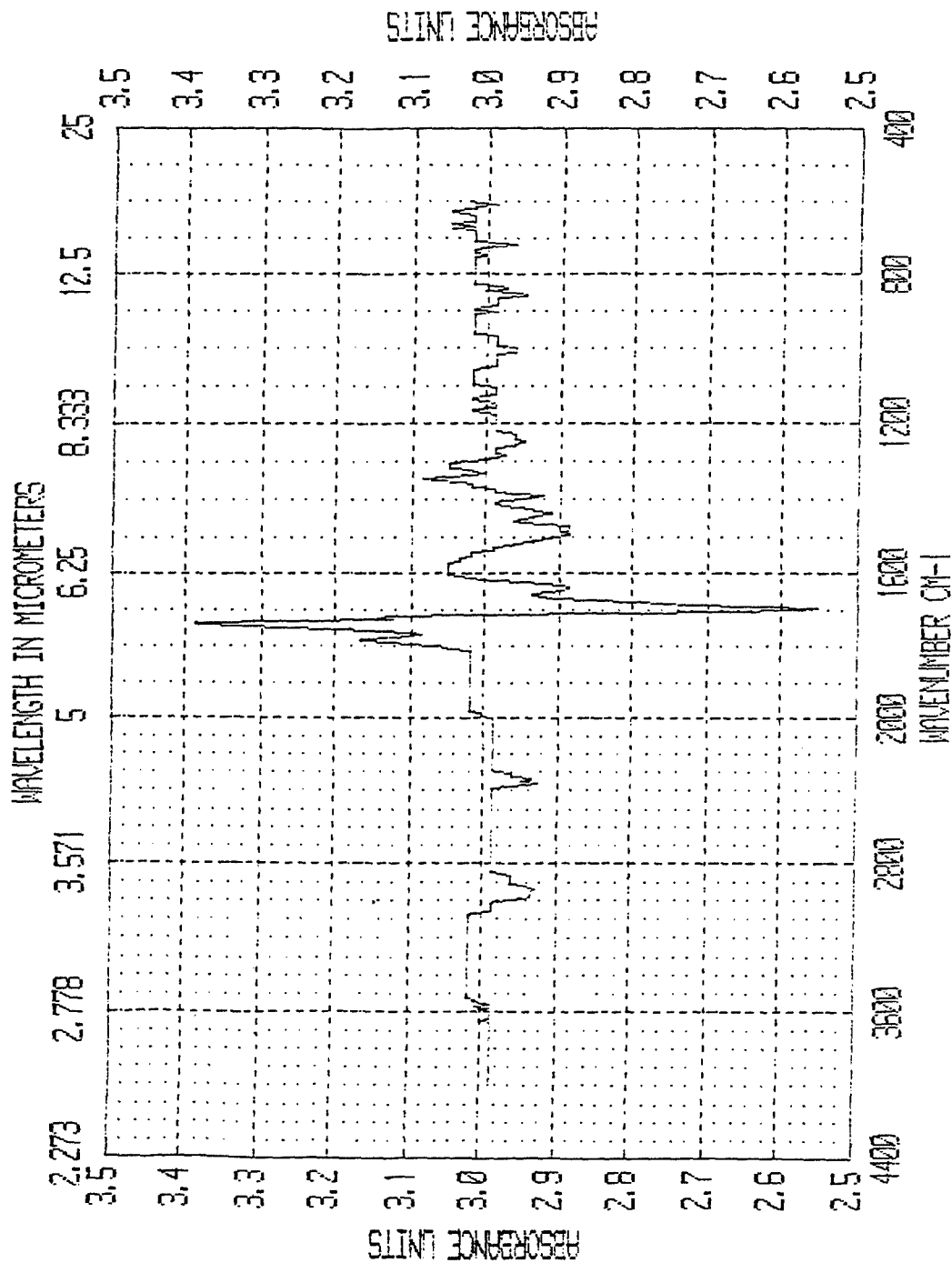


t=150 - 0 min. @260°C

Scan Name	Result	Apodized	Start	End	Scan Time	First Y
	4	no	3998.35	401.12	30 scans	3.0384
No additional information						
70/150 - 200%						



# BECKMAN

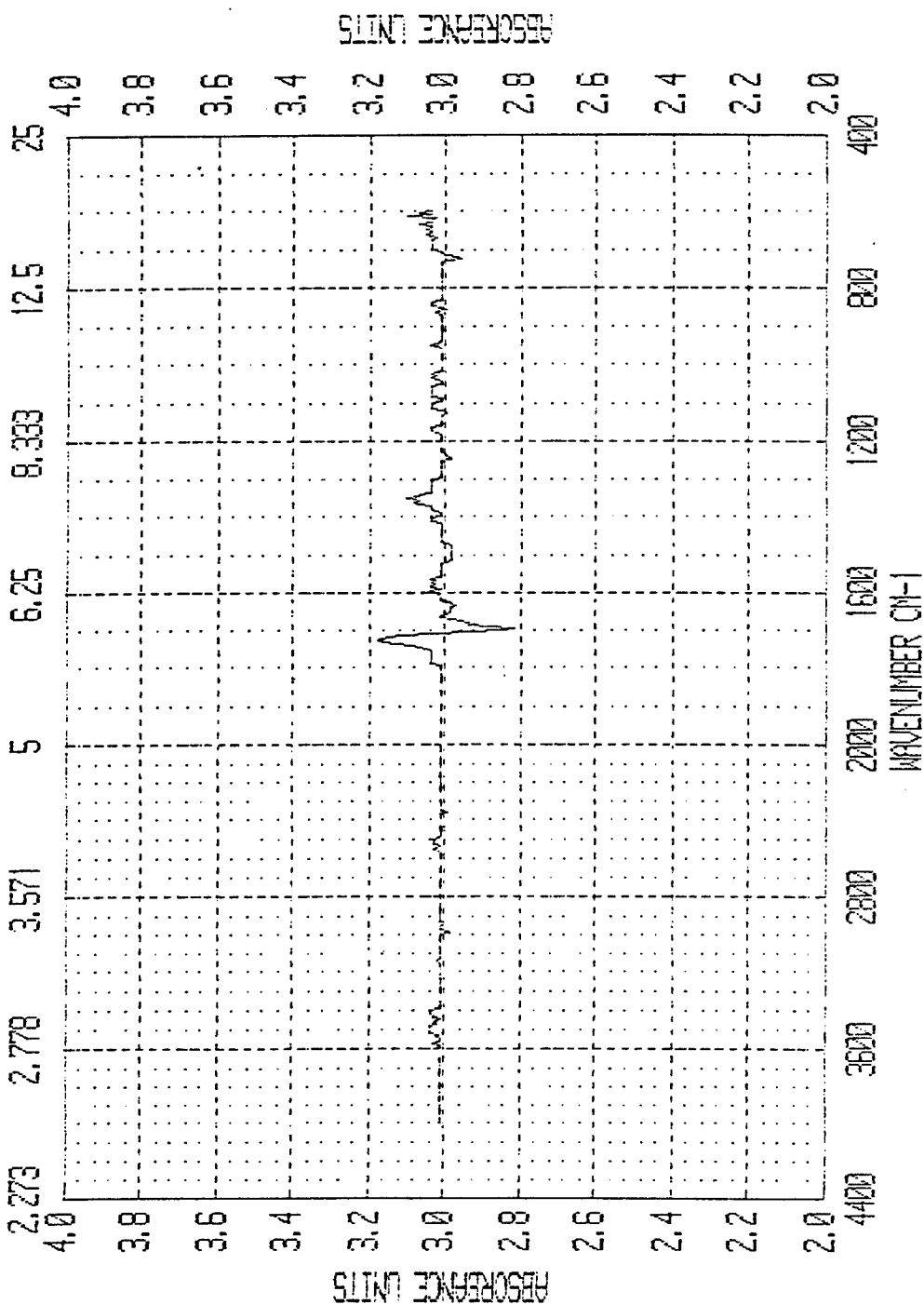


t=240 - 0 min. @260°C

Scan Name	Resolu	Apodized	Start	End	Scan Time	First Y
RESULT	4	no	3998.36	401.12	30 scans	3.0384
No additional information						
260/240 - 260%						

# BECKMAN

WAVELENGTH IN MICROMETERS

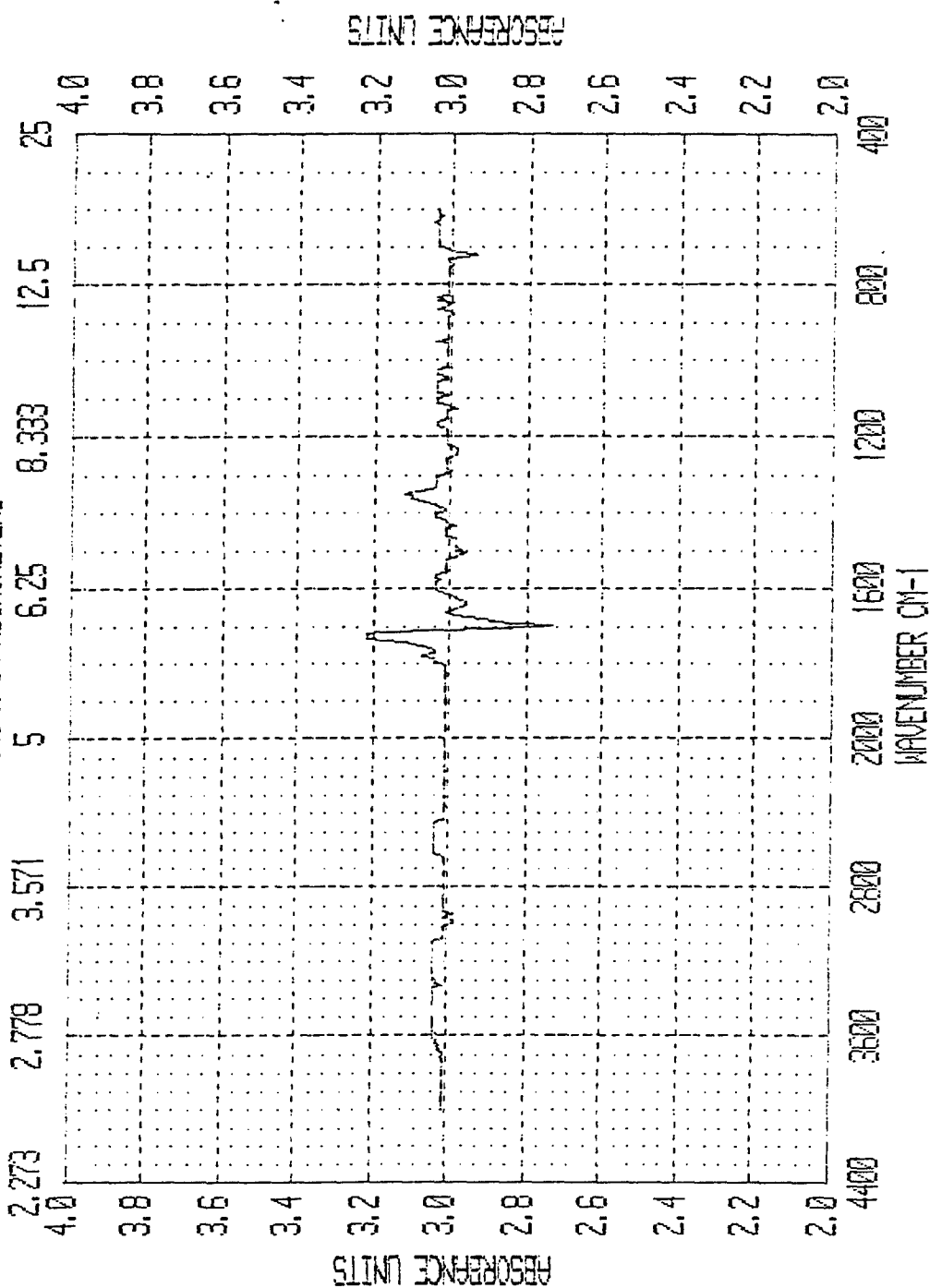


t=5 - 0 min. @280°C

Scan Name	Result	4	No additional information	3998.36	Start	End	Scan Time	First y
Resolu							10 seconds	3.0103
Apodized								
280/s - 280%								

# BECKMAN

WAVELENGTH IN MICROMETERS

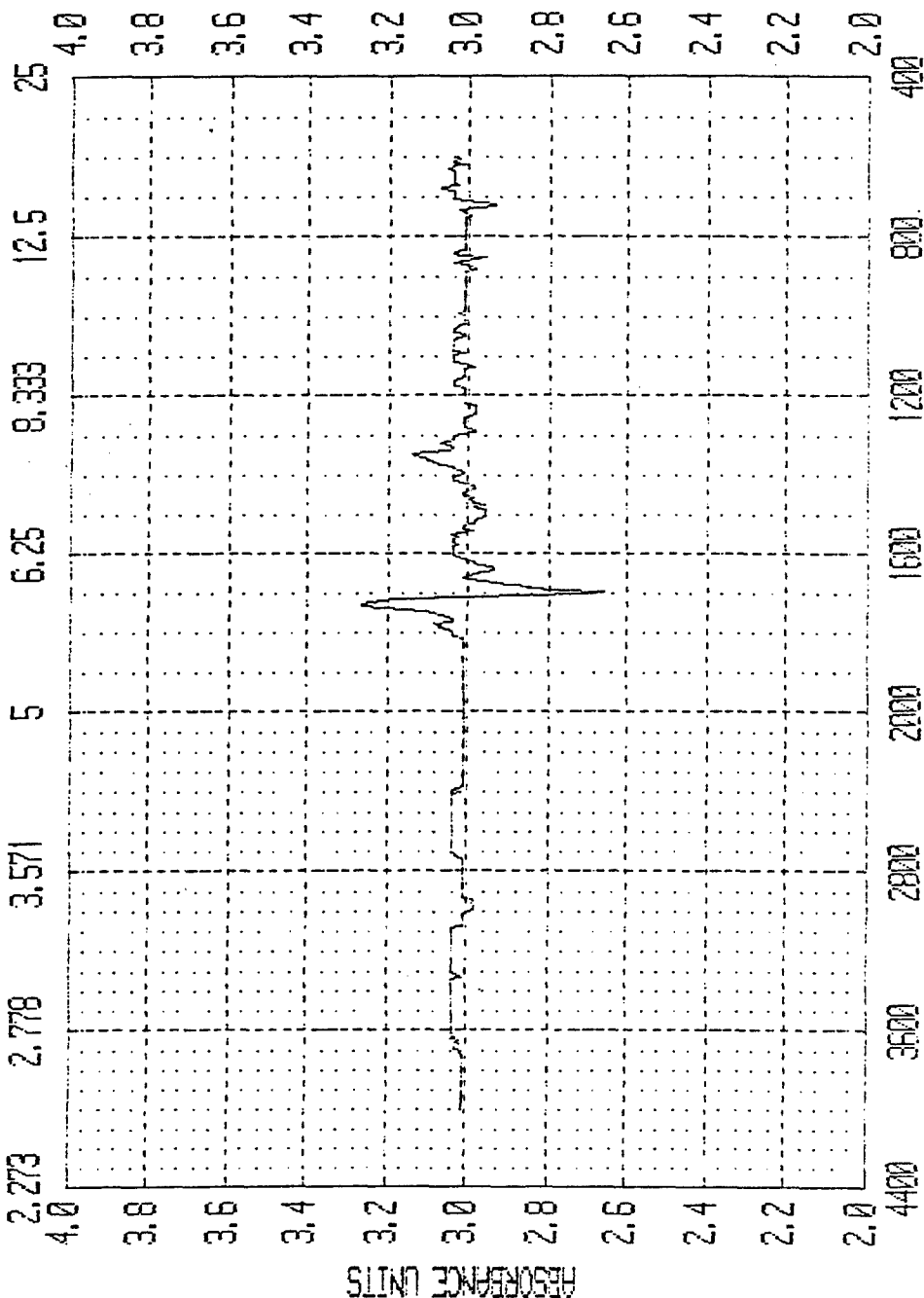


t=10 - 0 min. @280°C

Scan Name	Result	Apodized	Start	End	Scan Time	First y
4	no	no	3998.36	401.12	11 seconds	3.0103
No additional information						
280% - 28%						

# BECKMAN

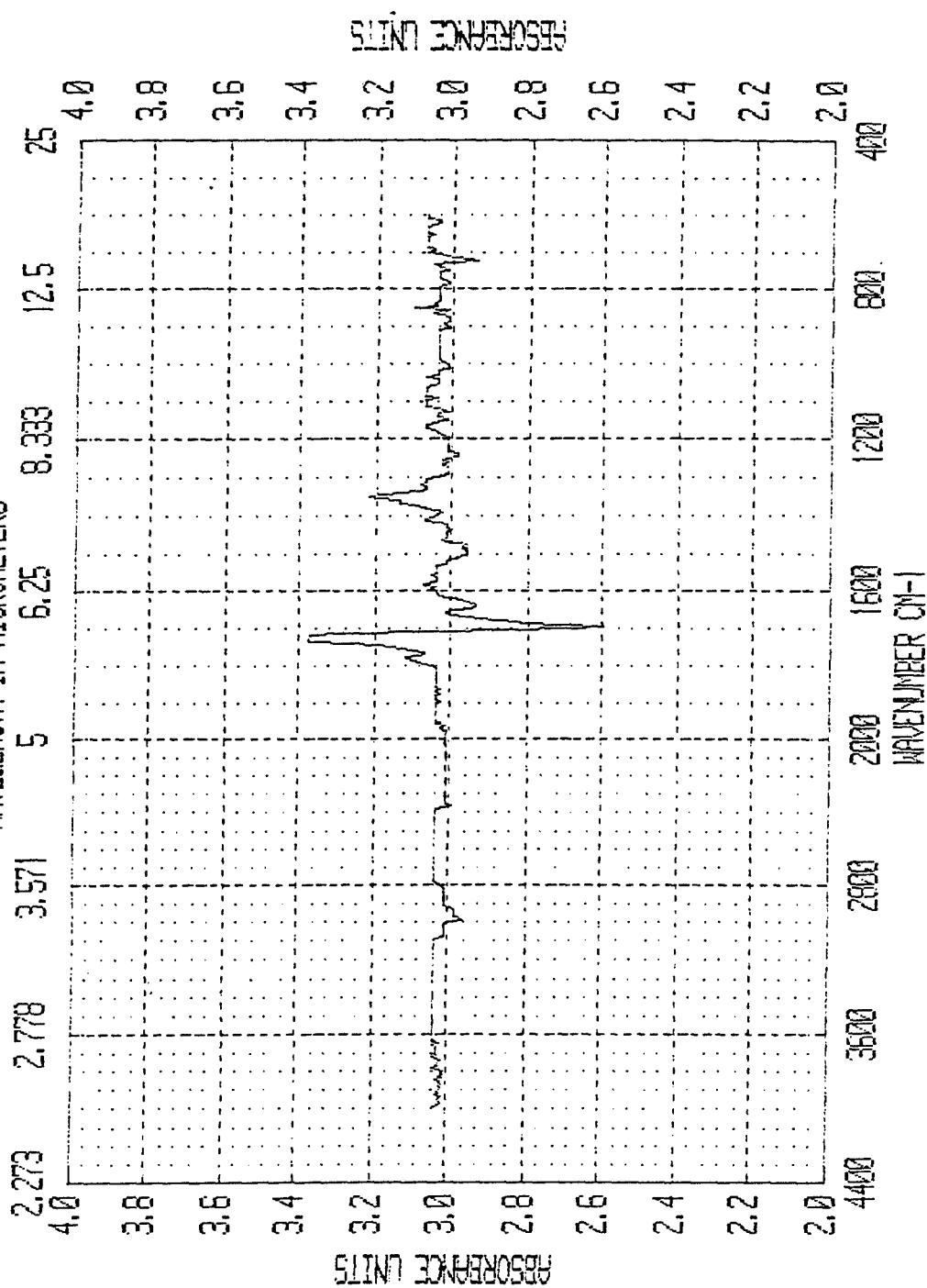
WAVELENGTH IN MICROMETERS



t=15 - 0 min. @280°C

Scan Name	Result	4	No additional information	3998.36	Start	End	Scan Time	First Y
Resolu	Apodized	no					10 seconds	3.0103
								280/15 - 280%

## WAVELENGTH IN MICROMETERS



t=30 - 0 min. @280°C

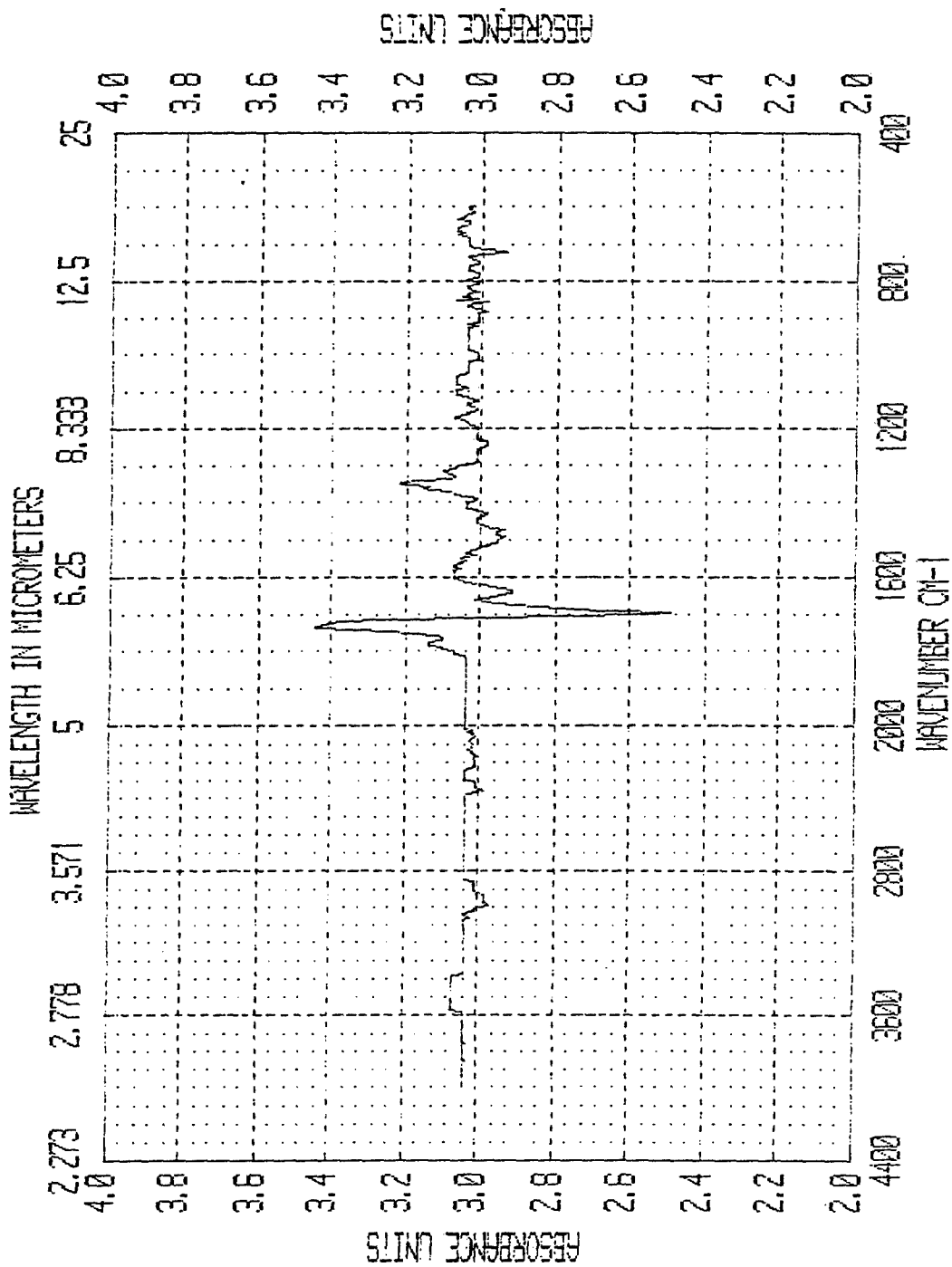
Scan Name	Resolved	Apodized	Start	End	Scan time	First y
RESULT	4	no	3998.36	401.12	10 seconds	3.0384
No additional information						
28% - 28%						

## WAVELENGTH IN MICROMETERS



280/40 - 280%

# BECKMAN

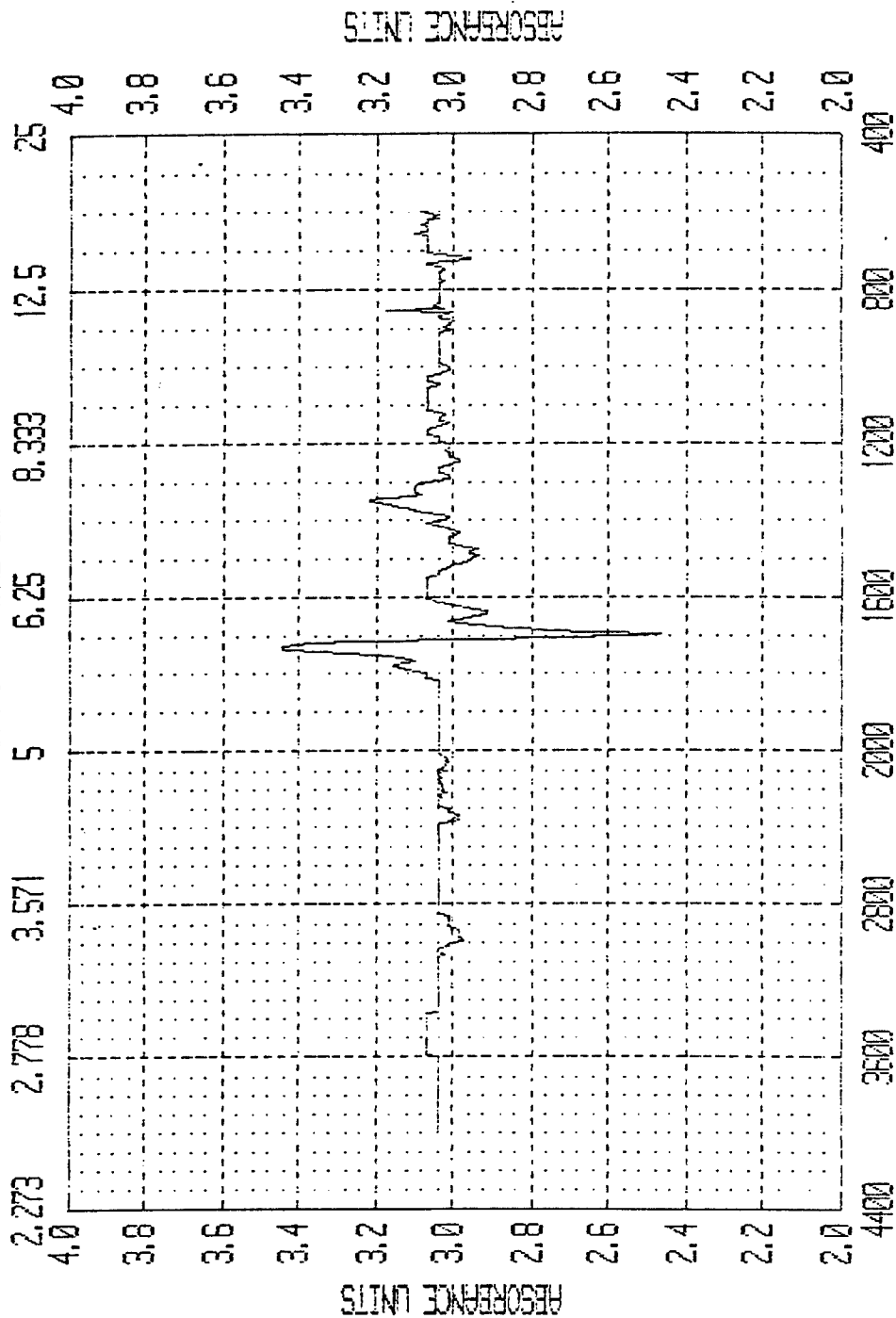


t=50 - 0 min. @280°C

Scan Name	Result	Start	End	Scan Time	First Y
Resolu	4	3998.36	401.12	30 seconds	3.0384
Apodized	no	No additional information			
280/50 - 280%					

# BECKMAN

WAVELENGTH IN MICROMETERS



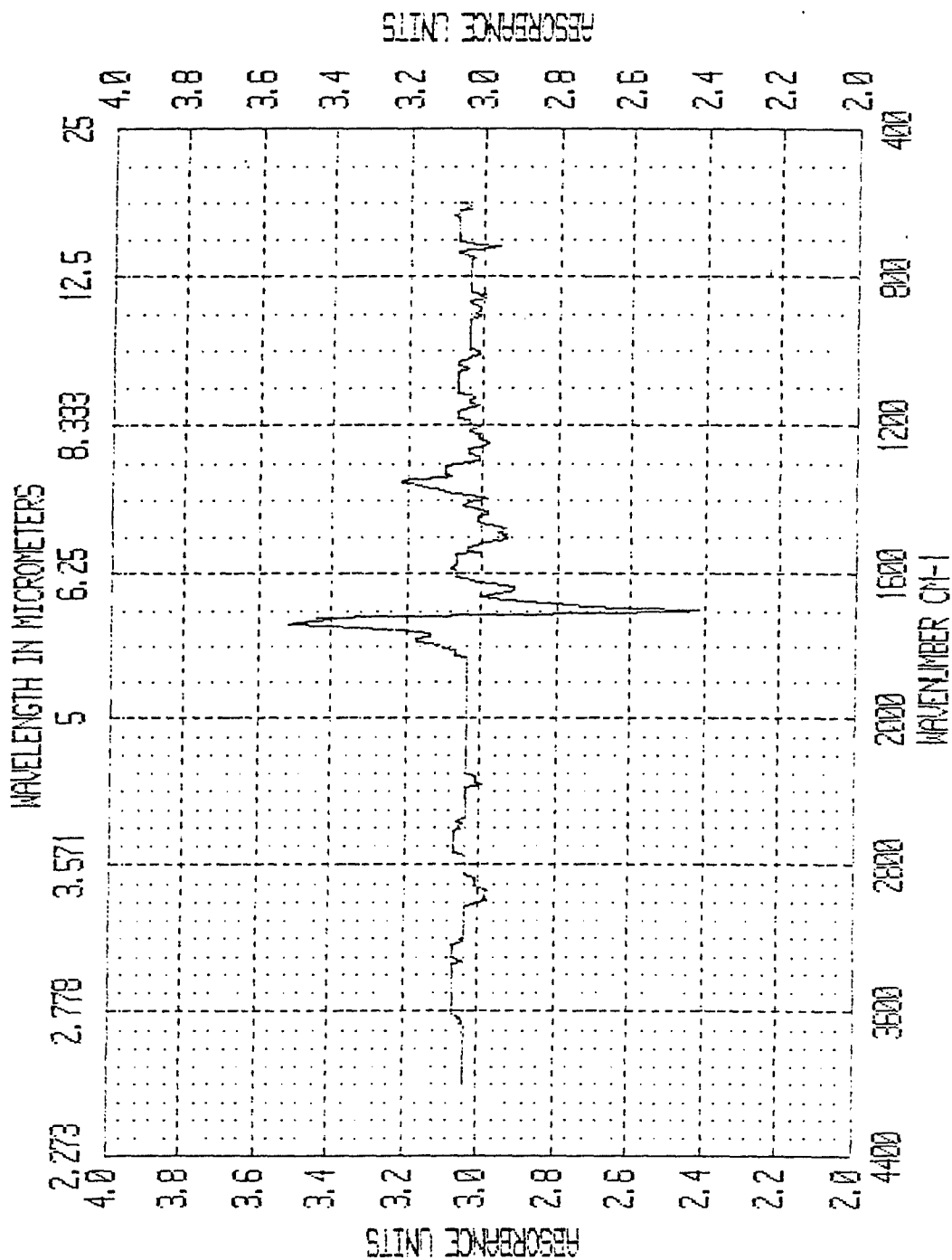
WAVELENGTH IN MICROMETERS

t = 60 - 0 min. @280°C

Scan Name	Result	No additional information	Start	End	Scan Time	First y
4	3998.36	28% - 20%	401.12	11 seconds	3.0384	



# BECKMAN

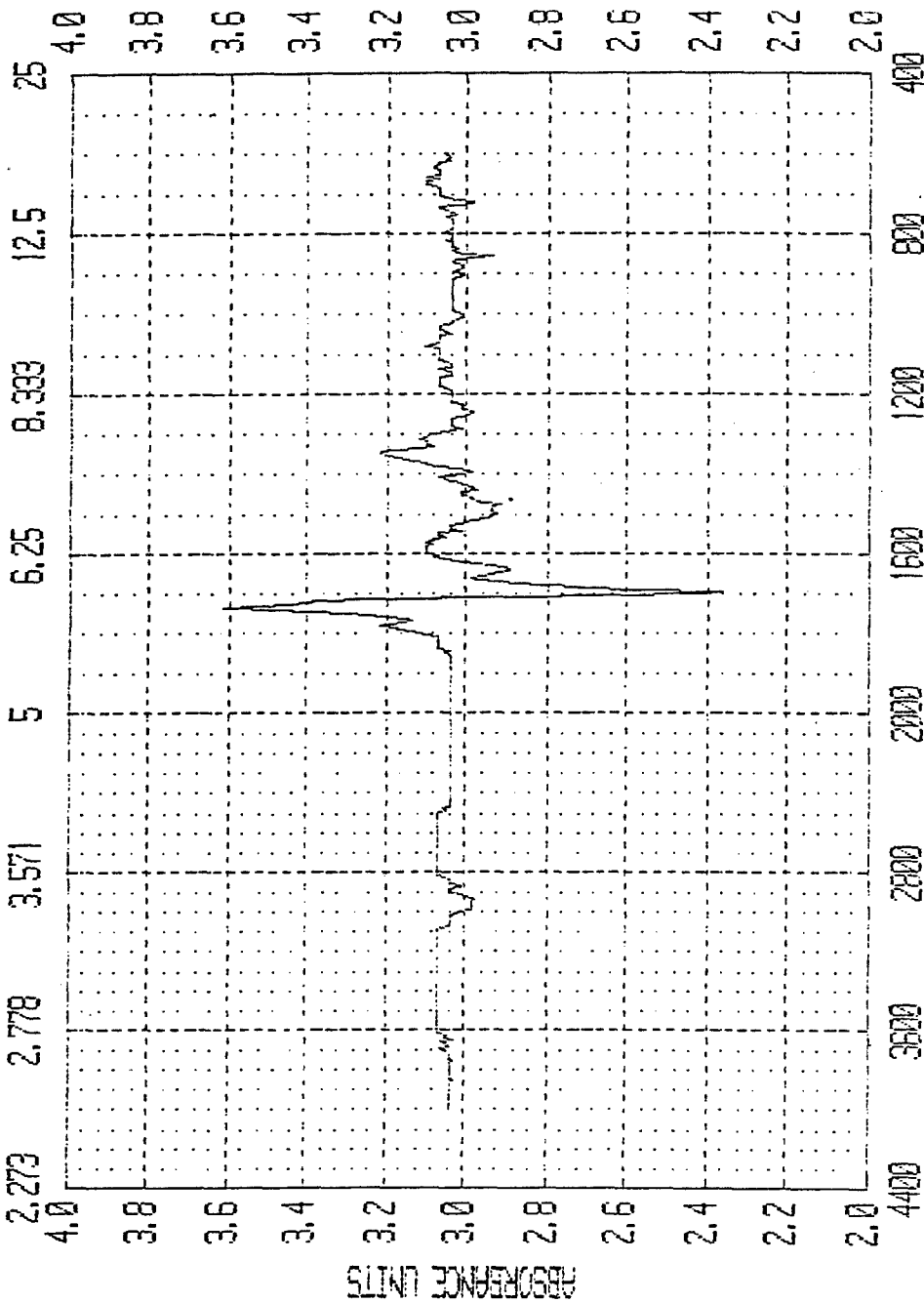


t = 90 - 0 min. @ 280°C

Scan Name	Result	Apodized	Start	End	Scan Time	First V
4	3998.36	no	401.12	9 seconds	3.0384	
No additional information						
280/90 - 280%						

# BECKMAN

WAVELENGTH IN MICROMETERS

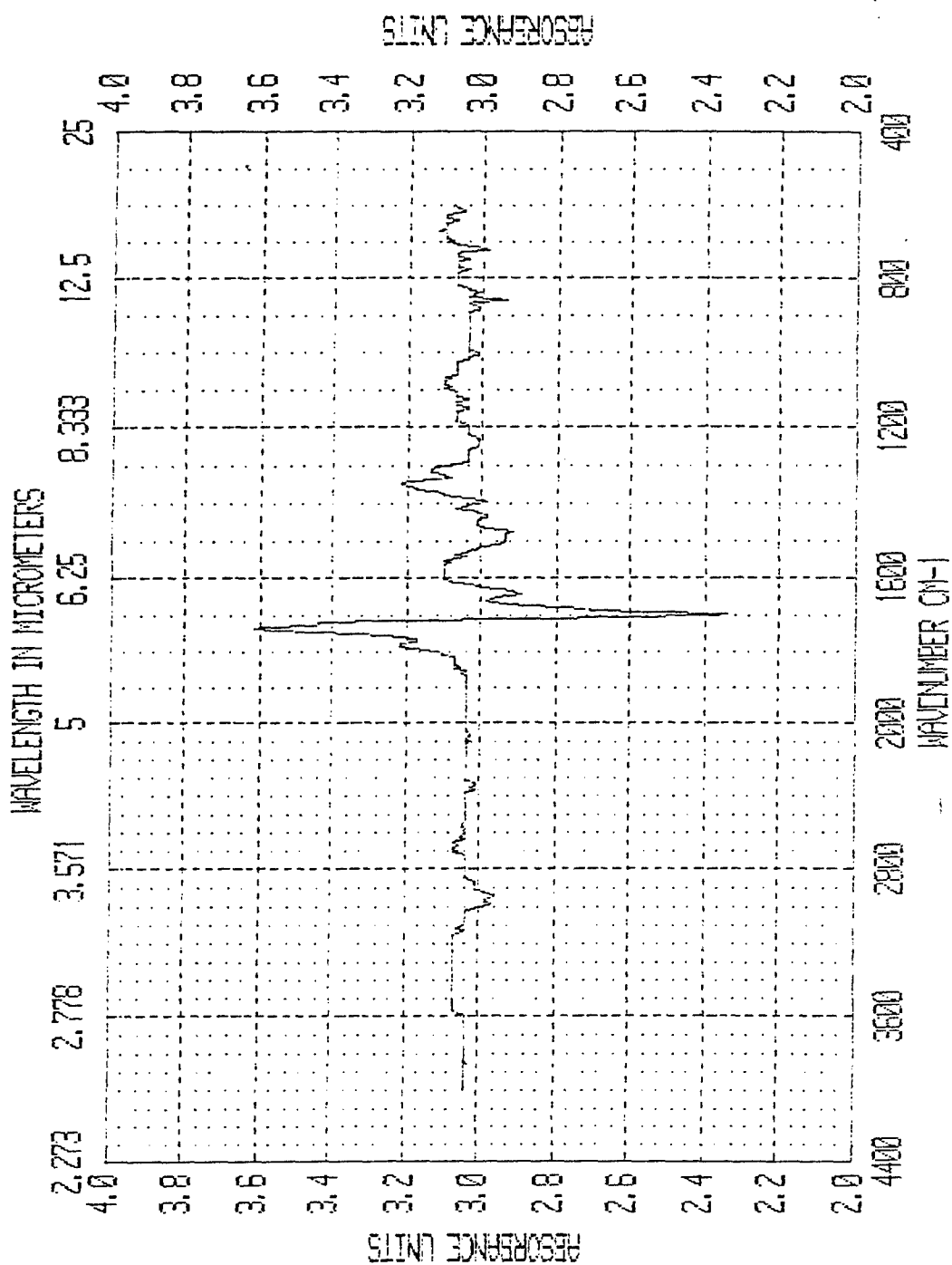


t= 130 - 0 min. @280°C

Scan Name	Result	4	No additional information	3998.35	Start	End	401.12	Scan Time	10 seconds	First y	3.0384
Resolu	Apodized	no									

280/30 - 280%

# BECKMAN



t= 180 - 0 min. @280°C

Scan Name	Result	Apodized	Start	End	Scan Time	First Y
4	no	3998.36	401.12	10 seconds	3.0384	
No additional information						
280/80 - 28%						